CONTINUOUS ANNULAR CHROMATOGRAPHY FOR THE SEPARATION OF CARBOHYDRATE MIXTURES

A THESIS SUBMITTED

BY

STEPHEN BRIDGES B.Sc.

FOR THE DEGREE OF DOCTOR OF PHILOSOPHY

Department of Chemical Engineering & Applied Chemistry
Aston University

MARCH 1990

The University of Aston in Birmingham

Continuous Annular Chromatography for the Separation of Carbohydrate Mixtures

Stephen Bridges (BSc) PhD 1990

SUMMARY

The continuous separation of beet molasses resulting in a sucrose rich product and a non-sugar waste product was carried out using a rotating annular chromatograph. The annulus was 12 mm wide and 1.4 m long and was packed with a sodium charged 5.5% cross-linked polystyrene ion exchange resin. Separation was achieved by the simultaneous mechanisms of ion exclusion, size exclusion and partition chromatography. The entire packed bed was slowly rotated while beet molasses was fed continuously through a stationary feed nozzle to the top of the bed. Each molasses constituent having a different relative affinity for the packing and the de-ionised water mobile phase describes a characteristic helical path as it progresses from the stationary feed point to the bottom of the rotating bed. Each solute then elutes from the annulus at a different angular distance from the feed and separation of the multicomponent mixture is thereby achieved.

When a 35% w/w sucrose beet molasses feed was used the throughput achievable was 45.1 kg sucrose m^{-3} resin h^{-1}.

In addition to beet molasses separation other carbohydrate mixtures were separated. In particular the separation of glucose and fructose by ligand

exchange chromatography on a calcium charged ion exchange bed was carried out.

The effects of flowrates, concentration, rotation rate, temperature and particle size on resolution and dilution of constituents in the mixtures to be separated were studied.

A small test rig was designed and built to determine the cause of liquid maldistribution around the annulus. The problem was caused by the porous bed support media becoming clogged with fines being introduced by eluent flows and off the resin. An outer ring was constructed to house the bed support which could be quickly replaced with the onset of maldistribution.

The computer simulation of the operation of the rotating annular chromatograph has been carried out successfully.

Keywords: **Chromatography, Annular, Molasses, Liquid Distribution.**

This thesis
is dedicated to my family

ACKNOWLEDGEMENTS

The author wishes to thank the following: Dr E L Smith and the Department of Chemical Engineering and Applied Chemistry for making available the facilities for research.

Professor P E Barker, who supervised the work and for his advice and guidance.

Mr N Roberts, Mr M Lea, Mr I R Murkett and all other members of the Department Technical staff for their time and effort.

The Directors of British Sugar PLC for the provision of funds for equipment and consumables. Mr N Broughton, Mr G C Jones and Mr D Sargent and other members of the British Sugar Research Group for their helpful advice and assistance.

Fellow Research Students in the separation and purification group for many useful discussions.

CONTENTS

LIST OF TABLES

LIST OF PHOTOGRAPHS

LIST OF FIGURES

CHAPTER ONE
INTRODUCTION

1.0 Introduction

In chromatography a mixture of chemical substances is separated due to the differential migration of each component through a system of two phases. The individual components of the mixture migrate through the stationary phase at a rate which is governed by the relative affinity each component has for the mobile phase compared with the stationary phase. Chromatography has proved to be a most versatile analytical technique but its application to industrial processes was hampered for many years by the preference for batch separations and by the loss of performance encountered with large diameter columns. The latter has to some extent been overcome so that one can find columns of up to 4 metres diameter in commercial use. Continuous operation of separation processes is often advantageous and more efficient for applications at the production scale, especially when the separation system is coupled to other continuous processes.

A continuous means of separation was used during the separation studies described in this work. The rotating annular chromatograph is a crossflow type system whereby the chromatographic bed moves perpendicularly to the direction of fluid motion within the bed. In particular the rotating annular chromatograph was used to separate various sugar mixtures of industrial relevance.

The production of sugar worldwide depends on the success of the harvest of the sugar producing crops. These crops vary with location - sugar beet in the temperate zones and sugar cane in the tropical zones of the world. The most common sugar produced in large quantities is sucrose, but since the late 1970's considerable interest has been shown in the production of

monosaccharides from starch sources such as maize, corn or rice by enzymatic inversion.

British Sugar PLC controls sugar production from sugar beet in Britain whereas Tate and Lyle Ltd is the main producer of sugar from imported sugar cane.

The production of sugar in the European Economic Community member countries is controlled by the commission to protect the sugar beet farmers in the community. There are three different quotas set for the quantity of sucrose produced by British Sugar from sugar beet:

Quota A - A high price is guaranteed by the E.E.C. for the sucrose produced in this quota.

Quota B - A lower price is guaranteed for sucrose produced within this quota. The B quota is 10% of the A quota in tonnage.

Quota C - Any C quota sugar produced must be exported outside the E.E.C., and hence it is quoted at the world market price. This price paid is much lower than the two other prices which currently makes it uneconomical to produce.

There is however an interest in the recovery of sucrose from beet molasses which could be sold under Quota C. Beet molasses is the final syrup spun off after repeated crystallizations in the extraction of sugar. The annual output of approximately 1.2 million tons from British Sugar is obtained from 8 million tons of sugar beet and this yields 0.3 million tons of molasses. British Sugar sells approximately 25% of the molasses to fermentation companies and about 60% as animal feedstock. The molasses however represents an important loss of extraction amounting to 12-16% of the sugar in beets.

The aims of this research were:

1 To run the rotating annular chromatograph using beet molasses as feedstock and to optimise the equipment's separating performance by evaluating various operating parameters such as feed rate, rotation rate and temperature.

2 To compare the separation performance of the rotating annular chromatograph using different particle size beds.

3 To run the rotating annular chromatograph using synthetic glucose/fructose mixtures as feedstock.

4 To run the rotating annular chromatograph using inverted molasses as feedstock and to compare the separation performance with that achieved with the synthetic glucose/fructose feed.

5 To model and develop a computer simulation program to predict throughputs, yields and purities of products under any operating conditions.

CHAPTER TWO
LITERATURE SURVEY

2.1 Principles of Chromatography

In chromatography a mixture of chemical substances is separated by being dissolved in a fluid (mobile phase) and passed through a packed bed of stationary phase. The individual components of the mixture migrate through the stationary phase at a rate which is governed by the relative affinity of the component for the mobile phase over the stationary phase. Components which interact more strongly with the stationary phase will migrate at a slower rate than those which have more affinity for the mobile phase. The result is that the components are separated into bands which elute from the stationary phase bed at different times. Figure 2.1 shows the hypothetical separation of a 3-component mixture. The separation of components within a given chromatographic device depends upon the relative affinity for the stationary phase and the fluid throughput.

2.2 Classification of Chromatographic Methods

2.2.1 Classification according to technique employed

There are three techniques of chromatographic operations that each of the four methods mentioned above can be carried out by, namely;

(a) Elution chromatography

(b) Frontal chromatography

(c) Displacement chromatography

Figure 2.1 Hypothetical Separation of a 3-Component Sample

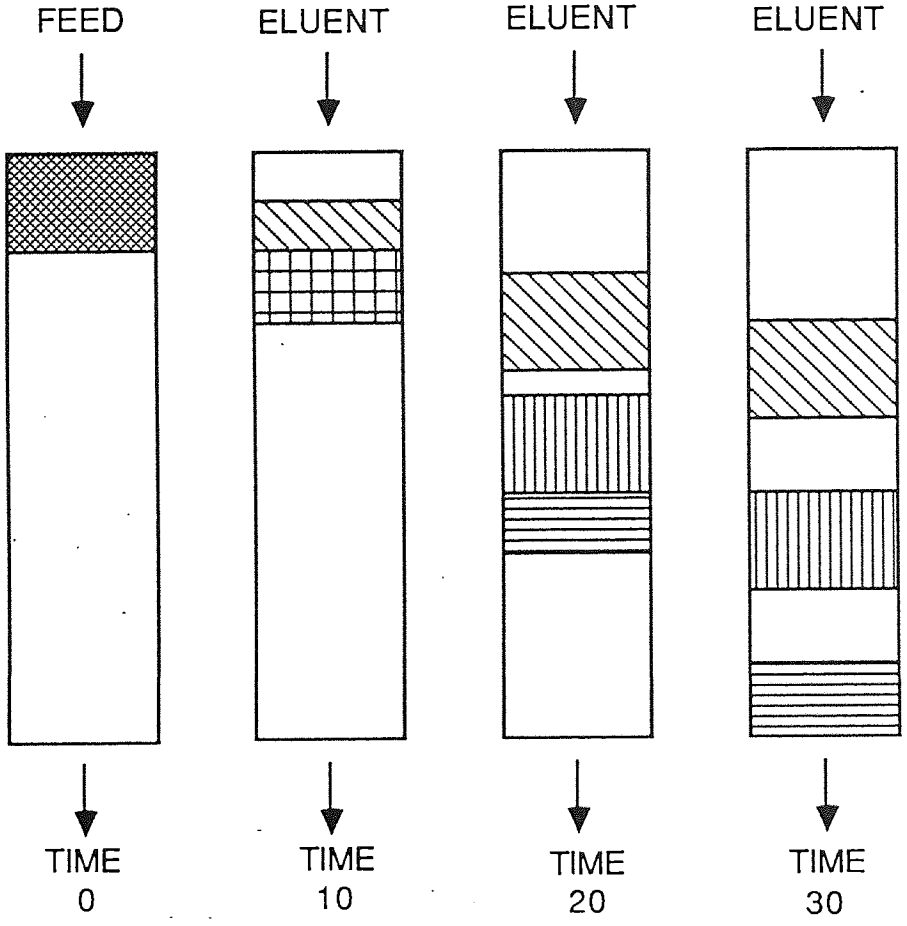

2.2.2 Classification according to phases employed

In chromatography, the components of the separation mixture are distributed between the two phases - the stationary and mobile phases. Depending on the nature of these phases we have four main chromatographic systems as follows:

A - Solid Stationary Phase	(a) Gaseous Mobile Phase "Gas-Solid Chromatography" (G.S.C.)
	(b) Liquid Mobile Phase 'Liquid-Solid Chromatography" (L.S.C.)
B - Liquid Stationary Phase	(c) Gaseous Mobile Phase "Gas-Liquid Chromatography" (G.L.C.)
	(d) Liquid Mobile Phase "Liquid-Liquid Chromatography" (L.L.C.)

In this work a Liquid-Solid Chromatographic System (system (b)) was used.

(a) Elution chromatography

A small quantity of mixture is injected onto a column and component separation is achieved by its distribution between the two phases. As different components migrate through the bed at different rates, both qualitative and quantitative separation of the mixture occurs.

(b) Frontal chromatography

A sample is introduced into the system continuously with the mobile phase. The less strongly adsorbed component migrates faster and is eluted pure until the accumulated strongly adsorbed component breaks through with the

mobile phase, after which there is no separation. This system can be advantageous when the separation of a powerfully adsorbed minor component from a mixture is required.

(c) Displacement chromatography

In this system, the mobile phase is more strongly retained by the stationary phase than the sample mixture. The sample is then pushed through the bed by the advancing mobile phase. This provides much poorer separation but increased sample loading can be applied to the bed.

2.3 Developments in Production Scale Chromatography

Chromatography is a batch process in its conventional implementation. An analytic chromatograph can provide a highly efficient separation of even very similar molecular species and the possibility of scaling up such processes for large-scale production has therefore attracted much attention. Were it possible to develop high throughput capabilities, chromatography could become the ultimate separation technique. Two principal approaches have been used to increase throughput: automated repetitive operation of large diameter batch columns, and the use of moving chromatographic beds that permit continuous introduction of feed and continuous withdrawal of products.

2.3.1 Batch chromatographic processes

A brief description of the commercial batch chromatographic processes used to separate carbohydrates is outlined in this section. A detailed literature search was carried out on many of these processes by Thawait (1).

2.3.1.1 The Finn-Sugar Process

In 1962 the Finnish Sugar Co Ltd became committed to the scaling-up of batch chromatographic processes. They specialized in the desugarisation of beet molasses, recovering sucrose by employing the ion-exclusion principle and also in the production of high purity fructose and high fructose corn syrups by ion-exchange on Ca^{2+} charged cross-linked polystyrene resins. In 1975 Finnish Sugar installed what was then the largest batch chromatographic molasses separation plant in the world, consisting of one 2.7 m inside diameter by 6 m high column, recovering up to 95% of the sugar in molasses at purities exceeding 92% (2).

In 1983 a new plant was completed for Amino GMBH in Frellstedt, Germany, for the recovery of beet molasses, at a reported cost of $7.6m. It employed seven resin filled 3.6 m I.D x 12 m high columns processing 60000 tons/yr of molasses (3). The typical product concentrations were about 21% w/v, 9% w/v and 5% w/v of sucrose, non-sugars and betaine respectively.

A Xrofin plant has also been installed by them in Thomson (Illinois, USA) producing over 13000 tons/yr of crystalline fructose from corn syrups using 17 separation columns (3).

2.3.1.2 The Pfeifer and Langen ion exclusion process (4)

A prototype 3 m diameter column containing 55m^3 of a sulphonated cationic resin in the sodium form, cross-linked with 4-5% divinylbenzene was brought on stream at Pfeifer and Langen in Germany in 1974. Molasses of 63 purity was separated by ion exclusion into a product fraction of high purity, e.g. 87, and low ash content and a waste fraction of low purity, e.g. 32, and high ash content. The fractions were concentrated separately in a multiple effect evaporator. 70% of the sugar could be recovered from the product fraction by crystallization and the secondary molasses which remained could be sold.

2.3.1.3 The Sudzucker process

In the Sudzucker process for the desugarisation of beet or cane molasses, the molasses is fractionated by means of liquid chromatography into a sucrose rich fraction and several non-sugar fractions. The stationary phase is a strongly acidic cation exchange resin with a low degree of cross-linkage and in the Ca^{2+} form. In a pilot plant with total resin bed volume 13.4m^3, beet molasses of purity 60, diluted to 50% dry substance was passed at 90°C into the resin column; after 0.06 bed volumes had been introduced, it was eluted with hot water. By using 3 columns in series, from each of which the molasses was eluted in turn, the duration of a cycle was reduced to $2^1/2$ hours and a fraction of purity greater than 90 and dry substance content 10-11% was obtained, from which more than 95% of the sucrose in the original molasses could be recovered.

The Sudzucker Process was developed by Munir (5) of Suddeutsche Zucker A.G, Mannheim, Germany.

2.3.1.4 The Boehringer process

C.F. Boehringer and Soehne GMBH (Germany) obtained a patent (6) for a process for the manufacture of pure solutions of invert sugar, starting from molasses. The molasses is hydrolysed preferably with H_2SO_4 and is then separated by ion-exchange chromatography on a cation exchanger in the salt form into a salt solution and an invert sugar solution. A separating length of 9m was used in 6 columns each 15cm ID and 2m high. A good separation is obtained by using a resin in the K^+ form which has been equilibriated with the acid hydrolyzate, e.g. containing 5-6% of exchangeable H^+ ions.
The chromatographic separation of the constitutents of beet molasses has been reported by Sayama *et al* (7). With the aim of recovering sucrose a 4% cross-linked divinylbenzene ion-exchange resin in the sodium form was employed. About 2 tons molasses/m^3 resin could be treated per day.

Fornalek *et al* (8) report on the development of a method for recovering sucrose contained in molasses by means of ion exclusion. Molasses previously diluted to 52° brix was passed at 85-90°C through a $10m^3$ column of Lewatit TSW40 resin in the Na^+ form, $0.7m^3$ molasses being put on at $4.5m^3/h^{-1}$. A recovery of 75% of the initial sucrose is claimed.

2.3.2 Continuous chromatographic processes

Continuous operation of separation processes is often advantageous and more efficient for applications at the production scale, especially when the separation system is coupled with other continuous processes.

A chromatographic process may operate continuously if there is a relative motion between the adsorbent phase and the point where the feed is

introduced into that phase. Under these circumstances the retention time differences of the components of the feed are transformed into physical displacements so that each component may be withdrawn continuously at fixed and characteristic distances away from the feed point.

Moving bed systems may be classified as: counterflow or crossflow. In counterflow systems the adsorbent phase and the mobile phase move in substantially opposite directions. In crossflow systems the relative motions of the two phases are at right angles to each other.

2.3.2.1 Counterflow moving bed systems

The Sarex process was developed by Universal Oil Products (U.O.P) primarily for the separation of fructose from glucose during the production of high fructose corn syrup from corn starch. It is one of the simulated countercurrent sorption processes known as the Sorbex Technique (9). Relative motion between fluid entry and exit points and the chromatographic bed is obtained by placing the adsorbent in fixed vertical columns and moving the fluid feed and exit ports down the column in small sequential steps so that product streams are of constant composition. The simulated moving bed overcomes difficulties associated with the control of solids on a large scale experienced by continuous countercurrent moving bed columns.

Barker and co-workers (10, 11, 12, 13, 14) have developed a system known as semi-continuous chromatographic refining. The countercurrent movement is simulated by the simultaneous opening and closing of specially constructed valves connected to the inlets and outlets of a number of stationary interlinked columns.

2.3.2.2 Crossflow moving bed systems

In crossflow systems the chromatographic bed moves perpendicularly to the direction of fluid motion within the bed. Martin (15) was the first to propose the concept of an annular chromatograph rotating with respect to a continuous feed stream and product collection points, as shown in Figure (2.2). The bed results from packing the annular space formed by two concentric cylinders. The annulus rotates about its centre while feed is continuously introduced through a fixed feed pipe immersed in the bed. A mobile phase is passed axially (downward) through the annular bed uniformly at all parts. The feed which is introduced continuously at a fixed point at the top of the annular bed is carried through the column by the mobile phase. For the time a feed molecule resides in the stationary phase its movement relative to the feed point is horizontal or circumferential. For the time spent in the mobile phase the molecule moves both vertically down and circumferentially. Thus the place at which the molecule emerges from the column in degrees of arc from the feed injection point will be a function of its retention time and the rate of rotation of the column. Each feed component will exit the chromatograph at different angles of displacement from the feed entry point. Products are then collected at fixed points beneath the annulus (see Figure 2.2). Each solute will display a stationary helical band which joins the feed entry point to the product exit point for that feed component.

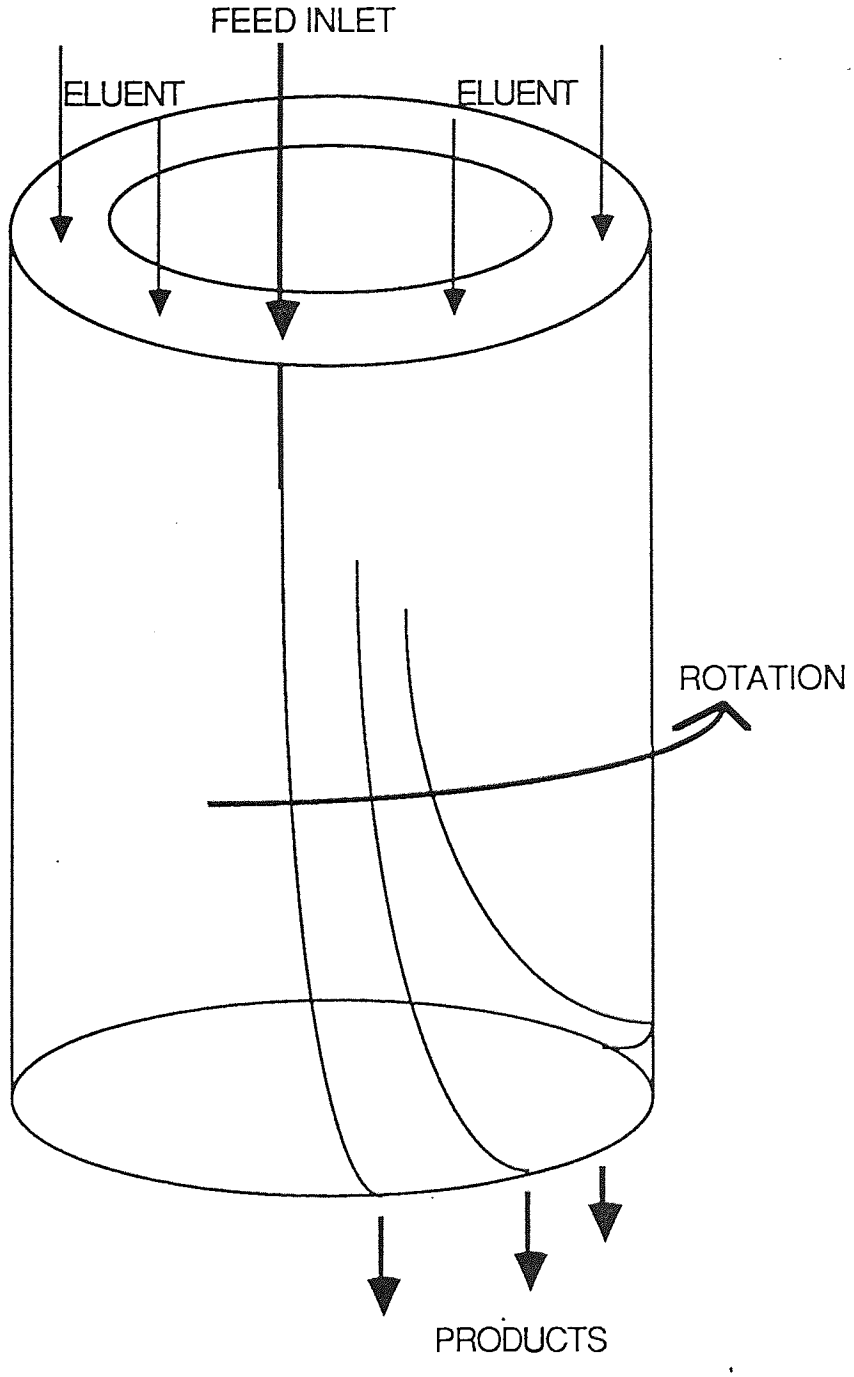

FIGURE 2.2 OPERATING PRINCIPLE OF THE ROTATING ANNULAR CHROMATOGRAPH

Giddings (16) recognized that some of the inherent disadvantages of batch type large scale systems are avoided by the annular approach. The cross-sectional area and hence capacity, could be made large for an annulus as compared with a batch column, while still keeping the annulus width narrow enough to avoid the loss in resolution experienced in batch columns with diameters greater than 25mm, caused by non-uniformity of packing.

Giddings also noted that properly spaced multiple feed points could be used to increase capacity by having the last component of a mixture exit just prior to the first of the second feed stream.

Svensson *et al* (17) used both a rotating annulus and a circular array of parallel columns to separate dyes. The composite column was designed to overcome flow maldistribution around the bottom of the annulus.

Equipment for separating volatile mixtures by gas-solid chromatography using the Svensson theme of a series of vertical columns was presented by Dinelli *et al* (18). They arranged a hundred vertical columns on a circular pitch and rotated them as a carousal at speeds of between 1 to 50 revolutions per hour. The carrier gas travelled down the columns with feed being injected successively into columns as they passed the fixed feed port. For the separation of cyclohexane-benzene mixtures on tricresyl phosphate as stationary phase at throughputs of $200cm^3hr^{-1}$, product purities of 99.9%.were achieved.

In 1969, Fox *et al* (19, 20, 21) published three papers covering the design and operation of a continuous annular chromatograph. They purified cow heart myoglobin and separated skim milk proteins from lactose and salt using molecular sieve gels. The low throughput inherent in their gravity fed device

led to some operating problems. It proved particularly difficult to obtain uniform flow throughout the entire annulus.

Continuous paper chromatography, using paper cylinders has been described by Solms (22) and others (23, 24).

Sussman (25, 26, 27) constructed a practical system called a continuous surface chromatograph. This system utilised two parallel annular discs. Separation occurs between a stationary phase coated onto surfaces between 50 μm and 150 μm apart. The primary application of this system was in the continuous monitoring and multi-component analysis of gases.

Moskvin *et al* (28) reported on the application of gradient elution chromatography in a rotating annular chromatograph. They worked with sorbent bed heights of 55mm in a column diameter 111mm, annulus width 3.5mm. The feed mixture was fed continuously at a stationary point in a top plate while different composition eluents were introduced simultaneously to effect separation. Continuous separation of calcium and strontium was achieved when making step changes in the concentration of their ammonium acetate eluent, going from 0.5M to 1.8M to 2.7M. Mercury, calcium and cadmium were also separated using eluents ranging from water to 6N HCl.

Moskvin and Mel'nikov (29) replaced a particulate sorbent bed with a sorbent in the form of uniform porous blocks. With a dispersed sorbent they believed the quality of separation was adversely affected by non-uniform packing and the non-uniform flow of solution through the sorbent due to channel formation and the wall effect. The porous blocks were formed by binding trisodiumphosphate with PTFE and then eluting with a 10% solution of ammonium molybdate in 2M HNO_3 to form ammonium molybdophosphate in the pores of the PTFE. The difference in the flow rates through each of 36 exit

positions were not greater than 20% of the average value, indicating that the sorbent block was of uniform porosity. Separation of rubidium and cesium was achieved using eluents of 1M and 5M NH_4NO_3.

Pronin *et al* (30) separated nickel and cobalt ions from solutions of their chlorides with the aid of a rotating annular chromatograph packed to a height 350mm. The annulus width was 4mm and column rotation was $180°hr^{-1}$. Since the device was limited to gravity flow, the components were considerably diluted on passage through the annulus and the throughput was restricted.

At the the Oak Ridge National Laboratory in The United States, work has been carried out for several years on continuous annular chromatography.

Scott *et al* (31) achieved pressurized operation of a rotating annular chromatograph using an air line to provide constant overpressure. The annulus was fabricated from Plexiglas and was 13mm wide and 500mm long with an outside diameter 284mm. The separation of nickel and cobalt from a synthetic process liquor was investigated using a 1M $(NH4)_2 CO_3$ eluent.

Since the initial development of the annular chromatography at ORNL various versions of the apparatus have been constructed and tested. The experimental units varied in diameter from 89 to 445mm with annulus widths varying from 6.4 to 50.8mm and bed lengths of 0.6 to 1.1m (32). One unit was built in stainless steel allowing operating at pressures of up to 150 psi and use of sulphuric acid eluents. These units have been applied to numerous systems including the separation of iron and aluminium in ammonium sulphate-sulphuric acid solution and the separation of hafnium from zirconium in sulphuric acid solution (33).

In a 60cm long, 27.9cm diameter continuous annular chromatograph of annulus width 12.7mm Howard (34) investigated the separation of fructose, glucose and sucrose solutions. He concluded that the industrially significant glucose-fructose fractionation could be performed in an optimally designed chromatograph on a production scale.

Byers and Holmes (35) described sugar separations on a pilot scale device 445mm diameter, 107cm sorbent bed depth and 31.7mm wide annulus. They found that the use of industrial feedstocks from corn and sugar beet sources gave comparable results to those of synthetic mixtures.

2.4 Chromatographic Models

2.4.1 Plate theory of chromatography

A profile as shown in Figure (2.3) is obtained when elution chromatography of a two component sample is carried out on a batch column. The concentration of each component as it is detected at the column outlet is plotted against the time of detection and these concentration-time profiles are called chromatograms. From Figure (2.3) we can recognize two characteristic features of chromatographic separation: differential migration of various components (solutes) in the original sample, and a spreading along the column of molecules of each solute.

Differential migration results from the relative distribution of each different solute between the stationary and mobile phases. This is expressed for each solute by the distribution co-efficient K_{DI} which is defined by:

$$K_{DI} = \frac{S_I}{M_I} \qquad 1$$

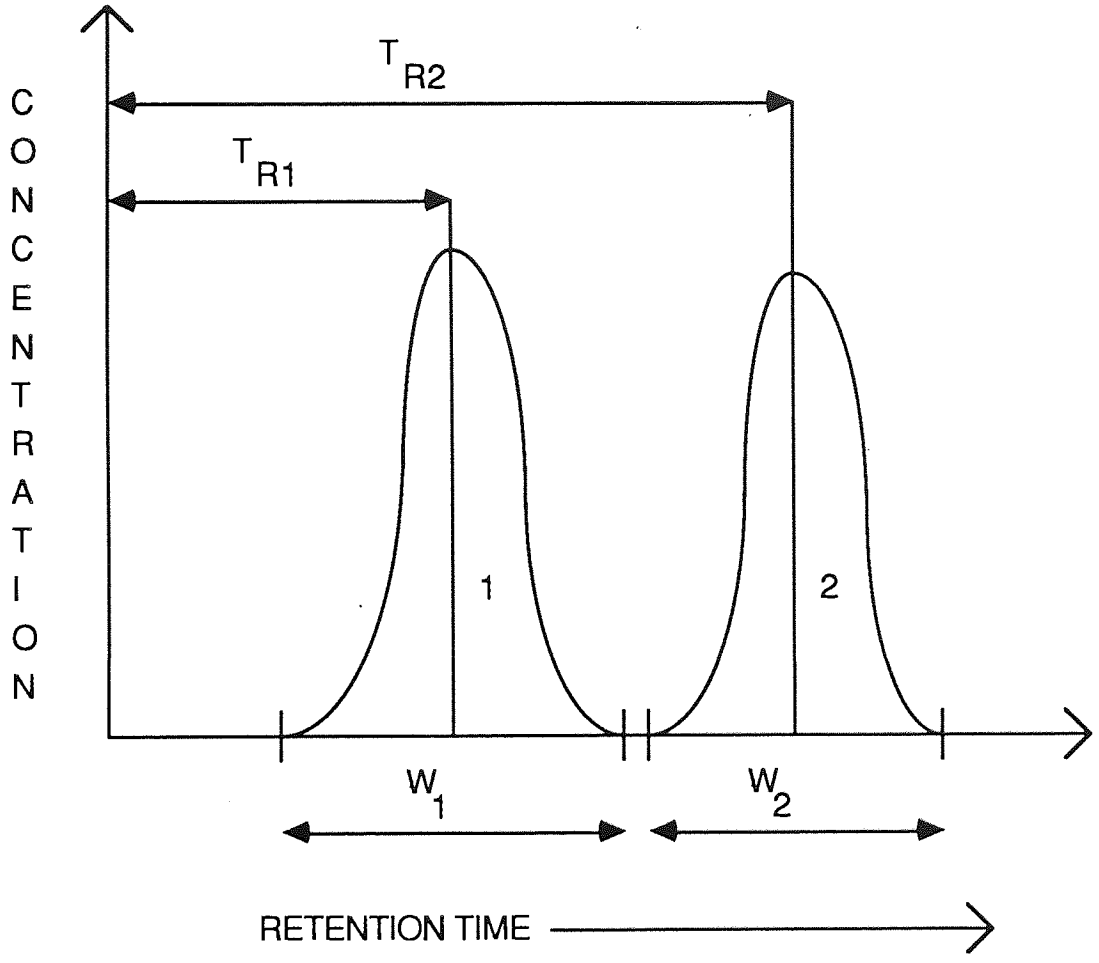

FIGURE 2.3 CHROMATOGRAM FOR THE SEPARATION OF TWO COMPONENTS

where

S_I = Concentration of solute I in the stationary phase

M_I = Concentration of solute I in the mobile phase.

The peak recorded at the column outlet always has a finite width and, although often approximately Gaussian in shape is actually asymmetrical to a greater or lesser degree. In an hypothetical "ideal" column a peak would maintain its initial profile as it migrated. An infinitely narrow injected peak would still be infinitely narrow at the outlet and the height equivalent to a theoretical plate (HETP) would be zero. In real (non-ideal) columns, peak spreading processes operate to broaden the peak as it migrates. Non-ideal peak spreading processes fall loosely into two groups. First, there are those processes which are present in every column and may be described as 'normal' processes. These are axial diffusion, non-equilibrium due to resistance to mass transfer between phases, and spreading due to non-equivalent flow paths in a packed bed. These processes are responsible for the terms in the well known van Deemter (36) expression for HETP and the numerous modifications to this equation that have since been made.

The van Deemter equation can be represented by:

$$HETP = A + \frac{B}{u} + Cu \qquad 2$$

where

A = Eddy diffusion term

B = Longitudinal diffusion term

C = Mass transfer term

u = Mobile phase velocity.

The second group of peak spreading processes depend on the system involved and are best described as 'slow kinetic processes'. Examples are slow desorption from sites of high adsorption energy and very slow diffusion controlled mass transfer between phases. Such processes usually lead to more asymmetrical peaks.

The theoretical plate model represents the column as a finite number of hypothetical well-mixed stages, the number of stages being a direct measure of all normal peak-spreading effects under linear conditions. Linearity implies that the concentration of solute is so small that all factors affecting retention are independent of concentration. A mathematical description of the chromatographic column can be obtained by considering one well mixed stage in which mass transfer occurs between the fluid phase and stationary phase (see Figure (2.5)). Martin and Synge (37) represented the HETP as a unit of column length sufficient to bring the concentration of a solute as it leaves the unit into equilibrium with the average concentration of the solute in the stationary phase throughout that unit. Scott *et al* (31) applied the plate theory to the rotating annular chromatograph. They divided the annulus into a series of equally sized segments arranged circumferentially with each segment consisting of a series of theoretical plates of identical fixed heights. All of the solute was assumed to be in the first theoretical plate at the end of the feed introduction period. The actual chromatographic process begins at the time, (t = O), when a reference segment just leaves the feed zone. Thereafter, the elution sequence occurs and the annular position of the reference, in terms of the stationary feed point, is dependant on time and angular speed of the annulus. Scott *et al* (31) were then able to relate the angular position, with respect to the stationary feed, at which the maximum value of solute concentration at the annulus exit occurs to pertinent process parameters:

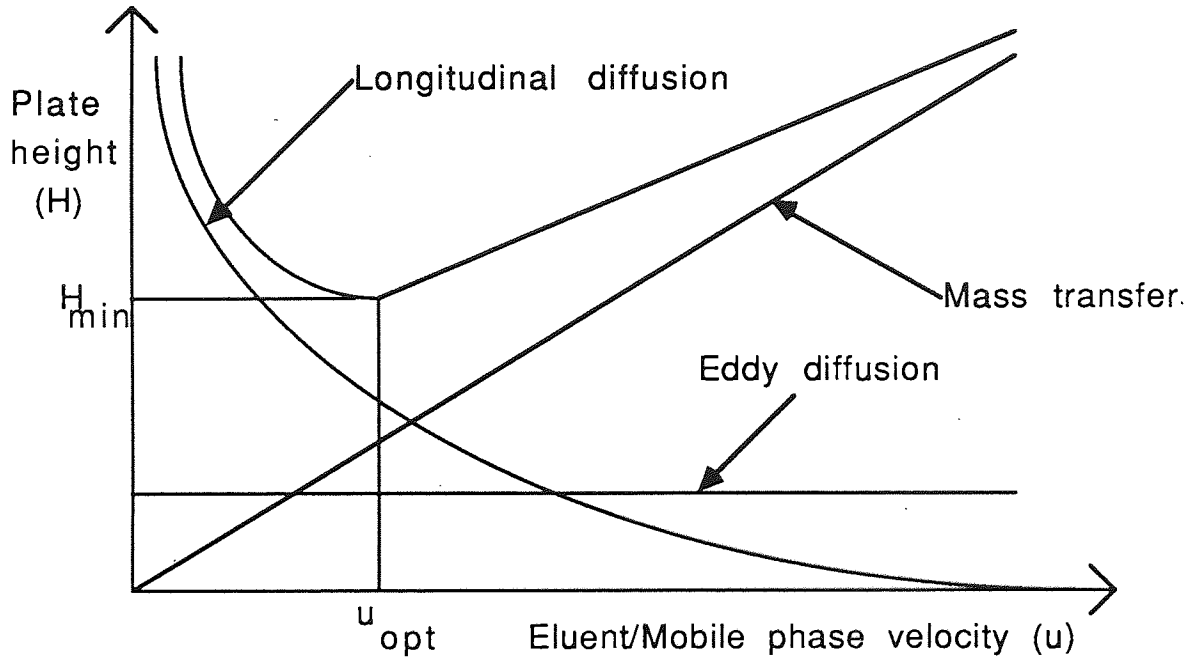

FIGURE2.4 The Theoretical Van Deemter Graph

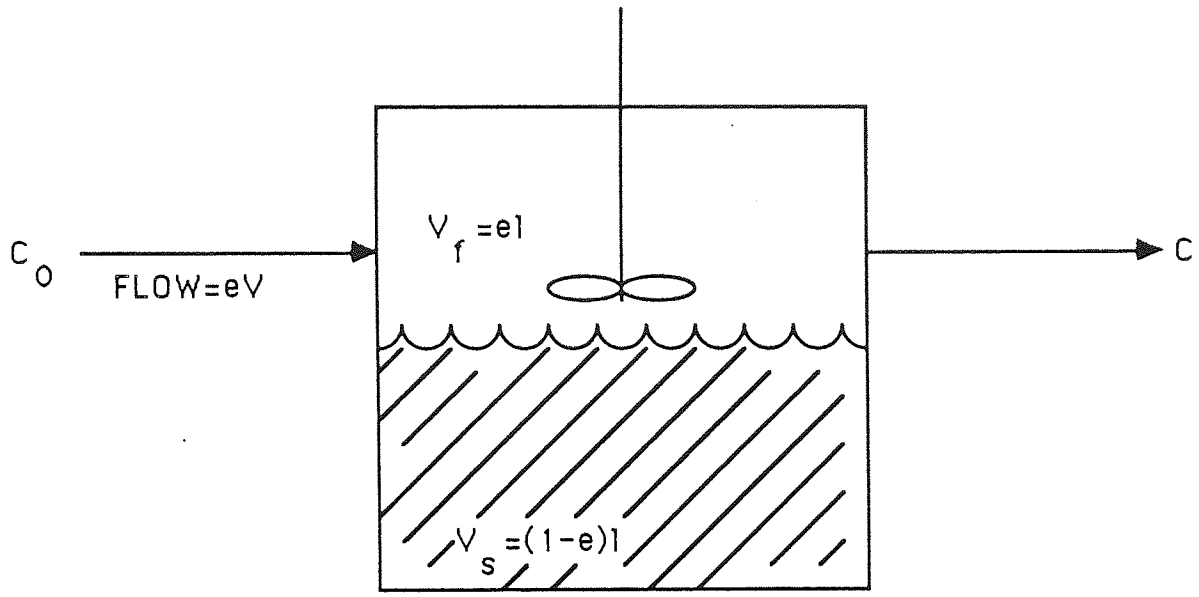

FIGURE 2.5 HYPOTHETICAL EQUILIBRIUM STAGE AS REPRESENTED IN THE PLATE THEORY OF CHROMATOGRAPHY

$$\bar{\theta} = \frac{\omega AL}{u}[e + (1 - e) K_{DI}] \qquad 3$$

where

$\bar{\theta}$ = Elution position (degrees)

ω = Rotation speed, (degrees per hour)

L = Vertical distance from feed to exit (m)

e = Column voidage

u = Mobile phase flow rate (m^3h^{-1})

K_{DI} = Distribtuion co-efficient

In order to establish conditions for separating two or more solutes, both the elution position and the width of the solute bands at the chromatograph exit must be predictable. Referring back to Figure (2.3) the abscissa time, t, can be converted to an angular measurement such as degrees by using the equation:

$$\theta = \omega t \qquad 4$$

where

θ = Angular co-ordinate, (degrees)

t = Time (hours)

ω = Rotation speed, (degrees per hour)

Since t is time from feed injection; θ is the angular displacement from the stationary feed point.

Bandwidths can be expressed as the baseline width of a peak, as the standard deviation of a peak, and so on. Using the former definition, Scott *et al* obtained the following expression for solute exit bandwidth;

$$W^2 = Wo^2 + 16\left[\frac{\omega}{u}\right]^2 HL\,[\,e + (1 - e)\,K_{DI}]^2 \qquad 5$$

where

Wo = Initial width of feed stream, (degrees)

u = Mobile phase velocity (= U/A), (cm s^{-1})

H = HETP, (cm)

W = Bandwidth, (degrees)

U = Mobile Phase Flowrate (cm^3 s^{-1})

A = Annulus Area (cm^2)

Wo can be estimated by:

$$Wo = \left[\frac{F}{U + F}\right] \times 360$$

where

F = Feed flow rate (cm^3 s^{-1})

Being able to predict a solute's elution position (θ) and bandwidth (W) for a given set of operating conditions allows a prediction of the measure of the separation between any two solutes in a feed mixture. The resolution of two adjacent bands 1 and 2 is defined equal to the distance between the two band centres divided by the average bandwidth:

$$R = \frac{\overline{\theta}_1 - \overline{\theta}_2}{1/2\,(W_1 + W_2)} \qquad 6$$

As well as being predictable by the plate theory and the multitude of other mathematical treatments of the chromatographic process, resolutions is a quantitative measure of separation obtainable from experimental chromatograms.

The plate model gives an immediate insight into the chromatographic process but it is the so called 'continuous' models which have been developed that allow for most of the major processes operating in the column.

2.4.2 Continuous Models of Chromatographic Processes

The differential mass balance equations for an element of the chromatographic column provides the starting point for the development of mathematical models to describe the dynamic behaviour of the system.

A batch chromatograph is first considered through which a mobile phase containing concentration c (z, t) of an adsorbable species is flowing (Figure (2.6)). If the flow pattern can be represented as axially dispersed plug flow the differential fluid phase mass balance is;

$$-D_L \frac{\partial^2 c}{\partial z^2} + \frac{\partial}{\partial z}(Vc) + \frac{\partial c}{\partial t} + \left[\frac{1-e}{e}\right] \frac{\partial n}{\partial t} = 0 \qquad 7$$

where

c = Concentration of solute in moles/volume in the mobile phase

n = Concentration of solute on the stationary phase in moles/volume of stationary phase

z = Space variable along the bed

t = Time

V = Interstitial velocity of fluid through the bed

e = Bed voidage

D_L = Axial dispersion co-efficient

Equation (7) involves no assumption about the mechanism of sorption. If there is a finite rate of transport of solute from mobile to stationary phases then this rate is assumed to depend upon the pertinent paramenters of the problem (38).

$$(1-e) \frac{\partial n}{\partial t} = F(c, n, V, e, \text{Solute, Mobile Phase etc}) \qquad 8$$

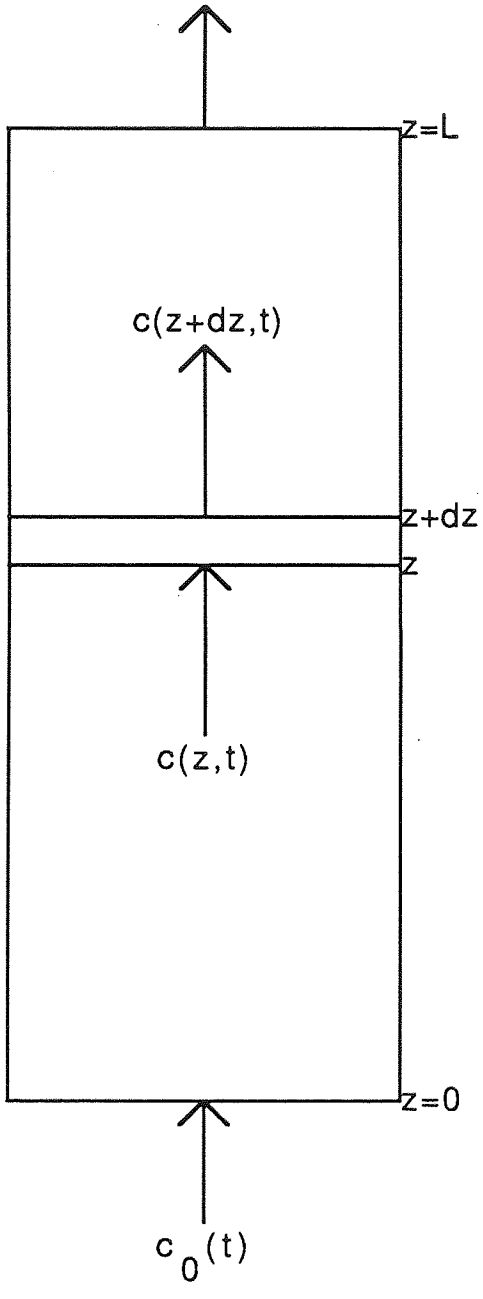

FIGURE 2.6 SIMPLE SHELL BALANCE

Although written as a single equation, the mass transfer rate expression is commonly a set of equations comprising one or more diffusion equations with associated boundary conditions, incorporating the equilibrium constraints to which the mass transfer rate expression must reduce at sufficiently long times.

The equilibrium relation is of the form

$$n^* = f(c) \qquad 9$$

where;

n^* = Equilibrium value of n

and the function f is in general temperature dependent.

For liquid chromatography the term $\frac{c\partial V}{\partial z}$ in equation (7) can be dropped.

Further simplifications lead to a variety of expressions for the concentration front c (z, t).

Numerical solutions have been attempted (39, 40) but it is generally analytic solutions which provide greater insight into the system behaviour. The simplest form equation (7) reduces to is when considering isothermal plug flow where a single chemical species is sorbed from a dilute solution under conditions of local equilibrium (i.e. at each point in the column there is equilibrium between solution and sorbed species). A form of expression originally derived by DeVault (41) then results, which shows how the basic pattern of behaviour of a chromatographic system depends on the form of the equilibrium isotherm, (i.e. equation (9)).

Assuming a linear equilibrium isotherm together with a linearized rate expression and dispersed plug flow, Lapidus and Amundson (42) obtained an analytical solution to equation (7).

Houghton's solution (43) assumed local equilibrium and allowed for non-linear isotherms and also for the effects of axial diffusion.

If one makes a steady state mass balance in a rotating annular chromatograph, ignoring radial gradients, one obtains:

$$\omega \frac{\partial c}{\partial \theta} + \omega \left[\frac{1 - e}{e} \right] \frac{\partial n}{\partial \theta} - D_\theta \frac{\partial^2 c}{\partial \theta^2} = D_Z \frac{\partial^2 c}{\partial z^2} - \frac{V}{e} \frac{\partial c}{\partial t} \qquad 10$$

where;

D_θ = Dispersion co-efficient in the θ - direction.

Wankat (44) noted that batch chromatography is an unsteady state one dimensional process separating a feed mixture on a time basis, whereas the rotating annular chromatograph is a steady state two dimensional process which separates a feed mixture in a spatial direction. If the dimensional translation form time to angular position is made (equation (4)) then equations (7) and (10) are identical if angular dispersion is assumed negligible. As confirmed by Begovich (32), angular dispersion in the rotating annular chromatograph is indeed found to be negligible.

Therefore, any of the numerous solutions of equation (7) can be readily applied to the continuous annular chromatograph.

The discussion so far has been restricted to systems containing only one sorbable species. In practical systems there is more than one solute in the feed mixture. The general principles governing the behaviour of multicomponent systems are similar to those of single-component systems. In linear chromatography the equilibrium relationship for each component is not affected by the presence of other components and the principle of superposition applies. In non-linear chromatography the sorption equilibrium for any particular component is affected by all other components present. The differential mass balance equations for individual components are therefore coupled. This coupling or "interference" between components is the central feature of multicomponent chromatography and the analysis of multicomponent sorption systems. The equilibrium theory of multicomponent sorption systems was first developed by Glueckauf (45). More general and complete treatments were developed by Rhee, Aris and Amundson (46) and by Helfferich and Klein (47).

CHAPTER THREE
PROPERTIES OF MOLASSES AND SUGARS

3 Properties of Molasses and Sugars

3.1 Molasses Formation and Composition

Molasses is the final syrup spun off after repeated crystallizations in the extraction of sugar. It is so low in purity that further crystallization from it is impractical. It is therefore discarded from the sugar end, carrying with it all of the non-sugars of the beet not eliminated by the juice purification process, the soluble impurities added in processing and the degradation products formed during processing. It also carries about one and one-half kilograms of sugar with each kilogram of impurities. It represents therefore an important loss of extraction, amounting to 12-16% of the sugar in beets (48). A typical approximate analysis of beet molasses is: dry substance 74-78%; sucrose 50-52%; nitrogenous compounds 12-13%; nitrogen free extract 9-10%; and ash 11-12%.

Betaine is the most abundant nitrogenous compound found in molasses, approximately 3-4% in British molasses. Table 3.1 indicates the approximate percentages of each of the main types of compounds found in beet molasses. The main differences between cane molasses and beet molasses are the high percentage of nitrogen compounds found in beet molasses and in terms of sugar content, beet sugar has a relatively lower percentage of reducing sugars present.

The sugar in the molasses is the largest single loss from the beet sugar refining process. This large loss in extractable sugar has prompted study and effort since the beginning of the industry to find means of reducing it. More complete exhaustion of the final syrups can be achieved by boiling to high density, cooling to low temperature and allowing longer periods of time for crystallization. However, as the density of raw molasses increase the viscosity

rapidly increases, making separation of crystallized sugar slow and unsatisfactory. Molasses can then be defined as a syrup from which no more appreciable amounts of sugar can be recovered by crystallization at economic cost.

Table 3.1
Composition of Beet Molasses

Dry Matter		74-78%
Sucrose		50-52%
Reducing sugars	0.2-1.5%	
Raffinose	0.5-2.0%	
Organic non-sugars of which:		
Nitrogen compounds	6-8%	
which include		
Betaine	3-4%	
Glutamic Acid	2-3%	
Non nitrogen compounds ie. Organic Acids, Lactic Acid, Malic Acid, Acetic Acids, Oxalic Acids and Hemicelluloses	6-8%	
Sulphated Ash		10-12%
of which:		
Sodium Na^+	0.3-0.7%	
Potassium K^+	2.0-7.0%	
Calcium Ca^{2+}	0.1-0.5%	
Chlorine Cl	0.5-1.5%	
Phosporous P	0.02-0.07%	
Others	5.5%	

3.2 Uses of Molasses

Molasses is a valuable by-product of beet sugar manufacture.

In order to recover sugar from molasses one can choose between two possibilities: one can either convert the sucrose component of the molasses into water - insoluble derivatives, separate them from the mother liquor by filtration and recover the sucrose after decomposition of the derivatives, or one can remove the non-sugar component of molasses through suitable chemical or physical methods so that a more or less pure sucrose solution can be recovered (5).

The Steffen process which utilizes the precipitation of sucrose as tricalcium saccharate has gained importance especially owing to the development of continuous processes, for example by Spreckels Sugar Division of Amstar Corporation (49).

Compared with sugar recovery from molasses by precipitation, the second method, ie. the removal of non-sugars, has been investigated rather intensively in the recent past. Some of these processes can reduce the amount of molasses produced or prevent its production altogether by removing a part or all of the non-sugars from the juices. Other processes which replace the non-sugars with less melassigenic ones, eg. the Quentin Process (50), increase the recovery of sucrose by decreasing its solubility. All of these processes work with ion-exchangers and so have the handicap of waste water disposal. Processes working according to the principle of ion exclusion as well as the chromatographic process developed by Südzucker (51) are better off in this respect. Gross (52) reported on the development of ion exclusion in 1971 and since then, as reported by Schneider and Mikule (53), an ion exclusion process has been developed to industrial scale.

For the occasions where sugar is not recovered from molasses, the molasses is in the main used for cattle feeding, either directly or in mixed feed production. Because of its high content of sugar and certain nitrogenous constituents, molasses is also a valuable raw material for the fermentation industries.

3.3 The Inversion of Sucrose in Beet Molasses

Sucrose inversion is defined as the hydrolysis of sucrose, a disaccharide, to form invert sugar, an equilibrium mixture of the two monosaccharides, fructose and glucose. The hydrolysis (or inversion) can be carried out either by acid hydrolysis, where the sucrose solution is mixed directly with mineral acids, or by hydrogen ion resin treatment where the sucrose solution is passed through a cation exchange resin in the hydrogen form, which allows continuous sucrose inversion, or by using enzyme hydrolysis.

$$\underset{\text{(SUCROSE)}}{C_{12}H_{22}O_{11}} + H_2O \longrightarrow \underset{\text{(FRUCTOSE)}}{C_6H_{12}O_6} + \underset{\text{(GLUCOSE)}}{C_6H_{12}O_6}$$

$$\underset{\text{INVERT SUGAR}}{\longleftrightarrow}$$

The terms invert or inversion are derived from the changes which occur in the optical rotation of sugar solutions (54), ie. invert sugar rotates polarized light in a direction that is opposite to that obtained with sucrose.

In this research,the inversion of sucrose in beet molasses was carried out using the enzyme invertase. The inversion took place at British Sugar Research Laboratories at Norwich where they had the equipment to invert the molasses in large batches.

The concentration of raw molasses is approximately 78% w/w total solids or 78 Brix. The inversion of sucrose in this molasses could not be carried out because of the high concentration of the total solids. Thus the molasses was diluted using de-ionised water to approximately 51 Brix before the inversion. The inverting molasses was left stirring for 17 hours and analysed to ensure complete inversion. To prolong storage life it was necessary to concentrate the inverted molasses to up to 65 Brix to prevent microbial growth.

3.4 Uses of Fructose

Fructose is established as a substitute to sucrose in beverages as well as various diabetic food products. Fructose can also be used as a raw material in the industrial manufacture of flavours and as a flavour enhancer in meat dishes.

Fructose is a natural sugar without any toxic properties, and has traditionally been used as an alternative to glucose in infusion therapy for patients with reduced tolerance to intravenous glucose. Fructose is 1.8 times sweeter than sucrose in cold solution and has a calorific value slightly lower than sucrose (3.7 Kcal. kg^{-1} compared to 4 Kcal. kg^{-1} for sucrose). The solubility of fructose in water is 15% higher than that of sucrose and fructose causes less dental plaque formation than sucrose according to some medical statistics.

The usage of fructose is expanding rapidly and though it is unlikely to replace sucrose completely it should become more favourable when new economical production methods have been developed and utilised. The separation efficiency and low energy intensiveness of chromatography favour its application in this field.

3.5 Chemistry of Glucose and Fructose

Carbohydrates have the general empirical formula $(C\ H_2O)_n$, where $n \geq 3$. They are divided into three basic categories:- Monosaccharides, Oligosaccarides and Polysaccharides.

The monosaccharides usually have between three and nine carbon atoms and contain only one aldehyde or ketone functional group or are derivatives of molecules that do. The oligosaccharides are generally two to ten monosaccharides linked together by the formation of glycosidic bonds. These are subdivided into disaccharides (e.g. Maltose and sucrose), tri-saccharides (e.g. raffinose) etc., depending on the carbohydrate units they contain. Carbohydrate polymers containing more than ten monomeric units are called polysaccharides and can have molecular weights of many million. Starch, glycogen and cellulose are examples of polysaccharides.

Glucose is the most common monosaccharide found in fruits, honey and other living material. Fructose is another common monosaccharide found frequently in fruits with glucose. Glucose is dextrorotatory with a specific rotation of $(\alpha)^{20}D = 52.7°$ in water while fructose is strongly laevoratory with $(\alpha)^{20}D = -132.2°$ (55). Thus glucose is often referred to as dextrose and fructose as laevoluse.

Both glucose and fructrose exist as different anomers, the α- and β- forms as shown in Figures (3.1) and (3.2). Such cyclic forms of sugars are called pyranoses. Except at temperatures over 60°C, the β - D - form of fructose makes up the majority of a fructose equilibrium mixture. Glucose equilibrium mixtures are relatively unaffected by temperature and the approximate composition is 40% α - D - form, 60% β - D - Form (56). The different fructose forms are particularly important when applying chromatography to separate glucose from fructose. The mechanism of this separation will be discussed in Chapter 4.

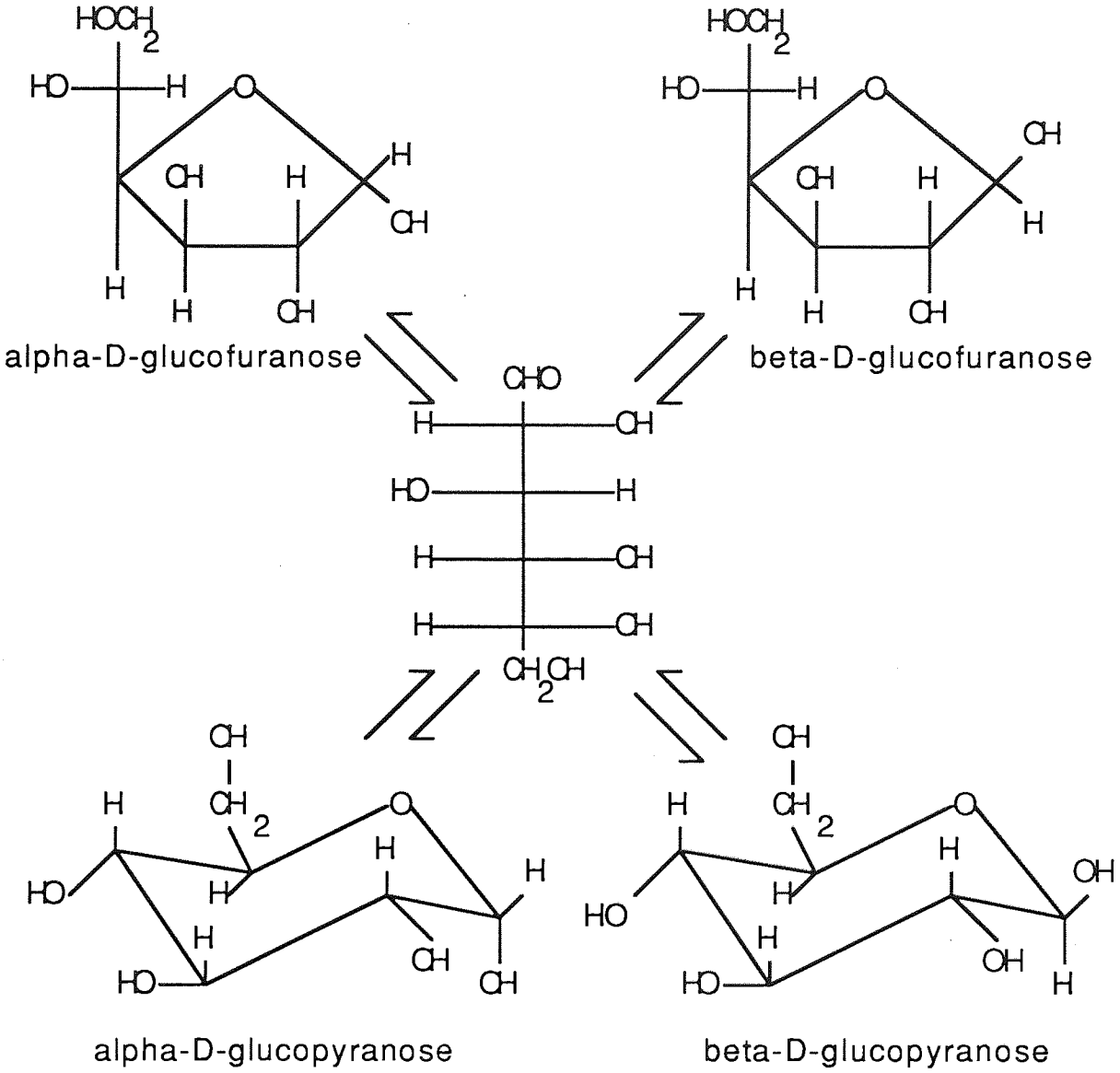

FIGURE 3.1 ANOMERS OF GLUCOSE

FIGURE 3.2 ANOMERS OF FRUCTOSE

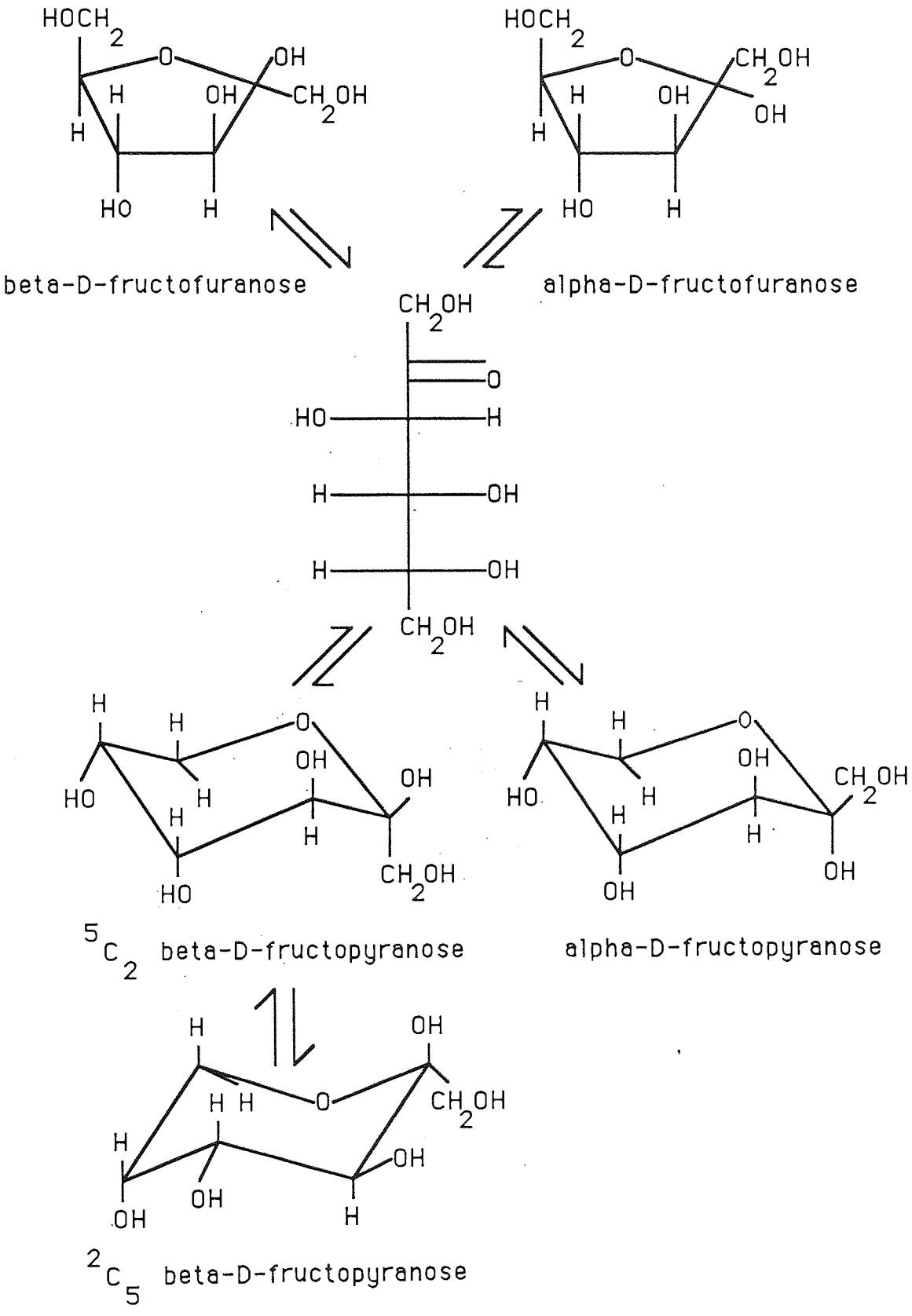

CHAPTER FOUR
EXPERIMENTAL DETAILS

4 Experimental Details

4.1 Experimental Apparatus

4.1.1 Introduction to Equipment Design

The rotating annular chromatograph was based on the design of Scott *et al* (31). The outer shell of the annulus was a glass pipe supplied by Schott Process Plant Ltd, Stafford with an internal diameter accurate to ± 4.0 mm. The longest pipe available in the diameter required was selected and this was 1500 mm long. It was decided to use glass so that observation of the chromatographic bed could be made. This facility proved extremely useful when it was seen how easily air could enter the bed. Ingress of air upsets the uniformity of the bed and if unchecked can lead to a deterioration of the resin beads themselves. The glass shell also allows observation of any microbial growth in the bed. This can be a problem when dealing with sugar solutions and if not prevented micro-organisms can clog the equipment.

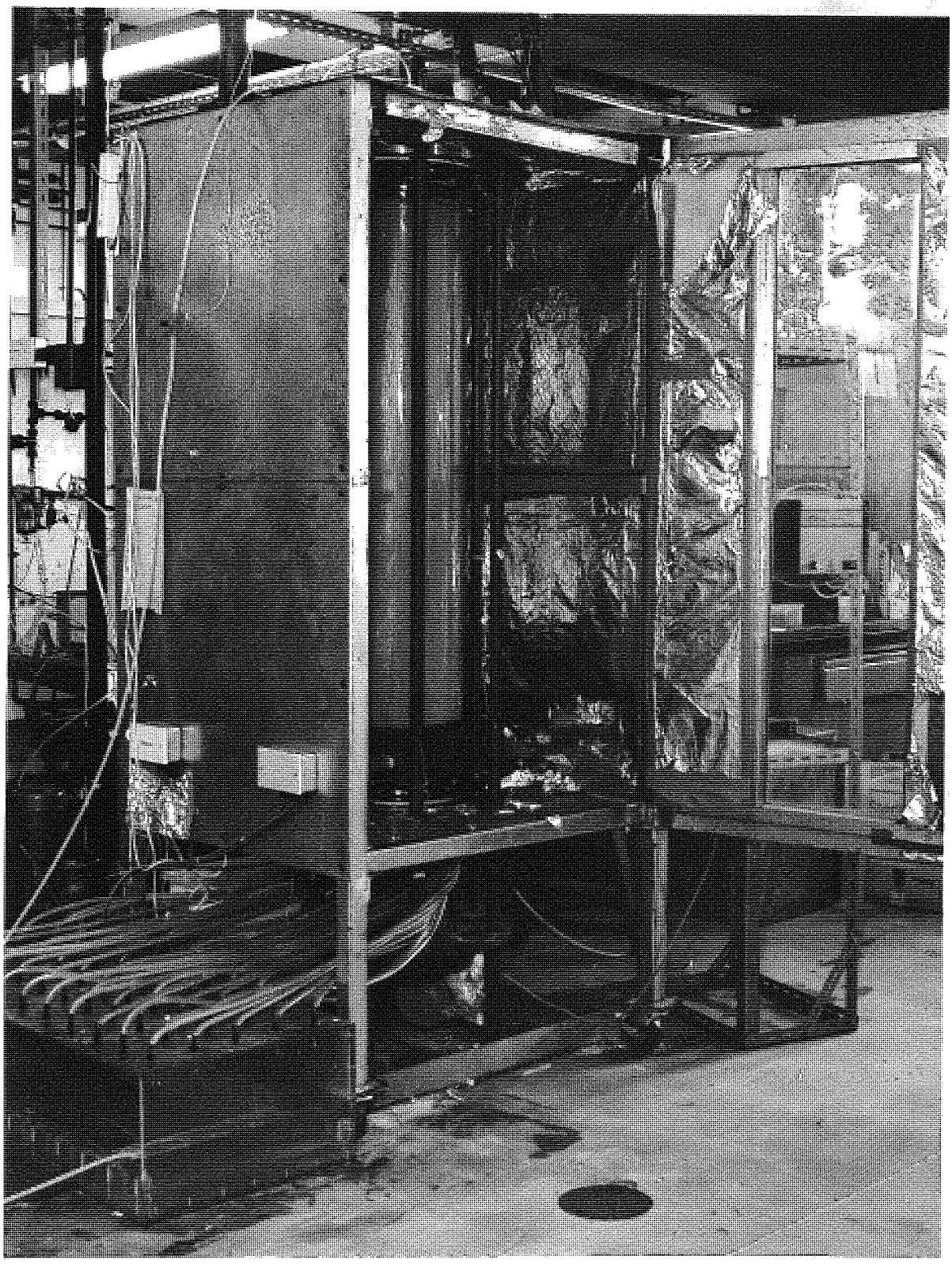

PLATE A

Photograph of Rotating Annular Chromatograph

Key to Figure 4.1

A	Glass Outer Column
B	Inner Stainless Steel Column
C	Upper Stainless Steel Flange
D	Lower Stainless Steel Plate
E	Stainless Steel Blanking Flange
F	Inlet Distributor
G	The Outer Framework
H	Feed Pipe
I	Liquid Level Controller
J	Pressure Relieve Valve
K	Overflow Pipe
L	Pressure Gauge
M	Manual Relief Valve
O	Polypropylene Product Collector
P	Drive Pulleys and Belt

Figure 4.1 Drawing of Chromatograph

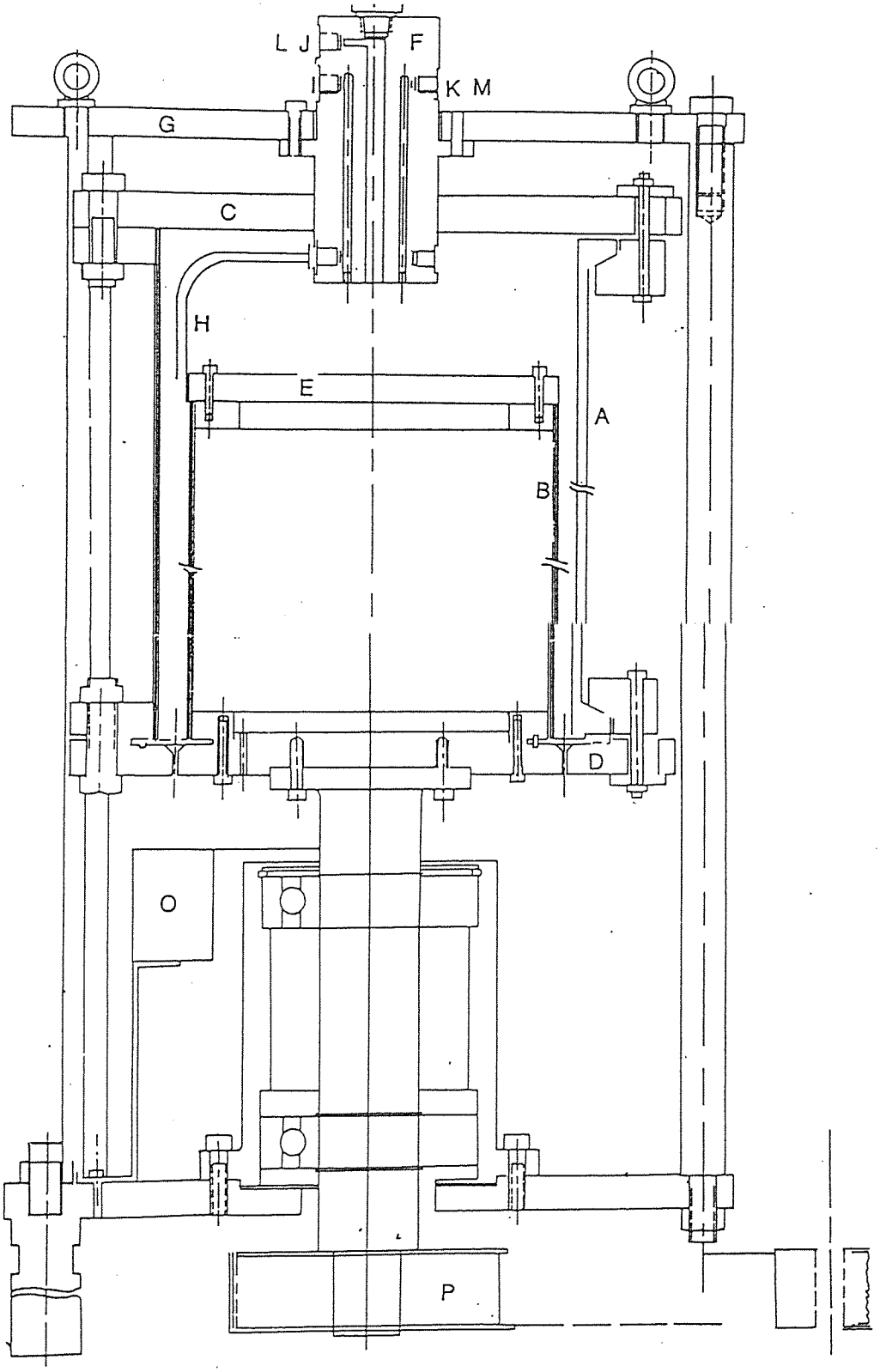

It was also useful to be able to observe the bed after packing the annulus. A well packed column would be one where horizontal uniformity was achieved and this was observable in the stratification of the resin bed.

A problem with using glass was its inability to withstand high pressures. The glass pipe chosen had a wall thickness of 8.0 mm ± 1.5 mm and was rated to a safe maximum working pressure of 101 kNm^{-2}.

4.1.2 The Annulus

The Annular Chromatograph was constructed from an outer borosilicate glass shell 297 mm internal diameter and 1.5 m length (Plate 1). This enclosed a type 304L stainless steel pipe (RGB Stainless Ltd., Smethwick) of outside diameter 273 mm (Figure 4.1B) and 1.4m in length to form an annulus. Two 25 mm thickness, type 316L stainless steel flanges (Figure 4.1C, D) were used to support the pipes at the top and bottom. The inner stainless steel pipe (B) was blanked off at its upper surface by a flat stainless steel flange (E). The inner pipe was 1.4 m long and so provided a headspace of 10 cm at the top of the chromatograph. The headspace gave sufficient height to include a liquid level controller and a central liquid distributor.

4.1.3 The Distributor

The upper stainless steel flange (C) had a centrally placed circular hole (9 cm diameter) in which the stainless steel inlet distributor was fitted. The distributor was held stationary by the outer framework which enclosed the apparatus (G). Two nitrile '0' rings were fitted into grooves around the distributor, and these formed a seal as well as the bearing on which the upper flange turned.

The distributor allowed the influx of de-ionised water as eluent and feed solution via various ports drilled through it. In the original design the feed pipe was fixed to the distributor in such a way that should the resin bed shrink too severely during operation the feed could possibly be fed above the bed and so be mixed with eluent leading to a complete breakdown in operation. An adjustable feed pipe was therefore devised which was again housed in the distributor but in such a way that it could be manoeuvred externally allowing the operator some flexibility as to the exact height of the feed nozzle. The feed pipe could be moved up and down within the bounds imposed by the distance between the upper stainless steel flange (C) and the underside of the distributor (F) through which the pipe was fed.

The feed pipe (H) was made of thin walled 5 mm 0.D stainless steel tubing and could be positioned to feed into the bed about an inch below the top of the bed. The distributor also housed the probes for a float liquid level controller (I), a pressure relief valve (J), an overflow pipe (K), a pressure gauge (L) and a manual valve for releasing the pressure built up in the apparatus during a run (M).

4.1.4 The Lower Plate (D)

The lower stainless steel flange which supports the two annulus-forming, concentric pipes contained one hundred exit holes evenly spaced beneath the centre of the annular space. In the original design each 3.2 mm diameter exit hole was counter-bored to a diameter of 7.0 mm and depth 3.0 mm. Into each counter-bore a porous polyethylene disc (Aston Manufacturing Co Ltd, Middlesex) was pressed. The polyethylene had a pore size 60-90 μm which was small enough to retain the resin bed whilst allowing the passage of liquid without creating prohibitively high pressure drops.

Following the completion of Thirkill's (75) experimental work on the chromatography the lower plate was modified. In the original design the ratio of exit hole area to annulus area was only 7.5% which meant that liquid reaching the base of the annulus was more likely to contact a surface than pass through an exit hole. Such liquid would be forced circumferentially and radially around the annulus until locating an outlet. During this traversing separated liquid streams are remixed leading to a deterioration in the performance of the equipment. To alleviate this problem of remixing, the ratio of exit hole area to annulus area was increased. The geometrical restrictions of a 100 holes on a circle of pitch 285 mm meant that the holes could not be widened to the width of the annulus without causing overlapping of holes. Nevertheless, by machining a V-groove into the lower plate the annulus width at the exit was brought down from 12 mm to 7 mm. At the exit were drilled through one hundred 7 mm diameter holes giving a ratio of hole area to annulus area of 61%. In place of the polyethylene discs a complete polyethylene ring was cut which fitted firmly into the groove, above the exit holes.

4.1.5 Auxiliary Equipment

4.1.5.1 The Motor Drive

The rotation of the chromatograph was achieved by means of an electronically controlled, variable speed DC motor (DC right angle geared motor, DRPM805A Type - Normand Electrical Co Ltd, Aylesbury) linked to a DC motor speed controller (Neco System 3, 3050 case version IP42 - Normand Electrical Co Ltd). A reduction in gearing was achieved by means of a toothed belt and two pulleys (J H Fenner and Son, Birmingham). The chromatograph rotated about two 150 mm diameter ball bearings situated beneath the chromatograph.

4.1.5.2 Temperature Control

The equipment was surrounded by an air bath (1.66 x 1.02 x 0.92 m) which was designed to operate at temperatures of up to 70°C. The temperature was controlled accurately by means of a DU82A temperature controller (Diamond H Controls Ltd., Norwich). Four 1kW heating elements (Eltron Ltd., London) and a fan (Woods of Colchester, Essex) were used to distribute the heat evenly. This oven construction provided useful protection should the glass column shatter and it had a perspex screen mounted in the door to allow observation of the annulus during a run.

De-ionised water was used as eluent and could be transferred to a stainless steel eluent storage tank either directly from the de-ioniser (The Elga Group, Bucks) or through an immersion heating vessel. A Techne TE-7 Heater (Techne, Cambridge) was used in the eluent storage tank to maintain the correct temperature of water entering the chromatograph.

Feed solutions could be preheated using an electrically heated heat exchanger.

4.1.5.3 Liquid Level Control

Ion exchange resins have to be kept moist to perform efficiently. When the chromatograph is not in experimental use, if the top of the column is open to the atmosphere the water in it will drain away and air will enter the bed. A float liquid level control system was used to regulate liquid height above the bed when the apparatus was not in use. The system operated such that on the liquid draining to a low level above the resin bed a pump was activated and de-ionised water was pumped into the column until a high level float was tipped which in turn switched off the pump.

4.1.5.4 Product Collection

Collection of product fractions was achieved using a stationary polypropylene annulus (O) which housed fifty 10 mm diameter holes. This was attached to the bars on the supporting structure of the annulus by 3 moveable clamps. Fifty lengths of PVC tubing were attached underneath the collector and these passed to a large perspex tank containing fifty 150cm^3 sterilen sample bottles (Appleton Woods, Selly Oak).

4.2 Analysis

4.2.1 Introduction to Analytical Procedures

This section describes the analytical equipment which has been used in this project. Analysis was carried out quantitatively on samples collected from the fifty collection points.

4.2.2 High Pressure Liquid Chromatography (HPLC)

4.2.2.1 HPLC System Description

The sugar composition and concentration in a sample were determined using HPLC. The HPLC analytical system shown in Figure (4.2) consisted of:

- A Bio-Rad 1330 Pump (Bio-Rad U K Ltd, Herts).
  This pump employs a two piston arrangement which operates out of phase by 180° thus minimising pulsations;
- A Bio-Rad column heater;
- A Bio-Rad differential refractometer type 1750;
- A Talbot ASI-3 Autosampler (Talbot Instruments Ltd, Cheshire);
- A Spectra-Physics Integrator Type SP4270 (Spectra-Physics UK Ltd, Herts);
- An Isomantle and a Baird and Tatlock (BDH Chemicals Ltd, Warwickshire) Temperature Controller was used to degas the eluent;
- An Anachem (Luton, Beds) debubbler was used to trap any air bubbles in the eluent delivery tubing;
- A 30 cm long by 0.78 cm diameter Aminex HPX-87C (Bio-Rad UK Ltd) Analytical column. The Aminex column was packed

with an 8% divinylbenzene cross-linked resin in the calcium form. The particle size was 9μm and the maximum pressure and temperature were 1500 psi and 85°C respectively. The pH range for the column was from pH 5 to 9.

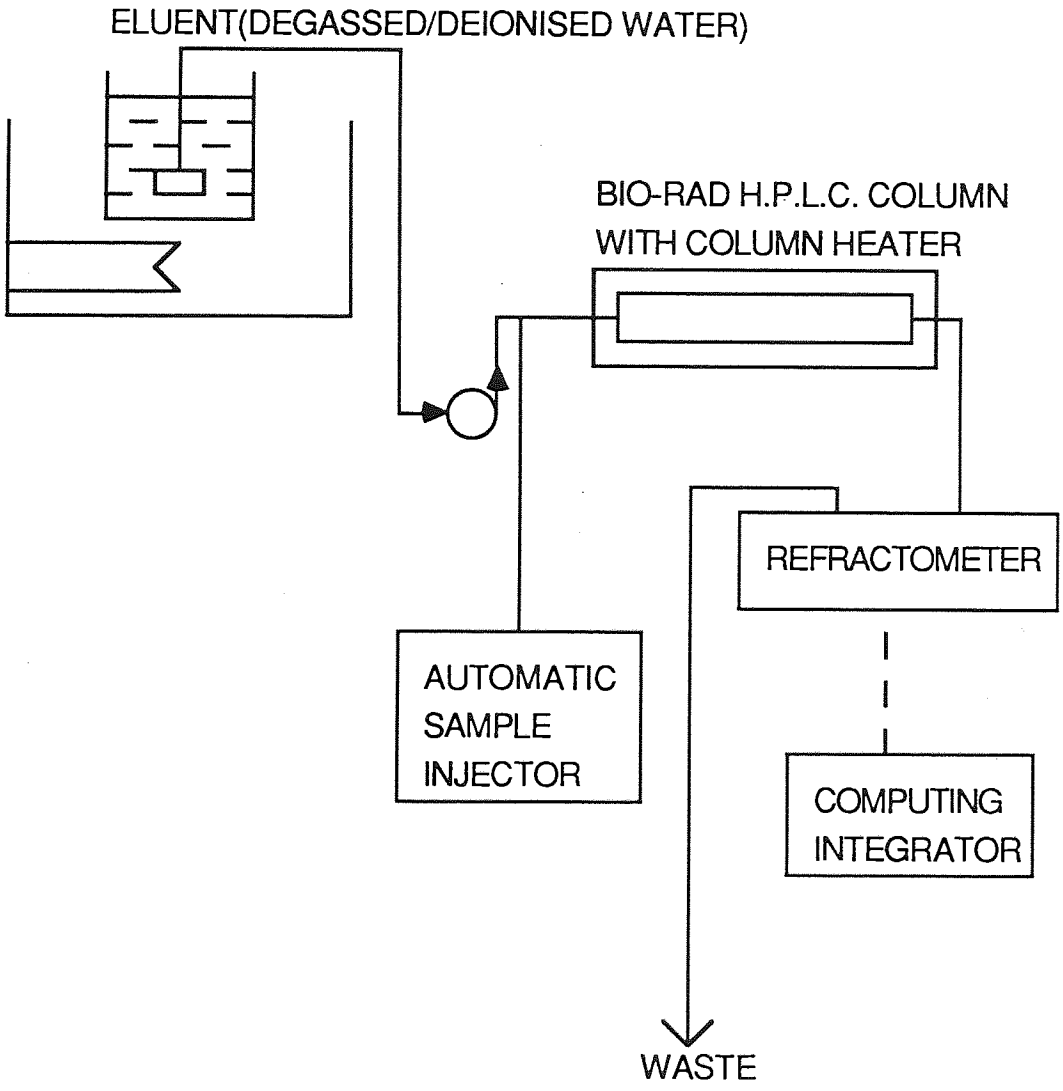

FIGURE 4.2 THE ANALYTICAL H.P.L.C SYSTEM

4.2.2.2 HPLC Operation

A 2 cm^3 sample was collected in a syringe and filtered through a 0.45 μm Gelman Filter (Brackmills) into 2 ml sample vial (Chromacol Ltd, London). A turntable on the autosampler could accommodate 60 of these vials.

By selecting the required sample, inject, analysis and delay times using the appropriate digital switches the autosampler was able to conduct the analysis of the required number of samples and was often left to do this overnight. A 0.02 ml sample loop was filled with a sample taken from a vial by a syringe and the contents of the sample loop was then flushed onto the Aminex column by de-ionised water flowing through the system at 0.5 ml min^{-1}. The components in the sample were resolved in the Aminex column and detected at the column outlet by the refractometer. Refractive index (R.I) is a universal property of all substances. Bio-Rad's R.I monitor measured the differential refractive index between a pure solvent and solutes in low concentration. An integrator socket on the refractometer's rear panel provided a 1 volt full scale output to the spectra-physics integrator. The integrator processed the R.I data and gave a sample chromatogram where individual components were identified by their retention times and component concentrations were determined by the areas under the chromatograph peaks.

4.2.3 Other Analytical Procedures

REFRACTIVE DRY SUBSTANCE (RDS)

The RDS of a sample is the percentage total solids in the sample on a dry basis and was determined using a refractometer (Bellingham and Stanley Ltd, London).

A shaded sodium lamp was used to eliminate any extraneous light. Water at 20°C was circulated through the prism jackets. Drops of the sample were placed on the lower face of the prism and the two prisms brought together slowly and clamped. The prism was then rotated until the edge of the shadow passed exactly through the cross-wires when viewed through the eyepiece. This gave a reading in degrees on the vernier scale. Tables were then used to obtain the refractive index of the sample. Further tables gave a relationship between the refractive index and the RDS values. The prisms were then cleaned and dried before re-use.

CONDUCTIVITY

Sample conductivity was a measure of the ionic matter in the sample. An alpha 800 digital conductivity meter (Aqua Scientific Ltd, Kent) with a A5005 glass flow through cell was used. The glass cell housed a pair of electrodes and was filled with a sample from a 2 ml syringe. The conductivity of the sample was measured in microsiemens.

COLOUR

Colour absorbance of a sample was measured using an ultra-violet spectrophotometer set at 420 nm wavelength.

4.3 Separation System

4.3.1 Introduction to Ion Exchange Resins

Ion exchange resins perform efficiently in a variety of applications in part because of their variable properties - including matrix, chemical type, functional group, cross-linkage, ionic form, and particle size.

Despite their diversity, ion-exchange resins do have certain properties in common. They consist of an insoluble porous lattice with attached ionic functional groups, and are available in the form of beads or, more rarely, granular particles. Resins also have an ionic form, an exchangeable counterion opposite in charge to, and associated with, the functional group.

In an ion exchange procedure, the counterions are replaced by sample ions that have the same charge and which are, in turn, bound to the functional groups. In addition to true ion exchange, other interactions can take place between the solutes and the resin which may supplement the ion exchange interaction or may be used in place of ion exchange to separate either ionic or non-ionic species.

The separations of sugars from polymeric and ionic materials and from each other on an industrial scale generally take place according to the following three main systems. (On a laboratory scale sugars may also be separated by additional chromatographic methods but these are not used on the industrial scale.)

4.3.1.1 Molecular Sieving

The porous matrix of an ion-exchange resin acts as a molecular sieve. It excludes molecules too large to enter the pores and retards the migration through the resin bed of those molecules capable of entering the pores, with the larger eluting first. For example, in the treatment of beet molasses the raffinose molecule elutes before the sucrose and the reducing sugars elute after. Similarly, if the 'cross-linkage' of the resin is controlled to the right degree the coloured compounds are excluded from the bead while the sugar molecule enters it. Betaine penetrates even further into the bead and is one of the last components to be eluted.

4.3.1.2 Ion Exclusion

Ion Exclusion, while utilizing an ion-exchange resin to effect a separation of both ionic and non-ionic materials does not involve a true exchange reaction.

Again, if one considers the separation of beet molasses. The ionizable compounds, such as sodium and potassium salts, amino-acids etc are excluded from the resin because of the Donnan Membrane Effect (57). Ionic substances in equilibrium with the resin will tend to have a higher concentration in solution, external to the resin bead, than that of the liquid phase inside the bead (58). The non-ionic substances will have the same concentration, both external and internal or perhaps greater internal concentration due to adsorption. If an impure sugar solution is contacted with the resin in the salt form, the sugar concentration inside will be the same as or greater than outside, but the ionic impurities will be less inside than outside. If the beads are then eluted with water, purification will have been

accomplished relative to ionic materials, even though the molecular size of the ionic compounds is smaller than the non-ionic sugar.

4.3.1.3 Ligand Exchange

In Ligand exchange chromatography, a metal which has been bound to a cation exchanger is used in turn to bind ligands.

Separation of glucose and fructose (polyols with five hydroxyl groups per molecule) is by ligand exchange. Ligand exchange occurs when water molecules held in the hydration sphere of calcium ions with the resin are exchanged for one or more hydroxyl groups of the polyol. A weak coordination complex is formed whose stability increases as the availability of hydroxyl groups increases. Separation will occur if one polyol provides more stable sites for ligand exchange. Fructose as compared to glucose has hydroxyl groups positioned to facilitate formation of complexes with the calcium. It was reported by Charley (59) that calcium ions and also barium, magnesium and strontium ions form soluble compounds in aqueous alkaline solutions with fructose, galactose, arabinose, maltose and lactose. According to Angyal's (60, 61, 62, 63) hypothesis only the β-D-Form of fructose has an axial-equatorial- axial hydroxide group arrangement required to complex with cations.

4.3.2 Resin Specification

The specification of ion exchange resins for industrial scale chromotographic separation is normally a compromise determined by conflicting factors, and depends on the particular mechanism of interest.

For industrial separations, strongly acidic cation exchangers are preferred to anion exchange resins because the latter are more expensive, of lower thermal and chemical stability, more easily fouled or poisoned, and more likely to contaminate food grade products.

The main parameters specified are the cross-linkage, particle size distribution, and ionic form used.

4.3.2.1 Cross Linkage

Generally specified as percent divinylbenzene copolymer (% DVB). The higher the % DVB the lower the porosity of the resin. A high cross-linkage gives good physical strength, minimal volume changes in service (all resins swell or shrink to some extent with changes in ionic form or when immersed in solutions of different concentration), and a high ionic concentration for efficient ion exclusion,. A low cross-linkage gives better diffusion into the beads. The cross-linkage determines which components will be absorbed, and which excluded, by the molecular sieve effect. Resins for industrial scale chromatographic processes generally contain 3-6% DVB, compared with 8% DVB in typical resins for ion exchange processes, and as much as 20% DVB in the physically strong macroporous type resins.

4.3.2.2 Particle Size

For a given flowrate, the pressure drop over a chromatographic column decreases with increasing particle size. The attainable resolution increases with decreasing particle size and with narrower size distribution ranges.

The resins used in industrial scale separations generally have a mean aperture in the range 300-500 microns.

4.3.2.3 Ionic Form

This has a marked effect on separation by ion exclusion or specific adsorption mechanisms.

The separation of fructose from glucose requires the resin to be in the alkaline earth metal form, normally calcium. Fructose, as compared to glucose, has hydroxyl groups positioned to facilitate formation of complexes with the calcium.

On the other hand, sucrose is separated from ionic impurities in beet molasses by ion exclusion on resin in the alkali metal form, normally sodium, and any exchange of calcium onto the resin in service causes markedly poorer separation.

4.3.3 Treatment of Ion Exchange Resin

4.3.3.1 Packing Technique

The difficulty in obtaining a uniformly packed bed has been one of the main reasons for the slow development of large scale chromatography. This difficulty should, however, not be exaggerated. Since the annular chromatograph rotates with respect to the collector, its composition and other properties must be constant within any cross section perpendicular to the direction of flow. In the direction of flow, however, the porosity and flow resistance as well as the nature of the sorbent may be allowed to change.

To obtain maximum uniformity of the annulus, the column was completely assembled except for the top plate. Rotation was started and the packing was poured in a continuous stream at a fixed point into the annulus.

4.3.3.2 Unpacking the Column

Resin and water as a slurry was drawn through an 8 mm polypropylene tube, the other end of which was attached to a side arm on a venturi. Mains water was passed through the venturi creating a vacuum at the side arm which drew off the resin slurry.

4.3.3.3 Backwashing the Resin

Backwashing was required after several months operation because fines and debris from the feed or eluent accumulate on the resin bed so that the separation efficiency of the column gradually decreases.

One possibility was to carry out the backwashing in a separate vessel. For the rotating annular chromatograph however a backwash ring was manufactured.

The ring was constructed in two halves to facilitate assembly underneath the base plate. Made out of polypropylene the ring encased the 100 exit holes and was sealed against the base plate by two '0' rings. The two halves were sealed together using a silicone sealant. Allen screws attached the ring assembly to the base plate and were also used to pull the two haves together.

Four 1/4" BSP Ports were tapped on the ring to accommodate CK - 1/4" - PK4-KU type Festo Plastic Fittings (Festo Pneumatics Ltd, West Bromwich, West Midlands) for the de-ionised water to be pumped through the ring and up through the column.

During the operation the impurities accumulated at the top of the resin bed and could therefore be removed in the course of backwashing.

However homogeneous the resin may be, the bed is always composed of beads which differ from each other as regards size. During the backwashing, the beads tended to stratify in the column in as homogeneous layers as possible. The separating and flow resistance in the layers was uniform and the liquid flow would take place as "plug-flow".

4.3.3.4 Regeneration

During the course of experiments with beet molasses the resin picked up calcium and magnesium ions from the molasses. H.G. Schneider and J. Mikule (53) have shown that the extraction of sucrose can be carried out economically only if the resin is loaded with calcium and magnesium ions at the most to the extent of 15-20% of its total capacity. If the rotating annular chromatograph holds 15 litres of resin having an ion exchange capacity of 1.6 equivalents per litre, then the resin initially contains:

$$15 \times 1.6 \times 23 = 552 \text{ g Sodium Ions}$$

If all the sodium ions are displaced by calcium ions from the beet molasses feed, then the resin will contain:

$$15 \times 1.6 \times 40/2 = 480 \text{ g Calcium Ions}$$

The beet molasses contains 0.039% calcium on dry substance. If all the calcium in this molasses feed is taken up on the resin by ion exchange, then the amount of molasses dry substance that would convert the resin entirely to the calcium form is:

$$480/0.00039 = 1.23 \text{ Tonnes}$$

If the molasses feed is 50% dry substance (w/w) - which is about 30% w/w sucrose - then it will require a minimum of 2.46 tonnes of this feed to completely convert the resin to calcium form.

In practice regeneration was more frequent than this. After 120 kg of 50% w/w molasses feed, 5% of the resin capacity would have been exchanged for calcium.

For full regeneration, four bed volumes of 10% w/w solutions of NaCl were used.

When using inverted molasses feed the resin is required to be in the calcium form. To convert from sodium to calcium ionic form four feed volumes of a 10% w/w solution of $Ca(N0_3)_2$ were used. With inverted molasses exchange with sodium ions reduces the separation efficiency and similar calculations to those outlined above are made to estimate operating life before regeneration.

4.4 Experimental Procedure

4.4.1 Introduction

On the completion of an experimental run the annular chromatograph was left in a safe state. Such a state required that air should not be able to enter the resin bed. The liquid level control system was designed to maintain a liquid head above the bed as water drained from the base of the annulus. However, it was found that if the column was isolated from the atmosphere then as water drained away a vacuum was created in the headspace above the bed. At a certain vacuum pressure further drainage was prevented and the water in the annulus would stay there until the vacuum was broken by opening the column to the atmosphere. Thus, the ingress of air was prevented and water was conserved as now the liquid level controller was not needed.

4.4.2 Feed Preparation

A feed solution of the required concentrations was prepared by dissolving the calculated weight of the sugars in deionised water. The feed solution was then transferred to a feed bottle (Figure 4.3, A). The feed pump (Figure 4.3, B) needed priming and the feed flowrate for the run had to be measured. To these ends the feed pump discharge line (Figure 4.3, C) had to be disconnected from the feed pipe (Figure 4.3, D). It was found that if the column vacuum was broken by opening the feed pipe to the atmosphere by disconnecting the feed pump discharge line resin would be sucked from the feed nozzle immersed in the resin bed and be spewed out at the other end of the feed pipe. The column vacuum could be broken first by removing a cap from one of the distributor inlet ports. These caps sealed off those inlet ports not in use for delivering eluent or feed into the annulus. Having broken the vacuum in the column (Figure 4.3, E) the feed line was disconnected from the feed pipe. To re-establish the vacuum a cap was affixed onto the feed pipe and then the cap first removed was fixed back onto the distributor.

The feed pump was primed with feed solution. Both feed and eluent pumps were positive displacement type pumps (MPL Pumps Ltd, Middlesex) where different flowrates were obtained by adjusting the percentage of full stroke of a reciprocating plunger.

If a run was being conducted at elevated temperature a heat exchanger (Figure 4.3, F) was introduced into the feed pump discharge line. The temperature in the heat exchange was controlled by a DU82A temperature controller (Diamond H Controls Ltd., Norwich).

Key to Figure 4.3

A	Feed Bottle
B	Feed Pump
C	Feed Pump Discharge Line
D	Feed Pipe
E	Chromatographic Column
F	Feed Heat Exchanger
G	Eluent Pump Discharge Line
H	Eluent Pump
J	Gearing Incorporating Speed Controller
K	Column Oven
L	Column Oven Heaters
M	Eluent Bath
N	Eluent Heater

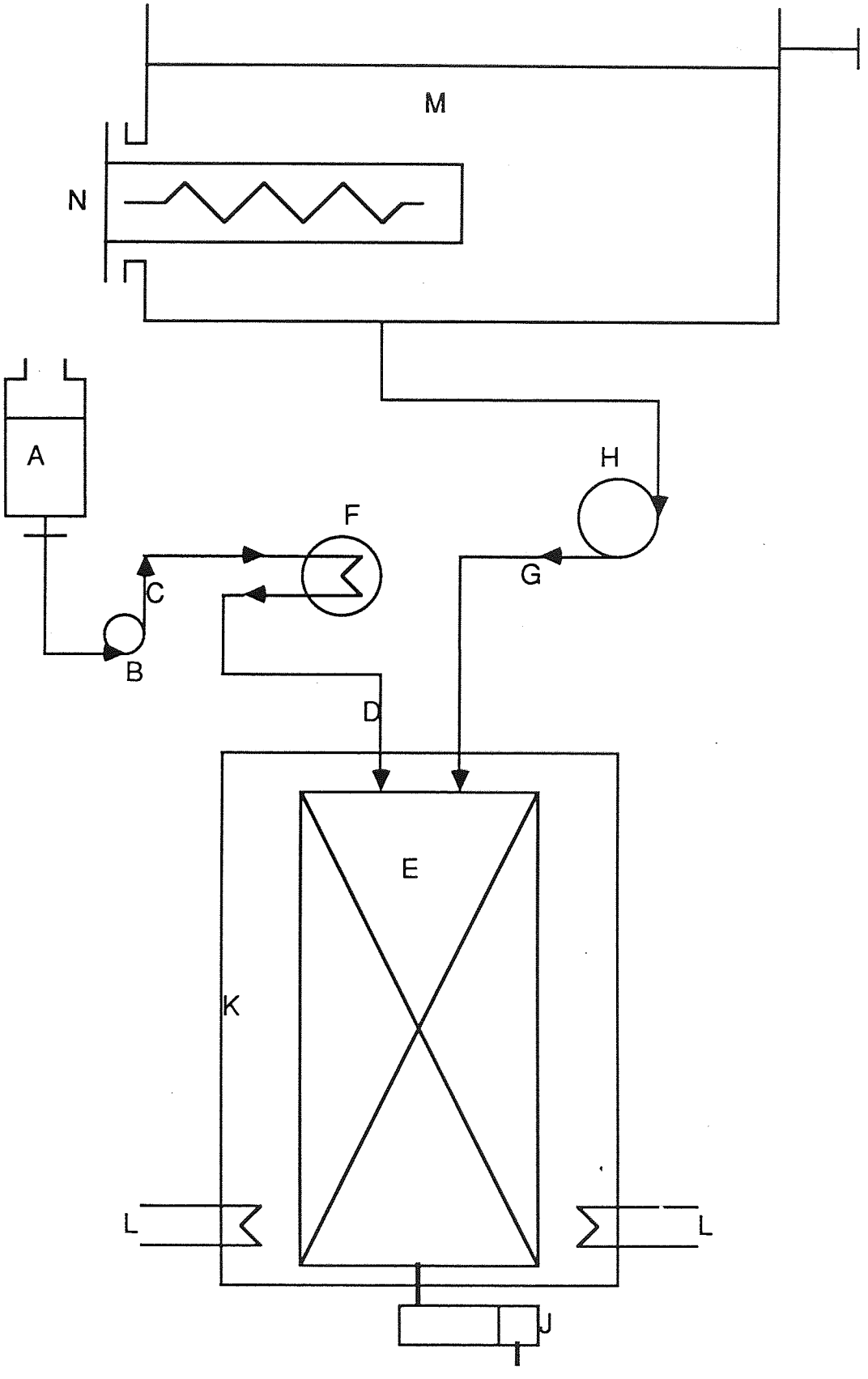

FIGURE 4.3 SCHEMATIC DIAGRAM OF APPARATUS

4.4.3 Start-Up Procedure

If the eluent flowrate needed measuring the eluent pump discharge line (Figure 4.3, G) was disconnected from the column at the distributor. A cap was used to close off the eluent inlet port in the distributor to maintain a vacuum in the column while the flowrate measurements were made. When the eluent pump (Figure 4.3, H) was delivering the required flowrate it was switched off and the eluent pump discharge line was reconnected at the distributor.

When the feed pump (Figure 4.3, B) was delivering the required flowrate it was switched off and reconnected to the feed pipe having first opened the column to the atmosphere by removing a cap from a distributor port not being used. This cap was subsequently replaced to maintain a column vacuum.

If the column rotation rate for the impending run was different from the preceding run the column rotation rate was adjusted and the motor drive system was started. Measurement of rotation speed was made using calibrated graph paper around the perimeter of the baseplate of the annulus and a pointer attached to one of the stationary tie bars.

For high temperature runs the heating elements (Figure 4.3.L) within the column oven (Figure 4.3, K) were activated by setting the oven temperature controller (Figure 4.3, L) at the required temperature setting. Two fans within the oven were switched on to protect the heating elements from overheating and to improve heat transfer. The temperature profile within the oven was monitored using fast response exposed junction thermocouples (Comark Electronics Ltd, West Sussex). The thermocouples were placed around the oven and were connected to a Comark 2501 digital thermometer.

As the column was being heated by the oven the eluent would be preheated in the water bath (Figure 4.3.M). The eluent pump would be continuously delivering eluent to the column and likewise a preheated feed would be continuously fed to the column. A column pressure drop would be created and liquid would start to leave at the exit of the annulus. When the exit liquid was at the required temperature the experimental run would begin.

For those runs at ambient temperature, once their respective discharge lines had been reconnected to the distributor the eluent and feed pumps were started. A column pressure drop would develop and the run would then begin.

4.4.4 Establishing Steady State

Steady state was reached when the concentration profile at the chromatograph exit was invariant with time. The time required to reach steady state varied with the operating conditions. Time had to be allowed for that component most strongly retained by the resin bed to elute from the chromatograph. This time depended upon the component distribution coefficient and also upon the eluent flowrate. It could be determined by repeatedly taking samples from selected positions around the annulus and monitoring their composition changes with respect to time. Knowledge of the time required to achieve steady state for a variety of experimental conditions could subsequently be applied to other conditions so that it was not always necessary to carry out repeated sampling.

4.4.5 Shut Down Procedure

Having collected samples from an experiment at steady state the column needed to be flushed free of feed components. Sugar solutions encouraged microbial growth and could not be left to reside in the column.

The feed bottle (Figure 4.3, A) was disconnected from the feed pump suction line (Figure 4.3, M). The feed bottle was washed out and refilled with deionised water containing 0.02% w/v sodium azide before being re-connected to the suction line. The sodium azide was used to prevent microbial growth and a similar concentration of it was added to the eluent bath.

If the experiment had been at elevated temperature the oven heaters and fans were switched off as also were the feed and eluent preheaters.

The column rotation was stopped and when the column had been flushed free of feed components the feed and eluent pumps were stopped. As liquid drained from the column the pressure drop over it fell until a vacuum was restored.

CHAPTER FIVE
EXPERIMENTS

5.1 The Separation of Sucrose from Beet Molasses (1)

5.1.1 Introduction

In the following section the separation of beet molasses on the rotating annular chromatograph is considered. The properties of beet molasses have been discussed in Chapter 3. The separation was carried out using Duolite C211/2558 ion-exchange resin in the sodium form. The Duolite resin had a mean aperture of 420μm with a minimum of 70% within 370-470μm (ie ± 12% of mean aperture) and 98% minimum within 315-550μm. This was a typical industrial scale chromatographic resin which had been used successfully to separate sucrose from non-sugars in molasses in batch chromatographic columns. The Duolite resin was 5.5% cross-linked with divinylbenzene which was suitable for the molasses separation but which was prone to shrinking under conditions of high sugar or salt concentrations due to osmotic effects.

5.1.2 Factorial Experiment on the Rotating Annular Chromatograph

5.1.2.1 Introduction

The experiments described in this section were carried out to determine the effects of factors on the performance of the rotating annular chromatograph. The term factor is used to denote any feature of the experimental conditions which could be assigned at will and includes temperature, rotation rate, feed rate, feed concentration and eluent rate. A considerable advantage is gained if the experiment is so designed that the effect of changing any one variable can be assessed independently of other variables. One way of achieving this objective is to decide upon a set of values, or levels, for each of the factors to be studied, and to carry out one or more trials of the process at each of the possible combinations of the levels of the factors. Such an experiment is

called a Factorial Experiment. The term experiment refers to the whole set of trials carried and not to an individual trial.

The following is an illustration of the arrangement of a factorial experiment. The performance of the annular chromatograph was measured by the degree of separation (or resolution) of the constituents of beet molasses feed achieved and also by the ratio of the maximum sucrose concentration at the column exit to the sucrose feed concentration.

The effects of four factors were studied: Rotation rate, Feed flowrate, Feed concentration and Eluent rate. Each factor was studied at two levels making a total of 2 x 2 x 2 x 2 = 16 different sets of experimental conditions.

The set of levels of all factors employed in a given trial is called the Treatment Combination. The outcome of a trial in terms of resolution between solutes and sucrose concentration is called the Response. The effect of a factor is the change in response produced by a change in the level of the factor. When a factor is examined at two levels only, the effect is simply the difference between the average response of all trials carried out at the first level of the factor and that of all trials at the second level. The average effect is called the Main Effect of the factor, and if the effect of one factor is different at different levels of another the two factors are said to interact.

NOTATION

For convenience a factor is denoted by a capital letter and the two levels of the factor are represented by adding subscript 1 or 2 to the capital letter. For example, letter A refers to feed rate and A_1 denotes a feed rate of 120 cm^3h^{-1},

A_2 a feed rate of 180 cm^3h^{-1}. The levels of the remaining factors are as follows:

B = Feed concentration. B_1 = 24% w/w sucrose,

B_2 = 35% w/w sucrose.

C = Rotation rate. $C_1 = 120°h^{-1}$, $C_2 = 180°h^{-1}$.

D = Eluent rate. $D_1 = 9lh^{-1}$, $D_2 = 12lh^{-1}$.

There are 16 treatment combinations each of which can be represented by applying the above notation. Thus, the treatment in which every factor is at its higher level is denoted by A_2 B_2 C_2 D_2. Each combination was tested once only and in order to eliminate any possible trends with time the treatments were carried out in random order. Table (5.1) outlines the experimental programme. The numbers represent the order in which the treatment combinations were performed. The first treatment was A_1 B_2 C_2 D_2, in other words, the feed flow was at 120 cm^3h^{-1}, feed concentration was 35% w/w sucrose, rotation rate was $180°h^{-1}$ and eluent rate was $12lh^{-1}$.

Table 5.1

Experimental Programme

		A_1		A_2	
		B_1	B_2	B_1	B_2
C_1	D_1	2	3	16	6
	D_2	13	15	4	11
C_2	D_2	10	12	5	7
	D_2	8	1	14	9

The separation performance in the rotating chromatograph was determined by using the analytical procedures outlined in section (4.2). A typical chromatogram resulting from the separation of beet molasses is shown in Figure (5.1). The ordinate, represents concentration while the abscissa represents angular displacement from the stationary feed point.

Figure (5.1) shows the sequence in which the different components of molasses were eluted from the column. The first to emerge were coloured compounds which are high molecular weight compounds. The colour fraction includes a variety of constituents which were in too low a concentration to be detected on the HPLC system.

The next to be eluted were the inorganic ions which were detected by conductivity measurements. The conductivity fraction like the colour includes many constituents present in very low concentrations.

Sucrose was eluted next followed by betaine, both of which could be detected by HPLC analysis.

The distance from zero to the maximum of the first peak is designated θ_1, while θ_2 is the distance to the second peak etc. Drawing tangents to the curves on both sides of the peak maximum and extending them to the baseline gives the baseline bandwidth, W. Resolution is defined as the ratio of the distance separating two solute peaks to their average bandwidth. In this section, resolution is calculated as being between a partioular component and sucrose.

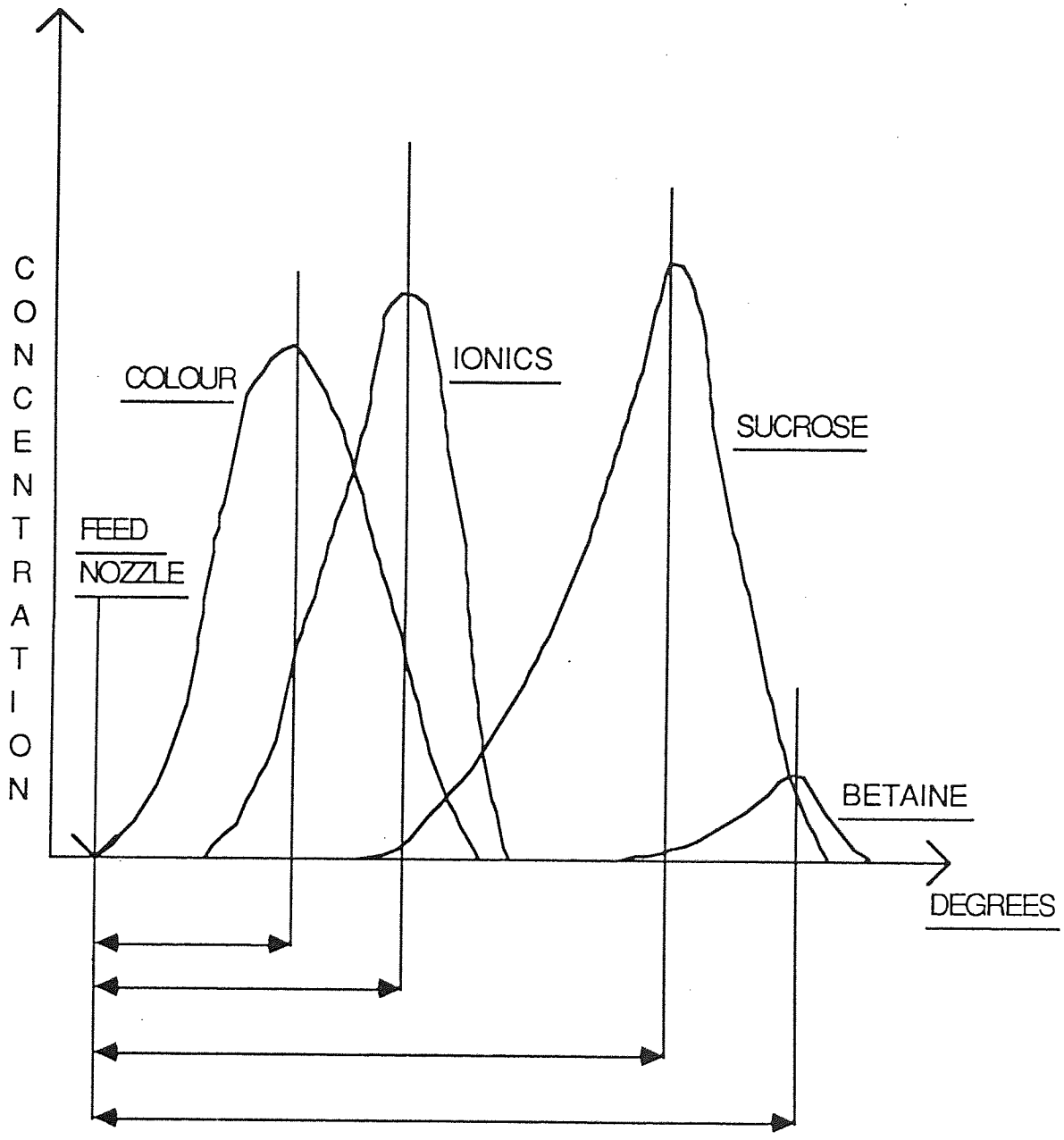

FIGURE 5.1 BEET MOLASSES CHROMATOGRAPH

Therefore:

$$R_{3-1} = \frac{\bar{\theta}_3 - \bar{\theta}_1}{1/2\,(W_3 + W_1)}$$

is the resolution between sucrose and the colour fraction.

The sucrose feed concentration was either 35% or 24% w/w but the sucrose product concentrations were much lower. The dilution suffered by the feed being separated represents a practical drawback with the separation process. A dilute sucrose solution necessitates higher evaporating costs to recover the sucrose. A measure of dilution was obtained by dividing the peak sucrose concentration by the sucrose concentration in the feed to give the sucrose concentration ratio (C_3).

5.1.2.2 Statistical Analysis

For each of the 16 treatment combinations there are 4 responses of interest. These are the three resolutions between sucrose and the remaining molasses constituents and the sucrose concentration ratio. For each run these responses are detailed in Appendix (A.1).

For the calculation of the main effects of each factor and also of the effects of interaction where a factor may be modified by the variation of others factors, Davies (64) outlines a systematic tabular method, The treatment combinations and the observations are written down in a "standard" order, as in the first two columns of table (5.2). The response here is the resolution between sucrose and colour. The first entry in column (1) is the sum of the first two responses (0.46 + 0.42); the second entry is the sum of the second pair (0.26 + 0.40) and so on until the top half of column (1) is complete by summing

the last pair (0.20 + 0.18). The lower half is derived from the response column by taking the differences of the same pairs, the first from the second in every case.

Columns (2), (3) and (4) are derived in a similar way. Column (2) being derived from the response column (1) by summing and differencing successive pairs and the other columns are each derived from the previous one in the same way.

The actual effects are then obtained by dividing the entries in column (4) by 8. In order to decide how much confidence could be placed in the apparent variation caused by a factor or interaction of factors a test of significance is made. A significance test involves a comparison of the effect with its standard error. The standard error is that variation in a set of data which is not attributable to any assignable cause. On the assumption that errors are distributed at random among the results (such an assumption is implied by the tests of significance) it is possible to calculate the odds against a given apparent effect of a factor being entirely due to error variations.

Table 5.2

Analysis of Resolution Between Sucrose and Colour Data

Treatment Combination	R_{3-1}	(1)	(2)	(3)	(4)	Effect = Col (4) /8	't' Value
$A_1B_1C_1D_1$	.46	.88	1.54	3.13	5.72	-	
$A_2B_1C_1D_1$	.42	.66	1.59	2.59	-0.88	-0.110	-7.3
$A_1B_2C_1D_1$	.40	.84	1.36	-0.47	-0.62	-0.078	-5.2
$A_2B_2C_1D_1$	.26	.75	1.23	-0.41	-0.34	-0.043	-2.9
$A_1B_1C_2D_1$	.45	.60	-0.18	-0.31	-0.18	-0.023	-1.5
$A_2B_1C_2D_1$	.39	.76	-0.29	-0.31	0.12	0.015	1.0
$A_1B_2C_2D_1$	.49	.85	-0.32	-0.27	0.50	0.063	4.2
$A_2B_2C_2D_1$	.26	.38	-0.09	-0.07	0.10	0.013	-9
$A_1B_1C_1D_2$	.35	-.04	-0.22	-0.05	-0.54	-0.068	-4.5
$A_2B_1C_1D_2$	.25	-.14	-0.09	-0.13	0.06	0.008	.5
$A_1B_2C_1D_2$	.49	-.06	-0.16	-0.11	0.00	0.000	0.0
$A_2B_2C_1D_2$	.27	-.23	-0.47	0.23	0.20	0.025	1.7
$A_1B_1C_2D_2$	.46	-.10	-0.10	0.13	0.08	0.010	.7
$A_2B_1C_2D_2$	.39	-.22	-0.17	-0.63	0.34	0.043	2.9
$A_1B_2C_2D_2$	.20	-.07	-0.12	-0.07	-0.76	-0.095	-6.3
$A_2B_2C_2D_2$	.18	-.02	0.05	0.17	0.24	0.030	2

A measurement of the error variation can be found from the differences in responses between replicated tests. To this end one of the trials was repeated a further three times. The trial chosen was that one where all factors were at a low level (this is treatment combination two in Table (5.1)). The results from this replicated trial are shown in Table (5.3).

Table 5.3

Responses for Replicated Trial

RESPONSES	TRIAL			
	1	2	3	4
Resolution Sucrose - Colour (R_{3-1})	.46	.48	.51	.45
Resolution Sucrose-Ionics (R_{3-2})	.51	.52	.49	.51
Resolution Sucrose-Betaine (R_{4-3})	.65	.70	.66	.62
Concentration Ratio (C_3)	.068	.040	.084	.110

To calculate the standard error for each response the standard deviation is first estimated. For the sucrose-colour resolution, R_{3-1}

$$\text{Mean } R_{3-1} = 0.48$$

Estimated standard deviation of responses

$$S = \sqrt{\frac{(0.46 - 0.48)^2 + (0.48 - 0.48)^2 + (0.51 - 0.48)^2 + (0.45 - 0.48)^2}{(4 - 1)}}$$

$$= \quad 0.026$$

Then the standard error of the response is:

$$S.E.\left[R_{3-1}\right] = \frac{S}{\sqrt{n}} = \frac{0.026}{\sqrt{3}} = 0.015$$

In the same way the following standard errors (S.E.) for each response are calculated;

Table 5.4

Standard Errors for the Various Responses

Response	S.E.
R_{3-1}	0.015
R_{3-2}	0.007
R_{4-3}	0.019
C_3	0.017

The procedure in a test of significance is to calculate the probability of finding a deviation as extreme or more extreme than the observed deviation. An appropriate significance test is the so called t-test. The t-test involves a comparison of the observed deviation with its standard error. If the observed deviation is significantly greater than the error can account for then the cause of the deviation is significant. For example, increasing the feed flow rate might cause the concentration ratio to increase. The average concentration ratio at low feed rate is subtracted from the average at the high feed rate to give the observed deviation which is then compared with the deviation accountable to the error. The observed deviation is called the effect of the feed rate.

$$t = \frac{\text{Effect}}{\text{Standard Error}}$$

The t-values for each treatment combination are given in table (5.2). The method outlined by Davies (64) in calculating table (5.2) ensures that each treatment combination corresponds to a particular effect. For example, the combination $A_2\ B_1\ C_1\ D_1$ corresponds to the effect of feed rate and in particular of increasing the feed rate while keeping the remaining factors constant. Thus the effect of feed rate has a t-value. The combination $A_2\ B_1\ C_2\ D_1$ corresponds to the effect of increasing both feed rate and rotation rate and its t-value of -1.5 is a measure of the interaction between these two factors.

To apply the t-test the assumption is made that only random (error) variation is responsible for a change occurring in a response. If the observed change has only a small probability of being attained if this assumption was valid, it is concluded that the assumption is not valid. α is called the Level of Significance used in the significance test, and the conclusion is usually expressed in some such form as a "A statistical test indicates a significant departure from the given assumption at the 100 α % level (e.g. 10% level)". This procedure implies that there is a chance of concluding erroneously that there is a departure from the given assumption, namely a 100 α % chance. Having calculated a t-value for a particular effect and stipulated a value for α reference is made to a t-table (see for example in reference (64)). The t-table makes it possible to determine whether the particular effect is responsible for the observed deviation in a response. For a certain α value e.g. $\alpha = 0.10$ the t-table will have a particular t-value which for $\alpha = 0.10$ is 6.31. If the effect t-value is say less than 6.31 then there is a greater than 10% chance that the observed deviation for the effect is in fact caused by random variation (error). In statistical experiments of this nature such a chance probability is sufficient

to maintain that there is no significant departure from the hypothesis that the observed deviation was due to random variation. However, if the effect t-value is greater than 6.31 then the observed deviation is not consistent with random variation and the particular effect is said to be significant. Of course, some discretion has to be exercised with t-values a little below or above 6.31 but before the statistical analysis proceeds the Level of Significance has to be stipulated and then adhered to.

For example, consider the sucrose-colour resolution response to changes in feed rate. From Table (5.2) the t-value for the effect of feed rate is -7.3. The negative sign indicates that the response decreases as the factor increases. Thus there is a greater than 90% chance that increasing the feed rate reduces the resolution. On the other hand the interactive effect of feed rate with rotation has a t-value 1.0 so that this effect is not significant.

Tables (5.5), (5.6) and (5.7) give t-values for the responses; resolution between sucrose and the ionics (R_{3-2}), resolution between sucrose and betaine (R_{4-3}) and the concentration ratio for sucrose (C_3).

5.1.2.3 The Effect of Feed Rate

The effect of feed rate on resolution and the concentration ratio is discussed in this section. Table (5.8) summarizes the t-values for the responses.

Table 5.5

Analysis of Resolution Between Sucrose and Ionics Data

Treatment Combination	R_{3-2}	(1)	(2)	(3)	(4)	Effect = Col (4) /8	't'
$A_1B_1C_1D_1$	.51	.92	1.70	2.79	4.71	-	
$A_2B_1C_1D_1$	.41	.78	1.09	1.92	-.83	-.104	-14.9
$A_1B_2C_1D_1$	.56	.62	1.17	-.75	-.87	-.109	-15.6
$A_2B_2C_1D_1$	.22	.47	.75	-.08	.23	.029	4.1
$A_1B_1C_2D_1$	.37	.65	-.44	-.29	-1.03	-.129	-18.4
$A_2B_1C_2D_1$	.25	.52	-.31	-.58	-.01	-.001	0.0
$A_1B_2C_2D_1$	.33	.60	.03	-.31	-.33	-.041	-5.9
$A_2B_2C_2D_1$	.14	.15	-.11	.54	.45	.056	8.0
$A_1B_1C_1D_2$	.35	-.10	-.14	-.61	-.87	-.109	-15.6
$A_2B_1C_1D_2$	.30	-.34	-.15	-.42	.67	.084	12.0
$A_1B_2C_1D_2$	.22	-.12	-.13	.13	-.29	-.036	-5.1
$A_2B_2C_1D_2$	.30	-.19	-.45	-.14	.85	.106	15.1
$A_1B_1C_2D_2$	.43	-.05	-.24	-.01	.19	.024	3.4
$A_2B_1C_2D_2$	.17	.08	-.07	-.32	-.27	-.034	-4.9
$A_1B_2C_2D_2$	0.0	-.26	.13	.17	-.31	-.039	-5.6
$A_2B_2C_2D_2$	.15	.15	.41	.28	.11	0.02	2.9

Table 5.6

Analysis of Resolution Between Sucrose and Betaine Data

Treatment Combination	R_{4-3}	(1)	(2)	(3)	(4)	Effect	't'
$A_1B_1C_1D_1$	.65	1.23	2.67	6.64	12.51	-	
$A_2B_1C_1D_1$	.58	1.44	3.97	5.87	-.63	-.08	-4.2
$A_1B_2C_1D_1$	.56	2.12	2.85	-.44	-.55	-.069	-3.6
$A_2B_2C_1D_1$	.88	1.85	3.02	-.19	.23	.029	1.5
$A_1B_1C_2D_1$	1.35	1.61	.25	-.06	1.47	.184	9.7
$A_2B_1C_2D_1$	.77	1.24	-.69	-.49	-1.35	-.169	-8.9
$A_1B_2C_2D_1$	.98	1.57	.11	.86	-.23	-.029	-1.5
$A_2B_2C_2D_1$	.87	1.45	-.30	-.63	-.09	-.011	0.6
$A_1B_1C_1D_2$	.72	-.07	.21	1.30	-.77	-.096	-5.1
$A_2B_1C_1D_2$	.89	.32	-.27	.17	.25	.031	1.6
$A_1B_2C_1D_2$	.65	-.58	-.37	-.94	-.43	-.054	-2.8
$A_2B_2C_1D_2$	.59	-.11	-.12	-.41	-1.49	-.186	-9.8
$A_1B_1C_2D_2$	.76	.17	.39	-.48	-1.13	-.141	-7.4
$A_2B_1C_2D_2$	.81	-.06	.47	.25	.53	.066	3.5
$A_1B_2C_2D_2$	.95	.05	-.23	.08	.73	.091	4.8
$A_2B_2C_2D_2$	.60	-.35	-.40	-.17	-.25	-.031	-1.6

Table 5.7

Analysis of Concentration Ratio Data

Treatment Combination	Concentration C_3	(1)	(2)	(3)	(4)	Effect	't'
$A_1B_1C_1D_1$	.068	.237	.470	.859	1.629		
$A_2B_1C_1D_1$	.169	.233	.389	.770	2.166	.27	15.9
$A_1B_2C_1D_1$	.103	.184	.421	1.221	.95	.119	7.0
$A_2B_2C_1D_1$	.130	.205	.349	.945	.058	.007	.4
$A_1B_1C_2D_1$	.067	.159	.371	.17	-.153	-.019	-1.1
$A_2B_1C_2D_1$	.117	.262	.850	.78	.218	.027	1.6
$A_1B_2C_2D_1$	.085	.187	.603	.019	-1.03	-.129	-7.6
$A_2B_2C_2D_1$	.120	.162	.342	.039	.914	.114	6.7
$A_1B_1C_1D_2$	.08	.101	-.04	-.081	-.089	-.011	-.6
$A_2B_1C_1D_2$	.151	.270	.21	-.072	-.276	-.035	-2.1
$A_1B_2C_1D_2$	.108	.500	1.03	.479	.61	.076	4.5
$A_2B_2C_1D_2$	.154	.350	-.25	-.261	.020	.002	.2
$A_1B_1C_2D_2$	.078	.143	.169	.25	.09	.011	.6
$A_2B_1C_2D_2$	.109	.460	-.15	-1.28	.218	.027	1.6
$A_1B_2C_2D_2$	.065	.310	.317	-.319	-1.53	-.191	-11.2
$A_2B_2C_2D_2$	.097	.032	-.278	-.595	-.276	-.035	-2.1

Table 5.8

t-values for the Effect of Feed Rate

Response	t-value
Resolution Sucrose - Colour (R_{3-1})	-7.30
Resolution Sucrose - Ionic (R_{3-2})	-14.90
Resolution Sucrose - Betaine (R_{4-3})	-4.20
Concentration of Sucrose (C_3)	15.90

The first point to note is that the significance of feed rate is different according to the response. For R_{3-2} and C_3 the effect of feed rate is highly significant.

As equation (6) shows resolution is determined by band peak positions and exit bandwidths of each solute. The effect of feed rate can be estimated using the plate theory of chromatography. With only the feed rate changing equation (3) predicts that θ for each solute is constant. However, as the feed rate increases the initial width of the feed stream increases which is the term W_o in equation (5). The effect of the feed rate on the H.E.T.P. is less easily reduced to a direct relationship though it is generally acknowledge (65) that in batch chromatography an increase in sample size reduced the column efficiency, i.e. it increases the H.E.T.P. The continuous rotating annular process and the batch process are analogous if one considers the annulus as a series of circumferentially arranged batch columns. . Thus equation (5) predicts that as the feed rate increases the exit bandwidth increases. As a consequence of constant peak positions and increasing exit bandwidths, the plate theory predicts that resolution decreases with increasing feed rate.

The negative t-values in Table 5 indicate that the resolution tends to decrease as feed rate increases. R_{3-1} and R_{3-2} are both significantly affected whereas less confidence can be placed in the result for the sucrose-betaine resolution. The variation in t-values may indicate the limitations of the plate theory in describing non-linear chromatographic systems, i.e. where the equilibrium isotherm is non-linear. The resolution between solutes may also have been affected by the presence of the remaining solutes such that each solute could not be considered separately as if the other solutes were not there.

The positive t-value for the concentration of sucrose in Table (5.8) shows that as the feed rate increases the ratio of the sucrose peak exit concentration to the feed concentration also increases. This is not surprising because as the feed rate increases the ratio of feed to the total flowrate (i.e. feed plus eluent) increases so that the quantity of water per molecule of sucrose falls.

5.1.2.4 The Effect of Feed Concentration

Table (5.9) shows the t-values corresponding to the responses being considered when the feed concentration changes.

Table 5.9

t-values for the Effect of Feed Concentration

Response	t-value
R_{3-1}	-7.3
R_{3-2}	-15.6
R_{4-3}	-3.6
C_3	7.0

There is considerable similarity between the effects of feed rate and feed concentration on the various responses. The solute exit bandwidths would be expected to increase as feed concentration increases since the greater quantity of solute molecules have a statistically greater opportunity to spread out more. The plate theory predicts constant peak positions as the feed concentration changes. Therefore the resolution between solutes would be expected to decrease as concentration increases. The sucrose-ionic resolution is again the most significantly affected.

Comparing tables (5.8) and (5.9) it might be supposed that feed rate and feed concentration are interchangeable factors. It should also be noted that an improvement in resolution between solutes can be attained by decreasing either or both of the feed factors but this improvement will be at the cost of a separation where sucrose suffers greater dilution.

5.1.2.5 The Effect of Rotation Rate

Table 5.10

t-values for the Effect of Rotation Rate

Response	t-value
R_{3-1}	-1.5
R_{3-2}	-18.4
R_{4-3}	9.70
C_3	-1.10

Table (5.10) shows that rotation rate affects the responses in different ways. For R_{3-1} and C_3 changes in rotation rate have no significant effect whereas both R_{3-1} and R_{4-3} are significantly affected but in different ways.

Equation (3) predicts that as rotation rate increases band peak position increases and equation (5) predicts that the exit bandwidth also increases. As rotation rate increases the ratio of the initial feed bandwidth to the exit bandwidth decreases and plate theory predicts that as this ratio tends to zero, resolution tends to be invariant with changes in rotation rate. As the rotation rate decreases the plate theory predicts that resolution tends to decrease eventually reaching zero at zero resolution. Thus, for each solute there would be a region where increasing rotation rate increases resolution and a second region where resolution would be constant. Therefore, for the colour, Table (5.10) would indicate that we were in the second region whereas for betaine which has different distribution co-efficient and H.E.T.P. values we would appear to be in the first region. The plate theory is however unable to account

for the significant decrease in sucrose-ionic resolution with increasing rotation rate.

The plate theory as developed for the annular chromatography by Scott *et al* (31) gives the following expression for the ratio of peak exit concentration to the feed concentration:

$$\frac{C_{EXIT\ PEAK}}{C_{FEED}} = \frac{1}{\sqrt{2\pi}\ (N - 1)} \qquad (11)$$

Thus the ratio is expected to be independent of rotation rate and the t-value in table (5.10) for C_3 confirms this. It should be noted however that equation (11) also shows that the concentration ratio is independent of feed rate. This is because the plate theory assumes that the feed flowrate is relatively small compared to the eluent flowrate and that changes in the feed flow have a negligible effect on the total liquid flow through the annulus.

5.1.2.6 The Effect of Eluent Rate

TABLE 5.11

t-values for the Effect of Eluent Rate

Response	t-value
R_{3-1}	-4.5
R_{3-2}	-15.6
R_{4-3}	5.1
C_3	-0.60

Although changes in eluent rate can be computed in Equations (2) and (4) by changes in the velocity, V, term, the eluent flowrate also affects the solute distribution co-efficients, K and the H.E.T.P., H. The latter can be predicted by Equation (2) once the various terms have been determined. Joshi (66) determined that the distribution co-efficients of various carbohydrates and also betaine and ionic solutes decreased as the eluent rate increased. Table (5.11) shows that the resolution tended to decrease as the eluent rate was increased. Since the concentration ratio was unaffected by the eluent rate changes made in the experiment it would seem that low eluent rates were favourable to optimize separation and product concentration.

5.1.2.7 The Effect of Interactions

Tables (5.2), (5.5), (5.6) and (5.7) also show some significant t-values for treatment combinations where two or more factors were varied. In particular the t-values and treatment combinations outlined in Table (5.12) are of interest.

Table 5.12

Major Interactive Effects

Treatment Combination	R_{3-1}	R_{3-2}	R_{4-3}	C_3
$A_1B_2C_2D_2$	-6.3	-5.60	4.80	-11.20
$A_2B_2C_1D_2$		15.10	-9.80	
$A_2B_2C_2D_1$		8.0		6.7

The first entry indicates that the interaction between feed concentration, rotation rate and eluent rate is possibly significant. This means that the effect of say feed concentration depends to some extent on the levels of rotation rate and eluent rate.

The t-values of the relevant effects for the response C_3 are:

Feed concentration	=	7.0
Rotation rate	=	-1.1
Eluent rate	=	-0.6
Interaction	=	-11.2

In other words, higher feed concentration increases the concentration ratio but the negative interaction with rotation and eluent rates shows that this increase is greater at lower rotation and eluent rates. Although rotation rate has no main effect on the concentration ratio it has an interactive effect such that if the ratio is to be increased by increasing the feed concentration then a lower rotation rate coupled with a low eluent rate is preferable. It is worth noting that the treatment combination A_1 B_2 C_2 D_1 has a t-value -7.60. This indicates that there is an interaction between feed concentration and rotation rate alone, independent of eluent rate. Thus, even at higher eluent rates, a low rotation rate should be used if the concentration ratio is to be increased by increasing feed concentration. The advantage of using lower eluent rates however is that the ratio will be increased further.

For the same treatment combination, A_1 B_2 C_2 D_2 the resolution t-values are:

	R_{3-1}	R_{3-2}	R_{4-3}
Feed Concentration	-5.2	-15.60	-3.60
Rotation Rate	-1.5	-18.4	9.70
Eluent Rate	-4.5	-15.6	-5.10
Interaction	-6.3	-5.6	4.80

There is a weak indication that high feed concentrations may reduce resolution R_{3-1} but a reduction is more confidently expected if the rotation and eluent rates are high. ("High" refers to the bounds of the experiment, e.g., a high rotation rate is $180°h^{-1}$ and a high eluent rate is $12lh^{-1}$).

Compared to the main effects, there is only a possible slight effect of the interaction on R_{3-2} and R_{4-3}.

For the treatment combination A_2 B_2 C_1 D_2 the relevant t-values for R_{3-2} and R_{4-3} are;

	R_{3-2}	R_{4-3}
Feed Flow Rate	-14.9	-4.2
Feed Concentration	-15.6	-3.6
Eluent Rate	-15.6	-5.1
Interaction	15.1	-9.8

Increasing the feed rate reduces resolution R_{3-2} but if the increase is accompanied by increases in the feed concentration and eluent rate then the resolution actually improves. The treatment combination A_2 B_1 C_1 D_2 has a t-value of 12.0 which would indicate that a significant factor in this improvement is the eluent rate increase. However for the resolution R_{4-3} an increase together of the three factors gives a marked decrease in resolution which is more significant than if either factor is increased alone.

For the treatment combination A_2 B_2 C_1 D_2 the relevant t-values for R_{3-2} and C_3 are:

	R_{3-2}	C_3
Feed Flow Rate	-14.9	15.9
Feed Concentration	-15.6	7.0
Rotation Rate	-18.4	-1.1
Interaction	8.0	6.7

For R_{3-2} a similar effect is observed as for the previous combination. Thus if feed flow or feed concentration are to be increased the increase of the one should be accompanied by an increase in the other plus an increase in either rotation or eluent rate if the resolution is to be improved. It is interesting that two factor interactions for R_{3-2} are not significant so that if only the feed flow and say rotation rate are increased the main effects of each reduce resolution but the reduction due to feed flow is not influenced by the changes in rotation rate.

5.1.2.8 The Separation of Sucrose from Non-Sucrose Solids

The statistical analysis outlined and discussed above indicates the difficulty in optimizing the performance of the continuous annular chromatograph to achieve high product concentrations and resolutions. The numerous interactions complicate the picture considerably. This is seen most plainly for the sucrose-ionic resolution R_{3-2} where individual increases in either feed rate, feed concentration or eluent rate each produces a fall in resolution whereas if all three are increased together the resolution increases. The same three increasing together however leads to a fall in the sucrose-betaine resolution. If the emphasis is to separate sucrose from ionics then the increase of all three is favoured in particular as high feed rates and concentrations give higher concentration ratios if carried out at low rotation rate.

The important aspect with regard to the molasses separation is the separation of sucrose from everything else. Thus a high resolution between sucrose and betaine is of little practical use if the sucrose is not effectively separated from the other constituents. Attention is turned to the RDS values of the samples.

RDS is a measure of the total solids concentration. If the sucrose concentration is subtracted from the RDS what remains is the non-sucrose concentration for the sample and it is the separation of sucrose from the non-sugars which is of interest.

Figure (5.2) shows the chromatogram for Run 16 with a sucrose profile and a profile for the RDS minus sucrose concentration. This latter can be abbreviated to MRDS standing for the modified RDS value. In figure (5.2) the MRDS profile has two peaks. The first peak corresponds to the inorganic ions and high molecular weight organics amongst others. The second peak corresponds to betaine and any glucose or fructose plus traces of components such as alanine, glycine and adenosine. These two peaks are labelled as MRDS1 and MRDS2. The resolution between sucrose and MRDS1 and MRDS2 can be calculated for Figure (5.2). For MRDS1 the resolution is 0.34, for MRDS2 it is 0.65. An estimate is made of the total solids represented by each MRDS profile by approximating each to a triangle and estimated the area of each triangle. Thus:

$$\text{Area MRDS1} = 1/2 \times 1.26\%\ \text{w/w} \times 9.2 = 5.79$$

$$\text{Area MRDS2} = 1/2 \times .70\%\ \text{w/w} \times 19.6 = 6.86$$

A 'weighted' resolution for each peak is then given by:

$$\text{For MRDS1, weighted resolution} = \frac{2 \times 5.79}{5.79 + 6.86} \times 0.34 = 0.31$$

$$\text{For MRDS2, weighted resolution} = \frac{2 \times 6.86}{5.79 + 6.86} \times 0.65 = 0.70$$

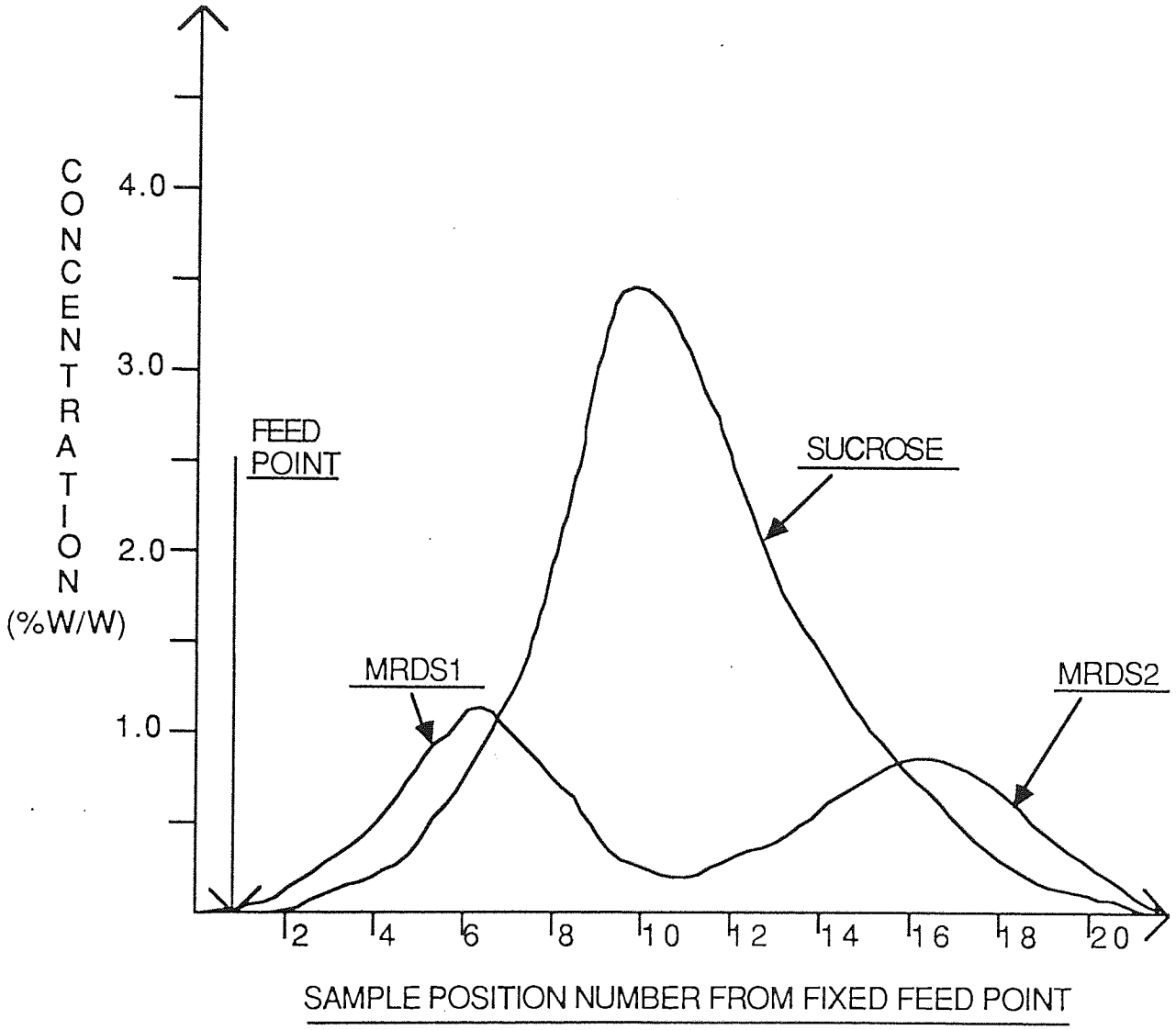

FIGURE 5.2 CHROMATOGRAM FOR RUN 16

The separation of sucrose from the other components is then given by the average of the two weighted resolutions:

$$\text{Sucrose - MRDS resolution} = (0.31 + 0.70)/2 = 0.51.$$

In the same way the sucrose - MRDS resolution is estimated for each of the 16 trials and a statistical analysis is carried out on the 16 responses to determine which effects are significant (see table (5.13)). The standard error, as for the previous analysis was estimated from the replicated trial and had the value 0.013.

From Table (5.13) two factors are significant, the feed rate and eluent rate. As both of these are increased the resolution between sucrose and the remaining solids decreases. A high feed rate has a higher initial bandwidth leading to a greater spread of the components at the annulus exit which is detrimental to the separation. At high eluent rates the components are transported through the column more rapidly and as a result there is less time available to achieve separation.

Table (5.13)

Analysis of Resolution Between Sucrose and Non-Sucrose Solids Data

Treatment Combination	Resolution MRDS-Sucrose	(1)	(2)	(3)	(4)	Effect	't'
$A_1B_1C_1D_1$	.48	.99	1.93	3.56	6.20		
$A_2B_1C_1D_1$	.51	.94	1.63	2.64	-.78	-.098	-7.54
$A_1B_2C_1D_1$	.59	.9	1.43	-.52	-.4	-.05	-3.85
$A_2B_2C_1D_1$	.35	.73	1.21	-.26	-.42	-.052	-4.0
$A_1B_1C_2D_1$	.49	.67	-.21	-.22	-.52	-.065	-4.0
$A_2B_1C_2D_1$	.41	.76	-.31	-.18	.14	.018	1.4
$A_1B_2C_2D_1$	.48	.74	-.25	-.42	-.48	-.06	-4.61
$A_2B_2C_2D_1$	.25	.47	-.01	0	.34	.043	3.31
$A_1B_1C_1D_2$	.37	.03	-.05	-.3	-.92	-.12	-9.23
$A_2B_1C_1D_2$	.3	-.24	-.17	-.22	.26	.033	2.53
$A_1B_2C_1D_2$	.47	-.08	.09	-.1	.04	0	0
$A_2B_2C_1D_2$	.29	-.23	-.27	.24	.42	-.052	-4.0
$A_1B_1C_2D_2$	.4	-.07	-0.27	-.12	.08	.01	.8
$A_2B_1C_2D_2$	.34	-.18	-.15	-.36	.34	.043	3.3
$A_1B_2C_2D_2$	.21	-.06	-.11	.12	-.24	.03	2.31
$A_2B_2C_2D_2$	.26	.05	.11	.22	.1	.01	.8

Apart from feed rate and eluent rate there is apparently no other significant factors which affect the sucrose-RDS resolution. There are some weak indications that feed concentration and rotation rate might possibly have some effect such that when each is increased the resolution falls. However, the main factors are feed and eluent rates and the t-values show that low values for each are beneficial to the separation of sucrose from the other constituents in beet molasses. From Table (5.13) the concentration ratio (C_3) increases with increasing feed rate and concentration and is unaffected by eluent rate. Thus, a low eluent rate is favourable to achieve a good separation of sucrose from the other solids and is not disadvantageous to the concentration ratio. The feed concentration of 35% w/w sucrose was not so high that the separation was decreased to any significant effect and a higher concentration would be permissible especially as the concentration ratio increased with feed concentration. Rotation rate had no significant effect on resolution or concentration ratio. However as the feed rate increases there is a tendency for the feed band to become so broad that some of the feed mixture escapes from the top of the resin bed. Although the feed pipe was adjustable and could be moved up and down there was a maximum depth within the bed to which the feed pipe would go. By increasing the rotation rate, higher feed rates can be tolerated before the feed spreads so much it starts to leave the top of the bed. The rotation rate would be of possibly greater significance if another feed pipe was used in the operation of the chromatograph. To increase the throughput of beet molasses two or more feed points could be utilized. If two feed points were used they would be stationed 180° apart at the distributor. With two sucrose peaks at the annulus exit column operation needs to be such that the sucrose peak from one feed line does not coincide with the bulk of non-sucrose solids from the other feed line. Appropriate rotation rate settings enable the use of two or more feed lines as a means of increasing feed throughput.

To achieve high throughputs and to minimize dilution a high feed rate is required but this has a tendency to reduce the separation between sucrose and the remaining solids. So for the feed rate a compromise has to be reached. With this in mind, some additional runs were carried out in which the feed flowrate was changed while keeping the remaining factors constant.

The values of the constant factors were:

Feed concentration	35% w/w sucrose
Rotation rate	120° h^{-1}
Eluent rate	12 lh^{-1}

The feed rate was varied from 160 cm^3 h^{-1} to 340 cm^3 h^{-1}. Three additional runs were carried out, Runs 17, 18 and 19 the results of which are in Appendix (A1).

The following sucrose - MRDS resolutions and concentration ratios were obtained:

Run Number	Feed Rate cm^3 h^{-1}	Resolution Sucrose - MRDS	Concentration Ratio C_3
17	260	.55	.22
18	340	.46	.28
19	160	.60	.13

Run 18 still showed a fair degree of separation between sucrose and the remaining solids and had a high concentration ratio. The peak sucrose concentration for this run was 9.74% w/w. Betaine, which has the highest

distribution co-efficient of the molasses components had a peak elution position at the annulus exit of 122.4°. Thus, Run 18 could have been carried out with easily two feed points and possibly three with the betaine from the third tending to overlap with the coloured solutes from the first. Because of these outstanding features a more detailed analysis was carried out on Run 18. The analysis was based on the assumption that sucrose is crystallizable and therefore an exit stream becomes a product stream if the purity of the stream is at least 65% sucrose and if the sucrose concentration of the stream is at least 5% w/w. Otherwise the exit stream is considered to be waste product. The following table shows the sucrose concentration and purity at the given exit positions:

Exit Position Degrees from Feed Point	Sucrose Concentration % w/w	RDS % w/w	Exit Stream Purity
64.8	0.55	2.23	24.7
72.0	2.18	4.75	45.9
79.2	5.94	8.48	70.0
86.4	8.66	10.76	80.5
93.6	9.74	9.79	99.4
100.8	7.85	7.93	99.0
108.0	4.73	4.82	98.1
115.2	2.37	3.05	77.7
122.4	0.93	2.02	46.0

The product portion of the effluent leaving the annulus lies between 79.2 and 108.0 degrees from the feed point. The liquid flowrate through this portion is given by:

$$(\text{ELUENT FLOW} + \text{FEED FLOW}) \times \left[\frac{108.0 - 79.2}{360}\right]$$

$$= (12000 + 408) \times 0.1$$

$$= 1240.8\ gh^{-1}$$

(NB/ The specific gravity of the feed was 1.2 so that $340cm^3h^{-1}$ of feed is equivalent to $340 \times 1.2 = 408\ gh^{-1}$ Beet Molasses).

The mean sucrose concentration in the product portion is 7.38%w/w. The mean RDS is 8.36%w/w and the mean purity is 89.4%.

The sucrose throughput in the product portion is:

$$\text{Sucrose Solids} = 1240.8\ gh^{-1} \times 0.0738 = 91.57\ gh^{-1}$$

And for non-sucrose solids:

$$\text{Non-Sucrose Solids} = 1240.8\ gh^{-1}\ (0.0836 - 0.0738) = 12.16\ gh^{-1}$$

The sucrose is recovered by the crystallization of the product stream. Crystallization continues until the sucrose purity of the uncrystallized product falls to 65%. At this point further crystallisation is prevented by the inhibiting effect of the non-sucrose solids present. Thus, although the sucrose flow in the product stream is $91.57\ gh^{-1}$ not all of this sucrose is recoverable. The crystallizable sucrose flow rate (S) is given by:

$$S = 91.57 - 65/35\ (12.16) = 69.0\ gh^{-1}$$

If three feed points had been used, the flowrate S would become:

$$S = 3 \times 69.0 = 207\ gh^{-1}\ \text{Sucrose.}$$

5.2 The Separation of Glucose from Fructose

5.2.1 Introduction

The various resolution values achieved for the separation of beet molasses were, without exception, all less than one. This means that the components were never completely resolved and so there was only a relatively narrow band from which a product stream of acceptable purity could be drawn. There are numerous means by which the separation could be improved. The experiments reported on in Section (5.1) showed that resolution generally improved if the eluent velocity was reduced or if the feed rate was reduced. However, such options are not always helpful when one of the aims of this work is to achieve high feed throughputs with as high as possible product concentrations. Another option is to increase the column length which in effect increases the time available for the separation to occur. However, a greater column length with result in greater dilution of solutes and on an industrial scale the tendency is to look for ways to reduce equipment size rather than the reverse. It was believed however that operation of the continuous chromatograph could be improved by reducing the particle size of the bed.

The Van Deemter equation for the height of an equilibrium stage for an isothermal system is given by Equation (2):

$$H = A + \frac{B}{u} + Cu \qquad 2$$

The term A is due to eddy diffusion

$$A = \lambda d p$$

The term B is due to molecular diffusion

$$B = 2\gamma D_M$$

And the term C is due to mass transfer

$$C = \frac{C_M dp^2}{D_M} + \frac{C_{SM} dp^2}{D_{SM}}$$

where λ, γ, C_M, C_{SM}, D_M and D_{SM} are constants.

The resulting equation has an optimum velocity which minimizes H. However, normal operation is in the region where pore diffusion controls and $H \alpha udp^2$. Thus, decreasing particle size decreases the H.E.T.P. and should increase the separation performance of the chromatograph.

5.2.2 Synthetic Feedstock Runs on Duolite Resin (Mean size 420 micron).

Before using a smaller particle sized bed it was decided to investigate further, the performance of the rotating annular chromatograph with a synthetic feedstock of composition 15% w/w glucose, 15% w/w fructose using the duolite mean size 420μm resin. The synthetic feed enables a relatively straightforward separation to be studied. With beet molasses the multicomponent nature of the feed added further to the complexities of the operation. These complexities could be seen in the numerous interactive effects (discussed in section (5.1)) which made it somewhat difficult to define the optimum operating conditions.

A simpler separation may simplify the picture and allow a clearer comparison between operations with different particle sized beds. In addition, the glucose-fructose separation has a practical significance when inverted beet molasses feedstocks are used. The bulk prices for both glucose and fructose are higher than for sucrose.

The separation of glucose and fructose is by ligand exchange, the mechanism of which has been outlined in Section (4.3.1.3). To achieve separation the ion-exchange resin needs to be in the calcium form as opposed to the sodium form for the beet molasses separation.

For the glucose-fructose runs a different experimental approach to the factorial design was undertaken. One of the limitations of the factorial method was that each factor such as rotation rate, feed rate etc. was studied at only two levels. In the beet molasses experiment these two levels or values were chosen arbitrarily. If the levels are too wide the likelihood of strong interactions between factors is increased and when an interaction is large the corresponding main effects have less meaning. If the spacing of the levels is too narrow then the conclusions drawn from the experiment are limited by the narrow conditions employed.

For the glucose-fructose runs the base conditions shown in Table (5.14) were chosen.

Table 5.14

Base Conditions for Glucose-Fructose Runs

PARAMETER	VALUE
Rotation Rate	120 Degrees h^{-1}
Feed Rate	4.0 $gmin^{-1}$
Feed Concentration	15% w/w Glucose, 15% w/w Fructose
Eluent Rate	150 $gmin^{-1}$

All the runs were carried out on the Duolite 420μm resin and at 20°C.

Twenty eight runs were undertaken. The feed concentration was maintained at the level shown in Table (5.14) throughout. The remaining three parameters were studied by increasing each on a one at a time basis. Thus while the rotation rate was being studied the other parameters were held at the base conditions. In addition the effect of increasing the rotation rate while keeping the ratio of feed rate to rotation rate (F/ω) constant was studied. Thus as the rotation rate increased the feed rate was also increased so that the feed to rotation rate ratio was constant. Finally, in a series of runs the eluent rate was varied while keeping the ratio of feed rate to the eluent rate (F/V) constant.

The run conditions for each of the twenty eight runs are summarized in Appendix (A.2). For each run the resolution between glucose and fructose was determined. The peak concentrations of each component at the annulus exit are also included in Appendix (A.2).

Figures (5.3) and (5.4) show the resolution and peak exit concentrations respectively plotted against rotation rate. The correlation between rotation rate and these variates is measured by the correlation co-efficient R. When the absolute value of R is unity, the points fall exactly on a straight line and the correlation is exact. When R = O the points scatter widely and the variates are independent. In assessing the significance of the correlation coefficient a statistical table exists (see for example, appendix in Ref (67)) which gives the significant points for various numbers of degrees of freedom.

For example, from Figure (5.3) the rotation rate was varied from 90 to 300 degrees per hour.

The resolution between glucose and fructose over this range can be related to the rotation rate by the equation:

$$\text{Resolution} = 0.40 + 0.0042\ (\text{Rotation Rate})$$

The correlation co-efficient for this relationship is R = 0.67. The equation suggests that the resolution increases slightly as rotation increases but how much confidence can be placed in the equation's validity?

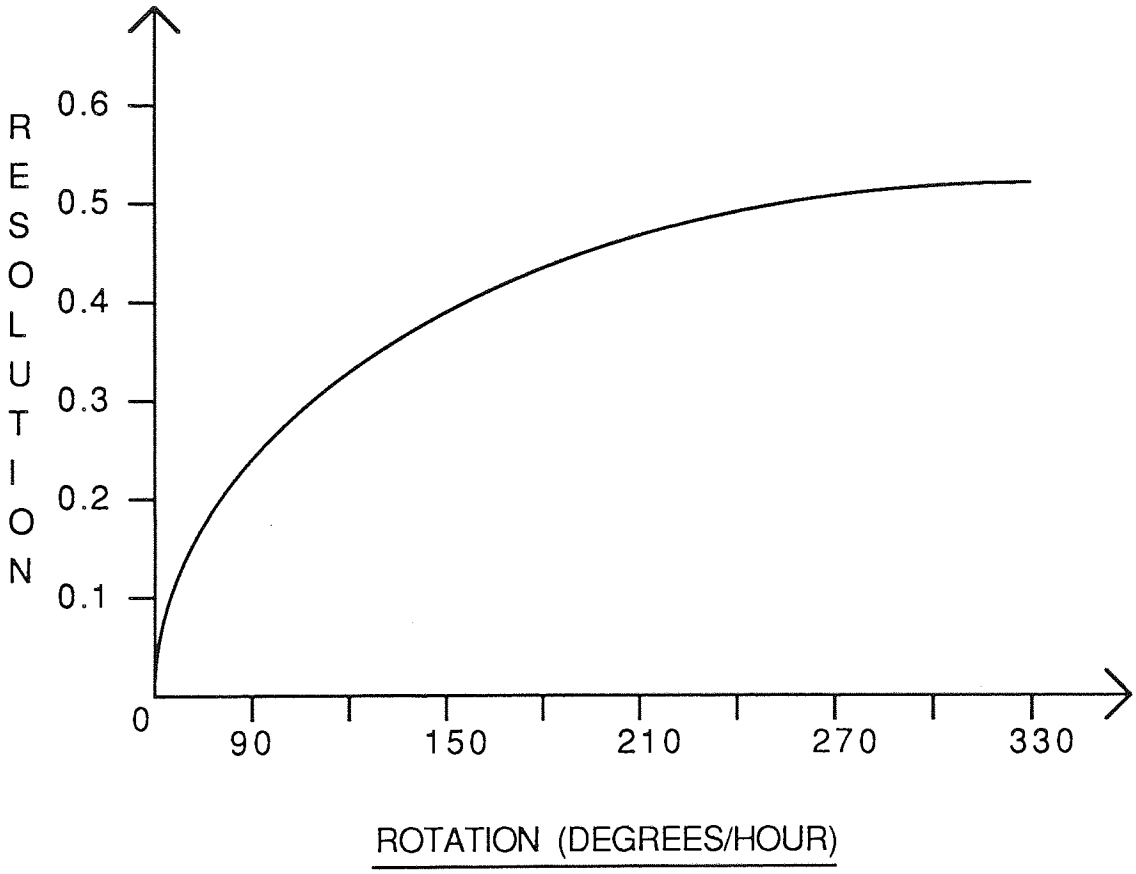

FIGURE 5.3 RESOLUTION VERSUS ROTATION RATE FOR GLUCOSE /FRUCTOSE SYNTHETIC FEED ON DUOLITE(420 MICRON) RESIN

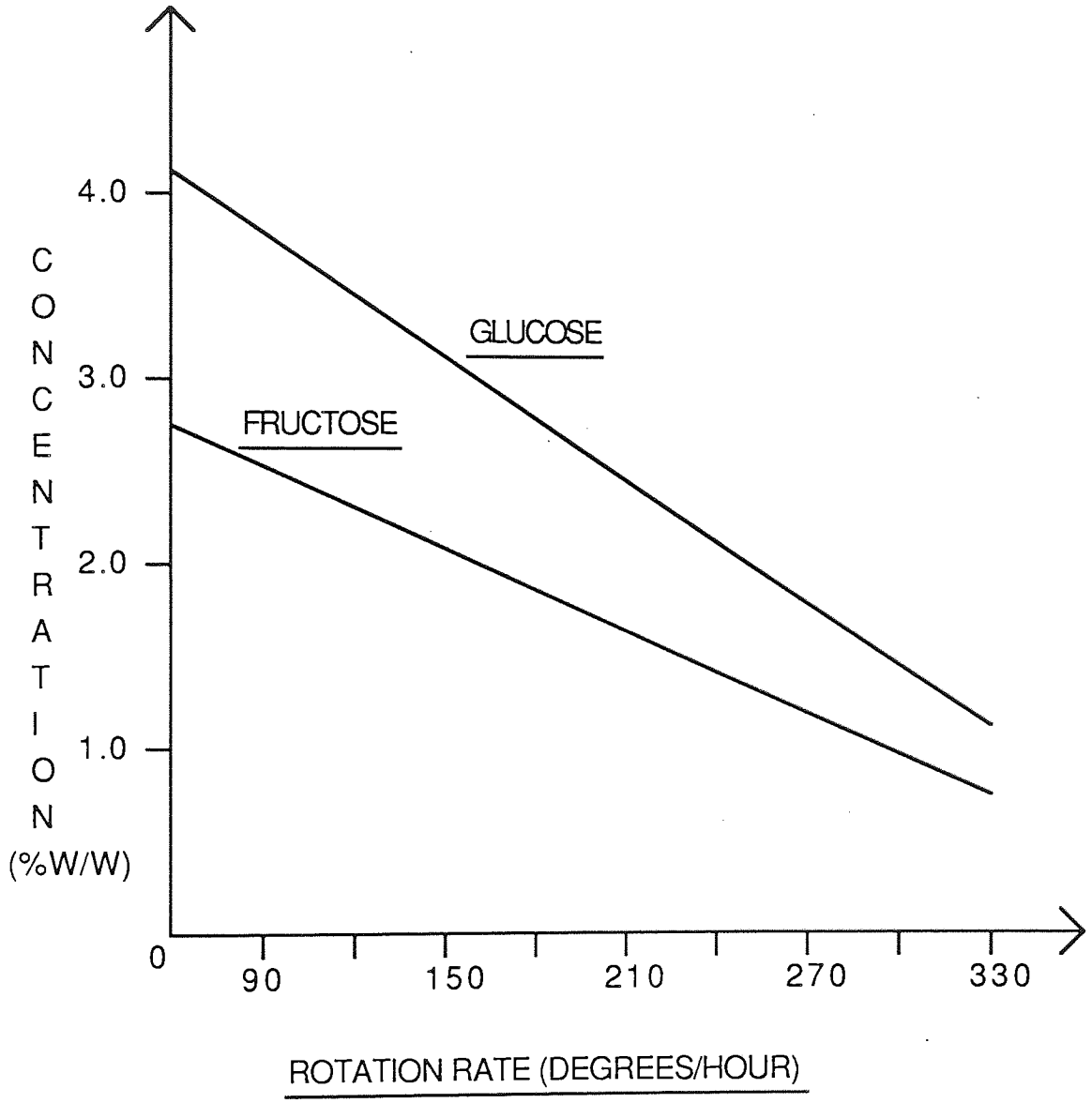

FIGURE 5.4 EXIT PEAK CONCENTRATION VERSUS ROTATION RATE FOR GLUCOSE/FRUCTOSE SYNTHETIC FEED ON DUOLITE(420 MICRON) RESIN

The equation was derived from seven observations and from Table E (67), the 10% significant point is 0.669. Thus there is a 90% probability that the correlation equation given above is valid and that the resolution between glucose and fructose increases slightly with rotation rate.

Figure (5.4) shows the plots for glucose and fructose peak exit concentrations versus rotation rate. The following correlation equations result from the data:

Glucose Peak Concentration (% w/w)

$= 4.6302 - 0.0108$ (Rotation ($°h^{-1}$)) $\quad R = 0.93$

Fructose Peak Concentration (%w/w)

$= 3.224 - 0.0079$ (Rotation ($°h^{-1}$)) $\quad R = 0.88$

The respective correlation co-efficients show that the two correlations are highly significant so that the peak concentrations of each solute decrease as the rotation rate increases.

In the previous experimental section (5.1) with beet molasses feed it was suggested that according to the plate theory the resolution between solutes tends to zero as rotation rate tends to zero but that beyond a certain point, as rotation rate increases the resolution is constant. Figure (5.3) shows that above $120°h^{-1}$ the resolution in fact increases slightly which suggests that high rotation rates favour separation. However the improvement is only small and may even be within the limits of experimental error.

There is no doubt though that the peak exit concentrations decrease as the rotation rate increases. This finding was not apparent with the Beet Molasses experiments in Section (5.1). As the efficiency of separation falls the height equivalent of a theoretical plate (H.E.T.P) increases so that the number of theoretical plates, N, in a given length of column decreases. According to

Equation (11), as N decreases, the concentration ratio increases so that where resolution is small the exit concentrations should be high compared to when the resolution is greater. Thus one might expect that the graph of exit concentration versus rotation rate to be the mirror image of Figure (5.3). Figure (5.4) shows a more significant decrease in concentration compared to the small increase in resolution as rotation rate increases. Another feature of Figure (5.4) is that the glucose concentration is greater than fructose. This is because fructose has a higher distribution co-efficient due to its complexation with the ion-exchange resin. As a result fructose is retarded by the resin so that it spends more time within the column compared to glucose. The higher column residence time leads to a greater dilution and therefore lower concentrations at the exit.

Table (5.15) below presents the correlation equations relating glucose/fructose resolutions and exit peak concentrations to the various column parameters. Figures (5.3) to (5.12) are the plots from which these correlations are acquired. Concentration units are % w/w and the abscissa units are those given in each figure. R_{10} is the 10% significant point value for the correlation co-efficient and R_{EX} is the experimentally determined correlation co-efficient. If $R_{EX} > R_{10}$ then the corresponding correlation equation is a reliable estimate of the relationship between X and Y.

Table 5.15

Correlation Equations Relating Glucose-Fructose Resolutions and Exit Peak Concentrations to Column Parameters

Ordinate (Y)	Abscissa (X)	Correlation Equation Y = f (X)	R_{EX}	R_{10}
Resolution	Rotation ($°h^{-1}$)	Y = 0.40 + 0.00042X	0.67	.669
Glucose Concentration (% w/w)	Rotation ($°h^{-1}$)	Y = 4.6302-0.0108X	0.93	.669
Fructose Concentration (% w/w)	Rotation ($°h^{-1}$)	Y = 3.224 - 0.0079X	0.88	.669
Resolution	Feed Rate ($gmin^{-1}$)	Y = 0.592 - 0.0236X	0.77	.729
Glucose Concentration (% w/w)	Feed Rate ($gmin^{-1}$)	Y = 1.8974 + 0.4916X	0.92	.729
Fructose Concentration (%w/w)	Feed Rate ($gmin^{-1}$)	Y = 1.0 + 0.4242X	0.89	.729
Resolution	Eluent Rate (lh^{-1})	Y = 0.6481 - 0.0012 X	0.93	.669
Glucose Concentration (%w/w)	Eluent Rate (lh^{-1})	Y = 4.6901 - 0.0076X	0.82	.669
Fructose Concentration (%w/w)	Eluent Rate (lh^{-1})	Y= 3.8696 - 0.008X	0.93	.669
Resolution	Rotation ($°h^{-1}$)(at Constant F/ω)	Y = 0.4229 + 2.202 x 10^{-4}X	0.25	.582

Glucose Concentration (%w/w)	Rotation ($°h^{-1}$)(at Constant F/ω)	Y= 2.79 + 0.0025X	0.35	.582
Fructose Concentration (%w/w)	Rotation ($°h^{-1}$)(at Constant F/ω)	$Y = 2.267 + 4.329 \times 10^{-4}X$	0.10	.582
Resolution	Feed Rate ($gmin^{-1}$) (Constant F/V)	Y = 0.6815 - 0.0452X	.96	.669
Glucose Concentration (%w/w)	Feed Rate ($gmin^{-1}$) (at Constant F/V)	Y = 2.4465 + 0.2799X	.91	.669
Fructose Concentration (%w/w)	Feed Rate ($gmin^{-1}$) (at Constant F/V)	Y = 1.4988 + 0.2488 X	.82	.669

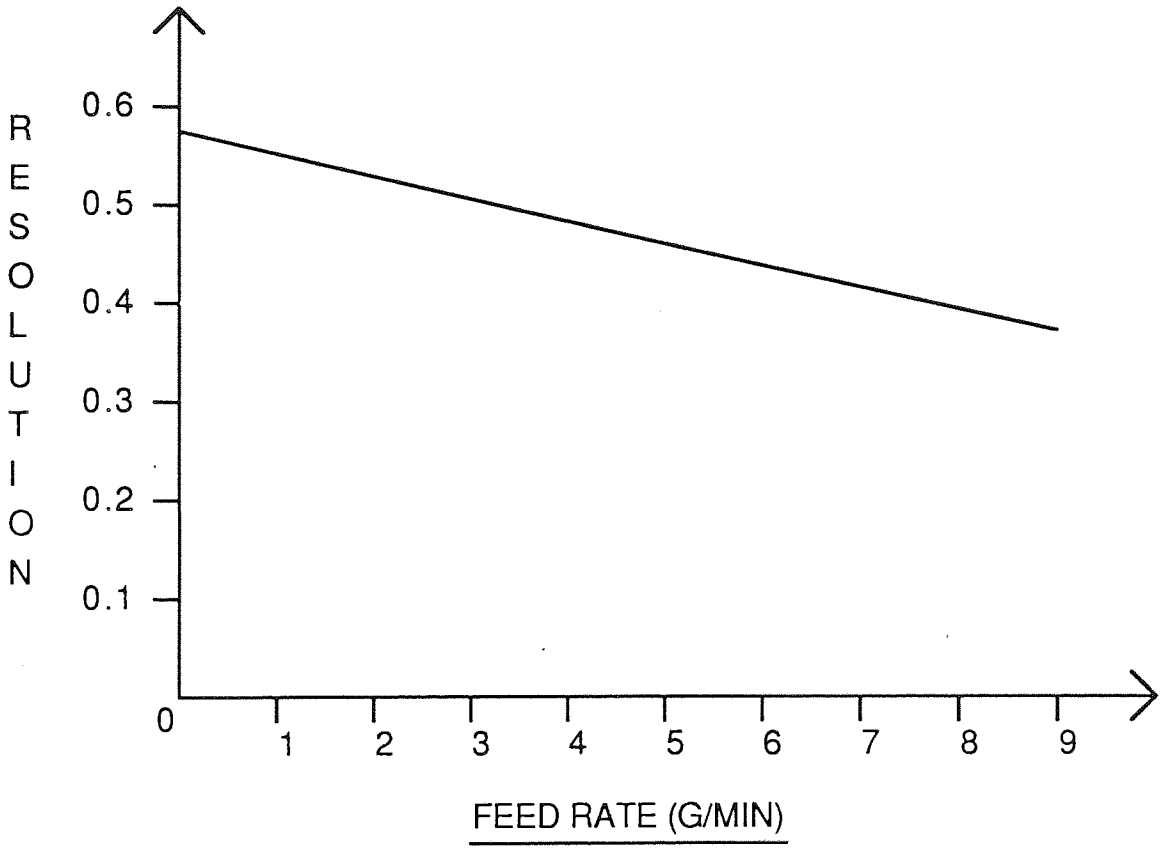

FIGURE 5.5 RESOLUTION VERSUS ROTATION RATE FOR GLUCOSE /FRUCTOSE SYNTHETIC FEED ON DUOLITE(420 MICRON) RESIN

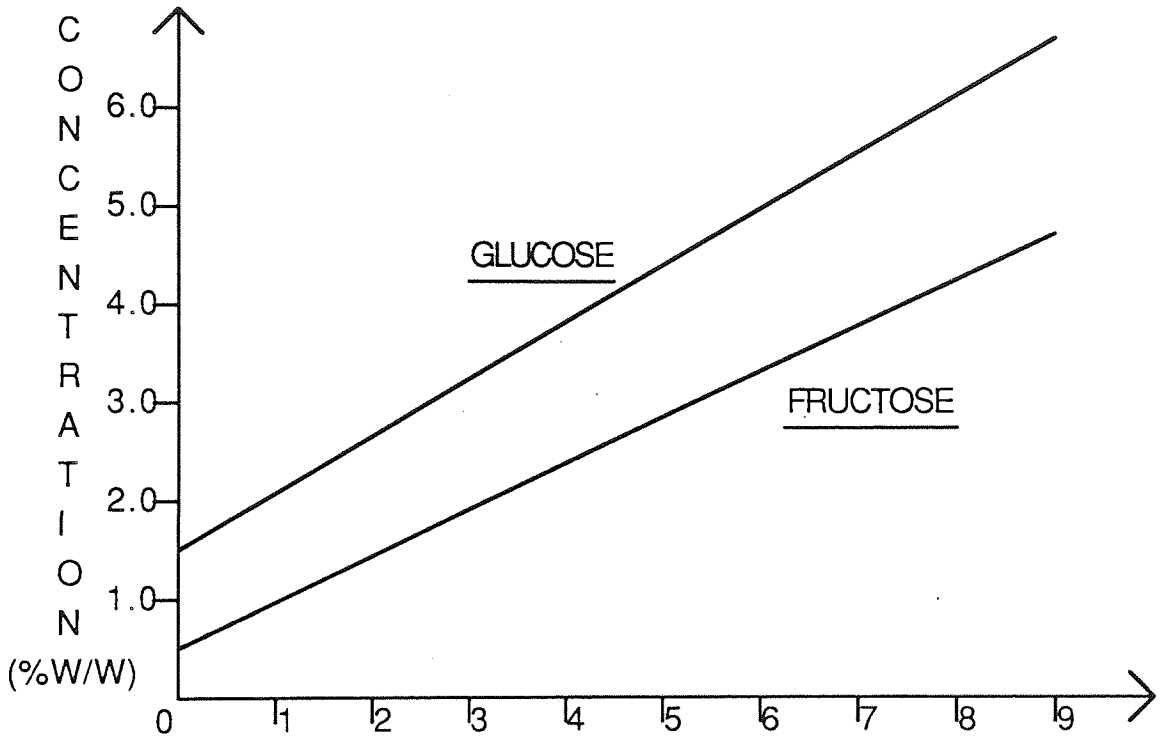

FIGURE 5.6 EXIT PEAK CONCENTRATION VERSUS FEED RATE FOR GLUCOSE/FRUCTOSE SYNTHETIC FEED ON DUOLITE(420 MICRON) RESIN

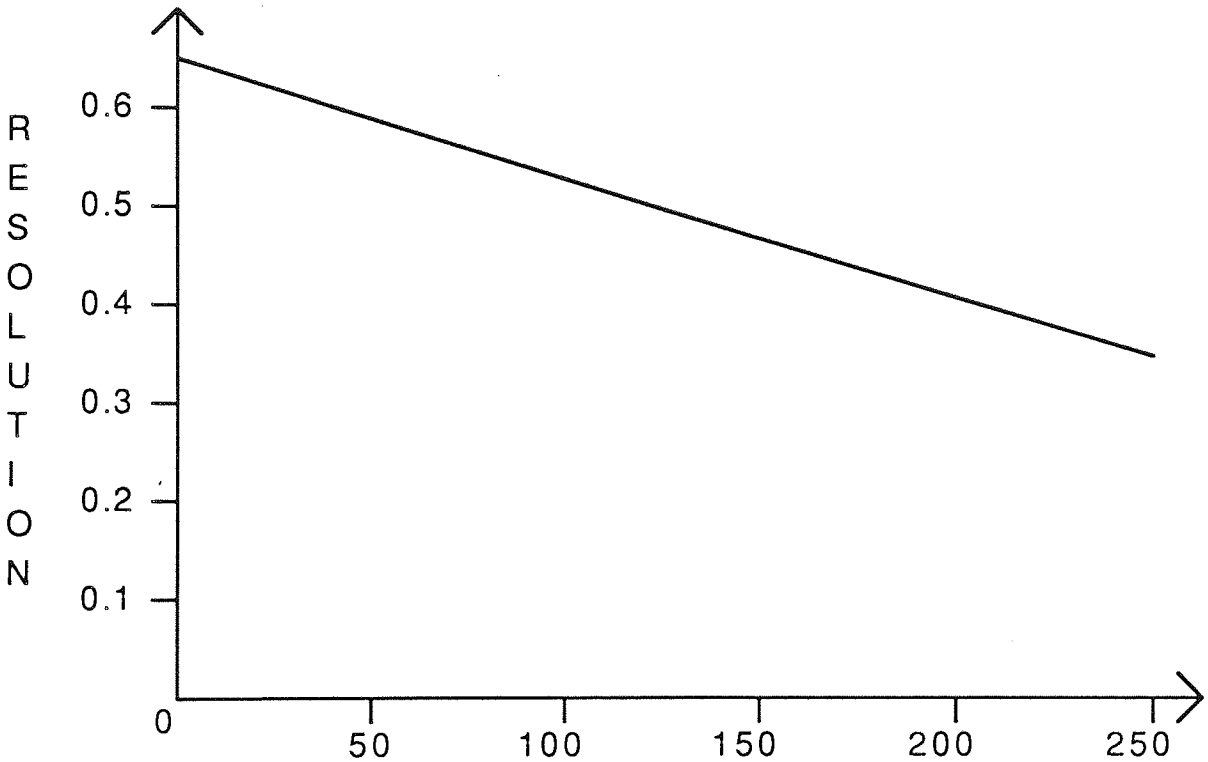

FIGURE 5.7 RESOLUTION VERSUS ELUENT RATE FOR GLUCOSE/ FRUCTOSE SYNTHETIC FEED ON DUOLITE RESIN

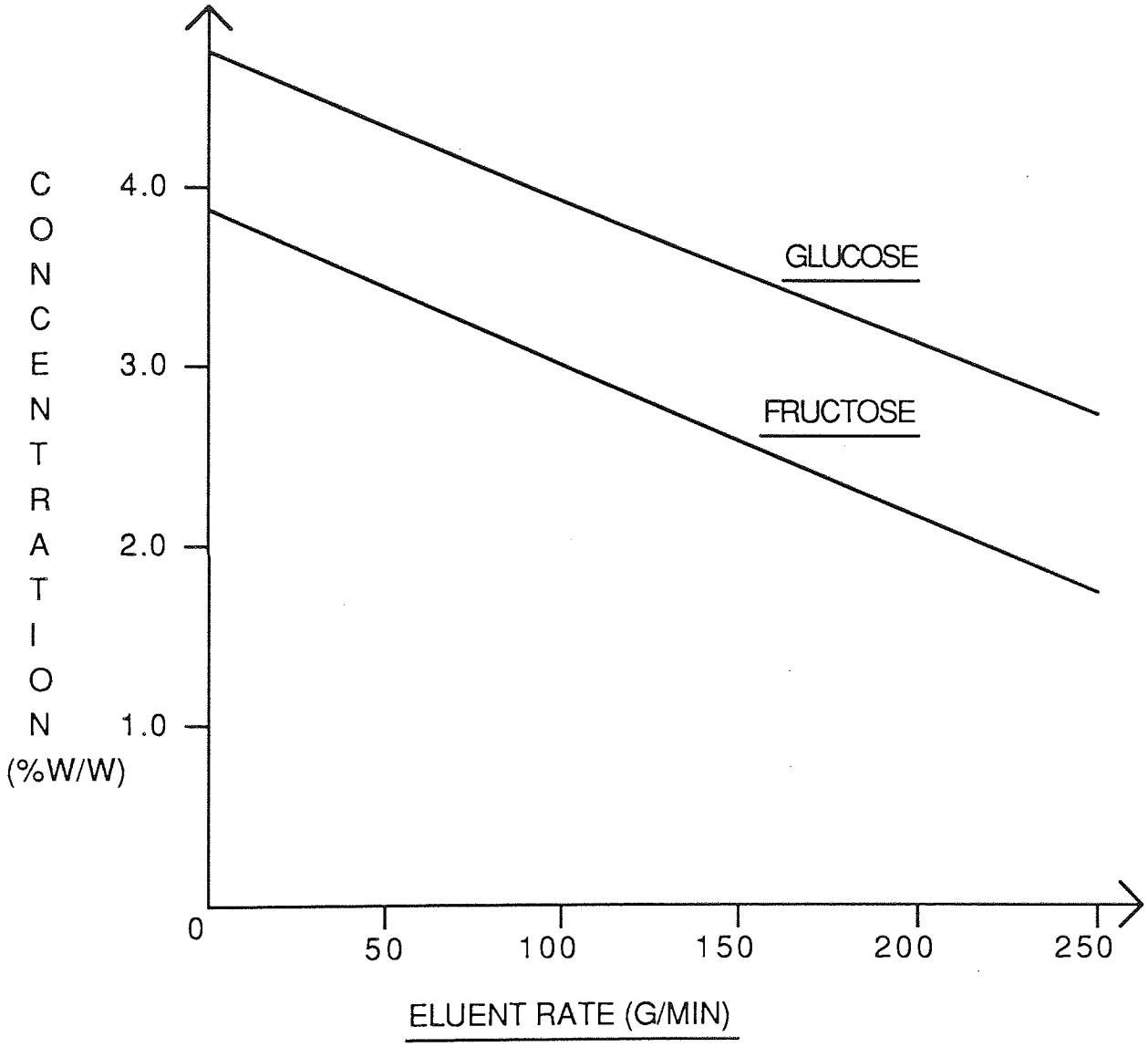

FIGURE 5.8 EXiT PEAK CONCENTRATION VERSUS ELUENT RATE FOR GLUCOSE/FRUCTOSE SYNTHETIC FEED ON DUOLITE (420 MICRON) RESIN

All three equations for the effect of feed rate show reasonable correlations. As the feed rate increases the resolution decreases and such an effect was observed in the beet molasses experiments in Section (5.1). However, the decrease in resolution is not as sharp as the increases in exit concentrations. If the equations were extrapolated outside the range of the data concentrations around 10% w/w would correspond to a resolution of 0.20 which is unacceptably low.

As the eluent rate increases, both resolution and concentrations decrease. Low eluent rates are thus favourable but care has to be exercised if the feed leaving the feed nozzle is not to be allowed to spread to such an extent that some of it escapes from the top of the bed.

One effect of increasing the rotation rate is that the feed is more thinly spread. If the resin bed is ever overloaded such that it has insufficient capacity to separate the feed according to the mechanisms outlined in Section (4.3.1) then the efficiency of separation falls. Overloading, should it occur, would take place at the top of the bed around the feed pipe. Thus as rotation increases the degree of overloading will decrease. However, if the feed rate to rotation rate ratio is held constant so that the quantity of feed per unit volume of bed is constant then the degree of overloading is also constant. Figures (5.9) and (5.10) show the effect of rotation rate at constant F/ω. The data does not correlate very well so that one effect of constant F/ω is that it introduces more scatter into the results. The low correlation between resolution and rotation indicates a less definite relationship than when F/ω was not constant. It is not therefore valid to say that, for example, resolution is constant as rotation increases at constant F/ω. Although the exit concentrations are similarly poorly correlated there does seem to be evidence when comparing Figure (5.10) to (5.4) that the exit concentration is not going to fall significantly as the

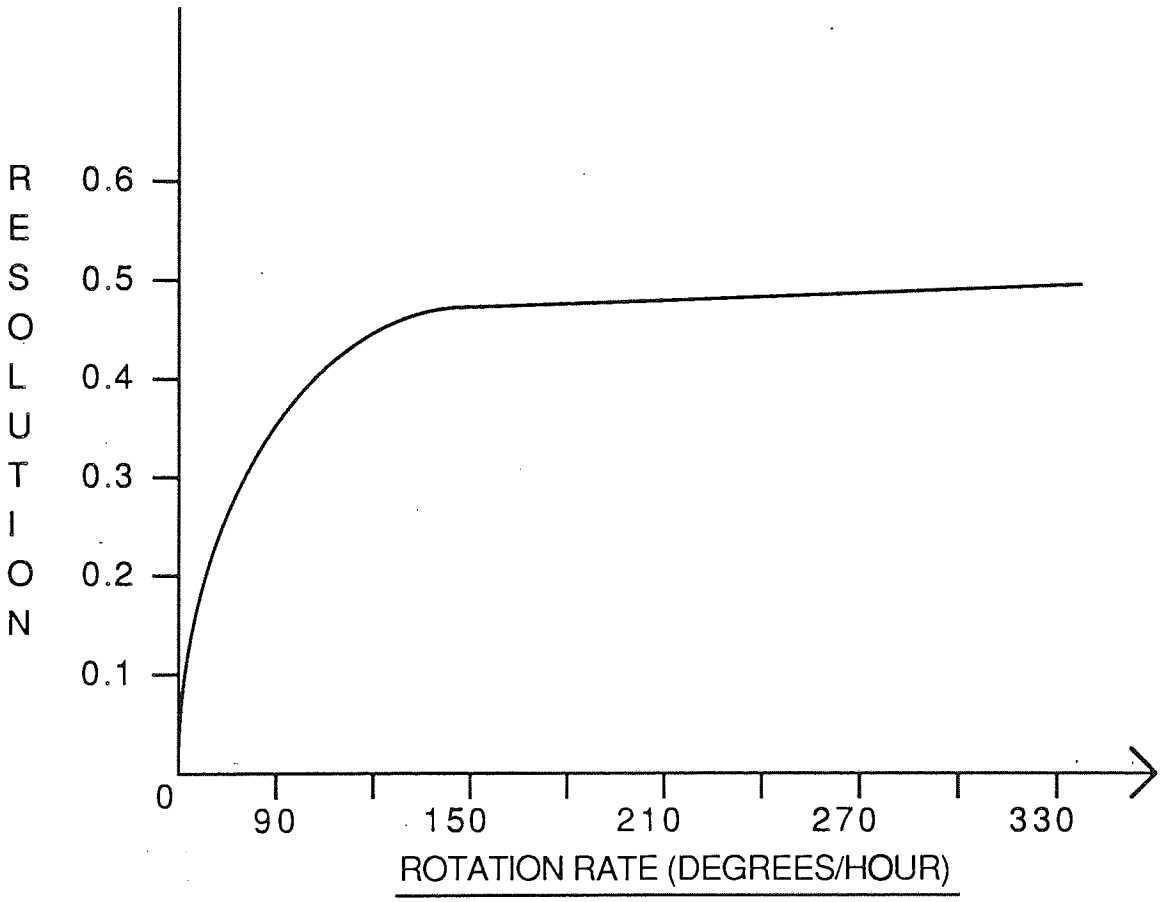

FIGURE 5.9 RESOLUTION VERSUS ROTATION RATE AT CONSTANT FEED TO ROTATION RATE RATIO FOR GLUCOSE/FRUCTOSE SYNTHETIC FEED ON DUOLITE (420 MICRON) RESIN

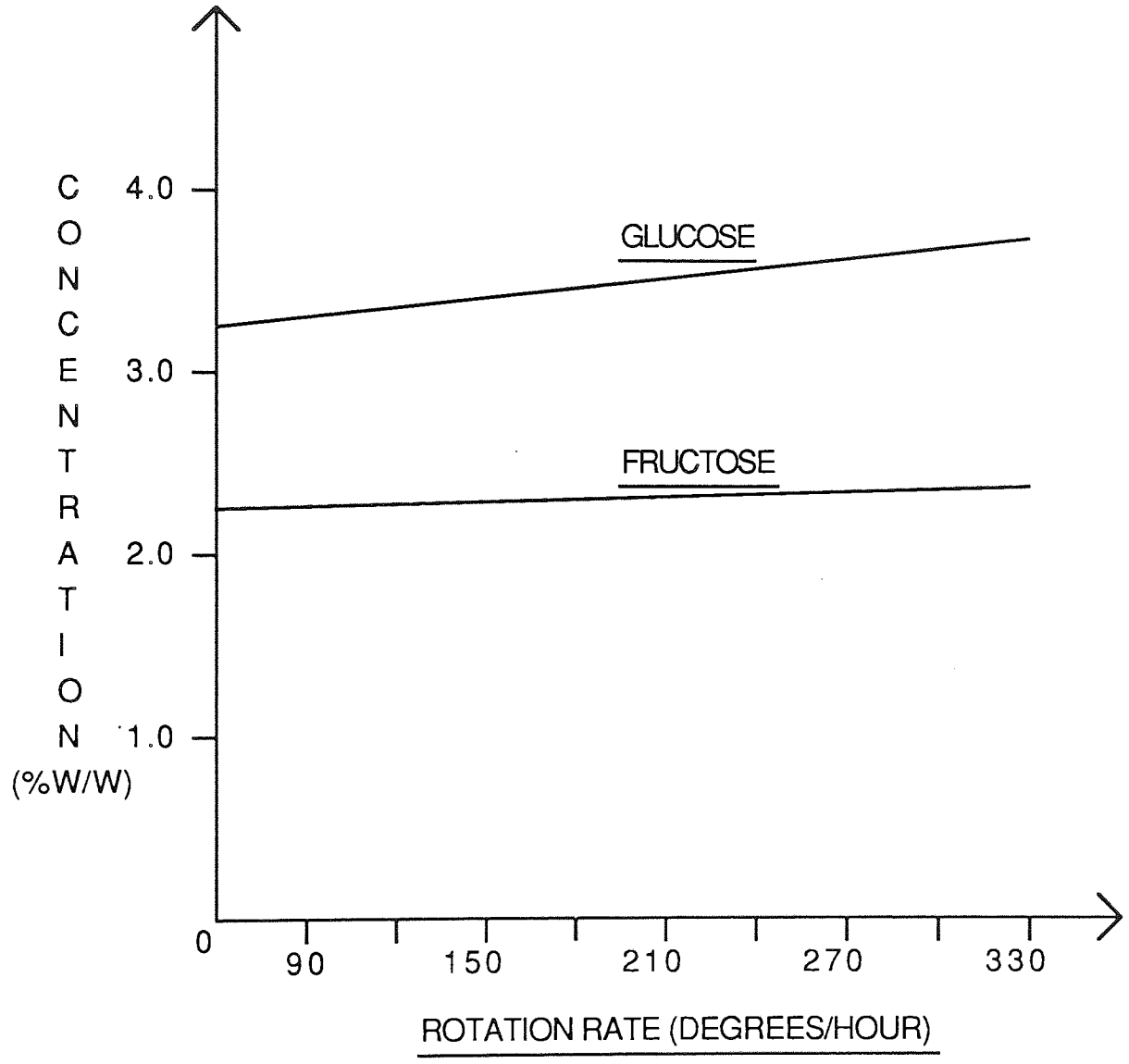

FIGURE 5.10 EXIT PEAK CONCENTRATION VERSUS ROTATION RATE AT CONSTANT FEED TO ROTATION RATE RATIO FOR GLUCOSE/FRUCTOSE SYNTHETIC FEED ON DUOLITE (420 MICRON) RESIN

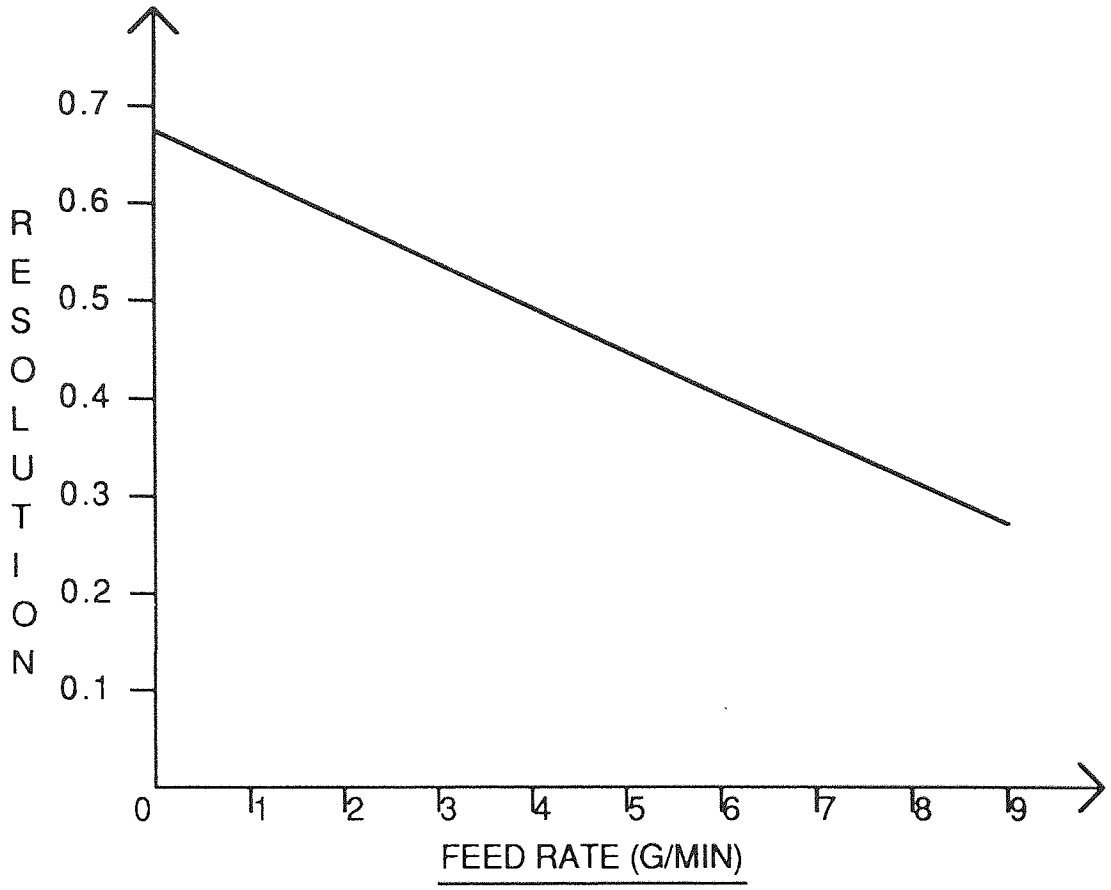

FIGURE 5.11 RESOLUTION VERSUS FEED RATE AT CONSTANT FEED TO ELUENT RATE RATIO FOR GLUCOSE/FRUCTOSE SYNTHETIC FEED ON DUOLITE (420 MICRON) RESIN

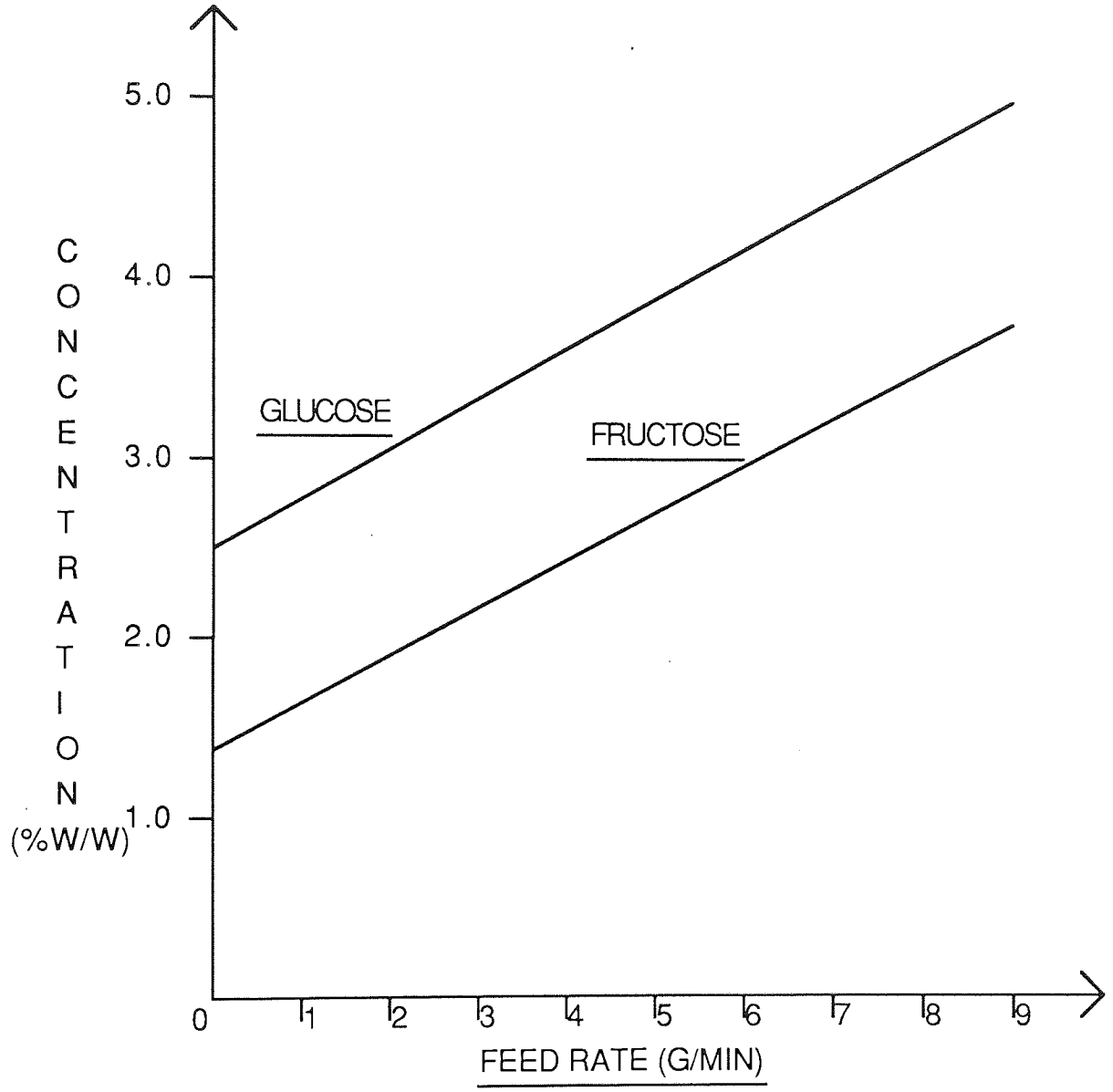

FIGURE 5.12 EXIT PEAK CONCENTRATION VERSUS FEED RATE AT CONSTANT FEED TO ELUENT RATE RATIO FOR GLUCOSE /FRUCTOSE SYNTHETIC FEED ON DUOLITE (420 MICRON) RESIN

rotation increases if F/ω is constant. This seems reasonable, due to an increase in feed flow. Figure (5.10) might be seen as a combination of Figures (5.4) and (5.6) with the diluting effect of high rotation being offset by the concentrating effect of high feed rates.

The effect of varying feed rate while keeping the feed to eluent rate ratio constant is shown in Figures (5.11) and (5.12). The increase in eluent and feed combined cause a more rapid deterioration in resolution than if feed alone is increased and the increase in concentrations is also less marked.

5.2.3. Synthetic Feedstock Runs on Dowex Resin (Mean Size 150 Micron)

The Duolite resin of mean particle size 420 micron was replaced by a Dowex cation exchange resin (Bio-Rad Laboratories Ltd, Watford). The resin had a 4% ratio of divinlybenzene to styrene (4% cross-linkage) and had a mean particle size 150 micron. The following glucose and fructose experiments were carried out using the Dowex resin in the calcium form The run conditions along with resolution and product peak concentrations are tabulated in Appendix (A3). The base conditions shown in Table (5.14) of section (5.2.2) still apply.

Figures (5.13) and (5.14) show glucose and fructose resolution and exit peak concentrations versus rotation rate. The following correlation equations were obtained:

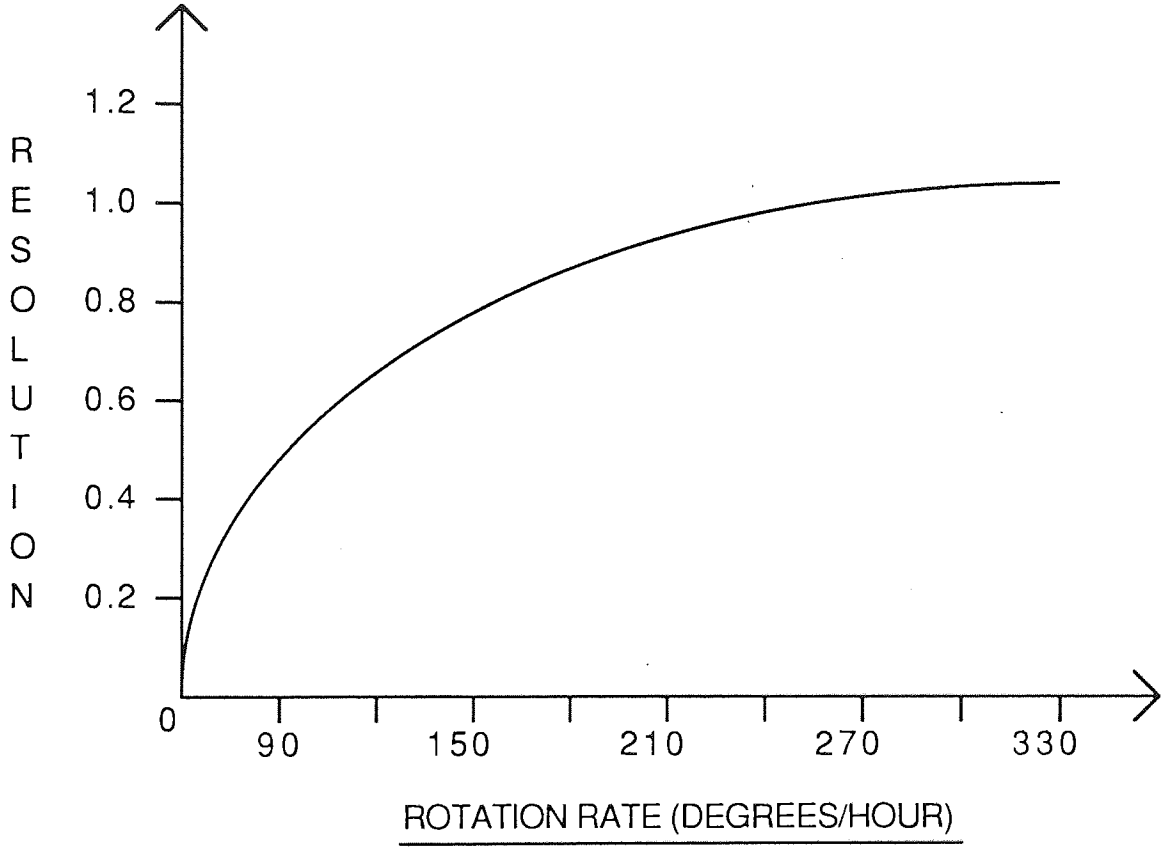

FIGURE 5.13 RESOLUTION VERSUS ROTATION RATE FOR GLUCOSE /FRUCTOSE SYNTHETIC FEED ON DOWEX (150 MICRON) RESIN

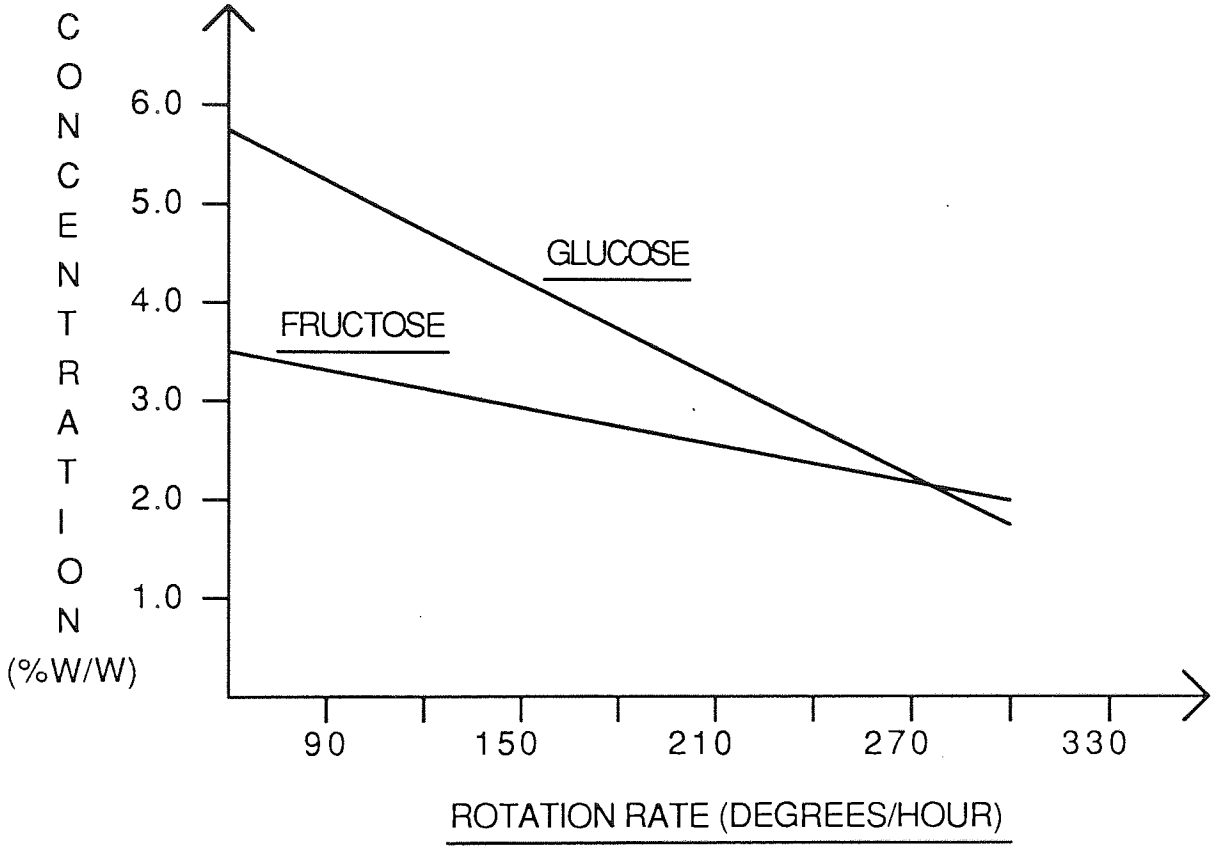

FIGURE 5.14 EXIT PEAK CONCENTRATION VERSUS ROTATION RATE FOR GLUCOSE/FRUCTOSE SYNTHETIC FEED ON DOWEX (150 MICRON) RESIN

Table 5.16

Correlation Equations Relating Glucose - Fructose Resolution and Exit Peak Concentrations to Rotation Rate

Ordinate (Y)	Abscissa (X)	Correlation Equation Y = f (X)	R_{EX}	R_{10}
Resolution	Rotation ($°h^{-1}$)	$Y = 0.844 + 7.13 \times 10^{-4} X$	0.30	.58
Glucose Concentration (% w/w)	Rotation ($°h^{-1}$)	$Y = 5.857 - 0.0138X$	0.84	.58
Fructose Concentration (% w/w)	Rotation ($°h^{-1}$)	$Y = 3.859 - 0.0067X$	0.92	.58

The resolution does not correlate very well but a comparison between Figures (5.3) and (5.13) shows the improvement in resolution achieved using the smaller size dowex resin. An approximate 100% increase in resolution was realized. The low correlation co-efficient was possibly because the column had only recently been packed with a new resin and time has to be allowed for the bed to reach its own "steady state". There is again a weak indication that resolution increase slightly with rotation rate.

The exit concentrations both decrease as rotation increases. This was expected since the same effect was found using the duolite resin. There is an approximately 25% increase in exit concentration with the dowex resin compared to the duolite. A smaller particle sized bed can generally be more tightly packed that a larger sized one. This closer packing reduces the column void volume and reduces the effect of dilution as a result. Thus the benefit of using smaller sized resin is two-fold. The resolution between glucose and

fructose is increased so that a greater percentage of the feed can be recovered as two pure products. In addition the higher exit concentrations would, in an industrial application, reduce the evaporating costs.

The rotation rate was further studied at a lower eluent flow of 100 $gmin^{-1}$. The following correlation equations were obtained:

Table 5.17

Correlation Equations Relating Glucose-Fructose Resolution and Exit Peak Concentrations to Rotation Rate

Ordinate (Y)	Abscissa (X)	Correlation Equation Y = f (X)	R_{EX}	R_{10}
Resolution	Rotation ($°h^{-1}$)	Y = 0.8348 + 0.0023X	.51	.669
Glucose Concentration (% w/w)	Rotation ($°h^{-1}$)	Y = 6.133 - 0.0134X	.94	.669
Fructose Concentration (% w/w)	Rotation ($°h^{-1}$)	Y = 4.8418 - 0.0098X	.83	.669

The trends observed were consistent with the previous findings on the effect of rotation. The resolution again appears to increase with rotation rate but with the lower eluent rate the increase is more pronounced. The resolution - rotation correlation is again not conclusive with considerable scatter existing between the experimental data. This particular correlation has been relatively low throughout the glucose-fructose runs. The concentrations however tend to correlate very well. At the lower eluent rate the concentrations are higher.

There is a proportionally greater increase in the fructose concentration than with glucose. This finding is consistent with the eluent rate - concentration correlation equations derived from runs on the duolite resin.

5.2.3.1 The Effect of Temperature

Fructose in solution can exist in three isomeric forms. The equilibrium concentration of each is temperature dependent and as the temperature rises the percentage of the complex forming isomer, β-D - Fructopyranose decreases. As a consequence the distribution co-efficient of fructose decreases as the operating temperature increases and the glucose-fructose separation becomes more difficult. There are, however, certain benefits to be gained from elevated temperature operation. Higher temperatures can lead to higher rates of mass transfer due to more rapid diffusion. In addition, for viscous feeds such as molasses, the viscosity falls as the temperature rises which makes for less problems with pumps and also within the separation column highly viscous feeds have a tendency to be troublesome. A phenomenon called "fingering" can occur where the feed band breaks up forming several irregular lines. Some of these lines can "slide" over others leading to a confused mode of operation in the region of the feed pipe.

The following correlation equations were obtained for the effect of rotation rate while operating at 50° C.

Table 5.18

Correlation Equations Relating Glucose-Fructose Resolution and Exit Peak Concentrations to Rotation Rate at 50°C

Ordinate (Y)	Abscissa (X)	Correlation Equation Y = f (X)	R_{EX}	R_{10}
Resolution	Rotation ($°h^{-1}$)	$Y = 0.74 + 5.89 \times 10^{-5}X$	0.02	.582
Glucose Concentration (% w/w)	Rotation ($°h^{-1}$)	$Y = 5.1885 - 0.0095X$	0.80	.582
Fructose Concentration (% w/w)	Rotation ($°h^{-1}$)	$Y = 4.4451 - 0.0079X$	0.58	.582

The resolution correlation indicates a very high degree of scatter in resolution data. The reasonable correlations for the concentrations suggest however that the experiments were not subject to unreasonably high variation due to some unmeasured effect. For example, if there was a temperature gradient across the column rather than a uniform 50° C then some variation might be expected in the results. It was however generally the case that the resolution appeared to be a little lower at the elevated temperature.

At higher temperature the peak exit concentrations were higher for fructose but lower for glucose. If the fructose distribution co-efficient was being reduced one would expect that the exit peak position of fructose would be at a smaller angle than for ambient conditions. For both fructose and glucose however the peak position increased by approximately 10° with operation at 50°C. Indeed, the peak positions were found to correlate quite well and it was

scatter in exit bandwidth data that led to the low correlation co-efficient for resolution at 50°C. There was no notable change in the bed as temperature increased, for example, the bed did not expand. It is possible that the unpredictability of the resolution at temperature was due to the various effects of temperature on the mass transfer and distribution co-efficient. Further temperature runs on different feedstocks were proposed and these will be reported upon in another section in this chapter.

5.2.4 Inverted Molasses Separation on Dowex Resin (Mean Size 150 μm)

The inversion of sucrose to form the two monosaccharides, glucose and fructose, was mentioned in section (3.3). The inversion of sucrose in molasses was carried out at the British Sugar Research Laboratories in Norwich. Due to the high concentration of total solids in raw molasses it had to be diluted to approximately 51% w/w solids before the inversion by enzyme took place. The inverted molasses was then concentrated up to 65% w/w solids to prevent microbial growth during storage before use. HPLC analysis showed that this inverted molasses contained 21% w/w glucose, 21% w/w fructose with the remaining 23% w/w solids being made up by principally betaine (approximate 4% w/w), nitrogen free extract and inorganic ash. Prior to a run the inverted molasses was diluted so that the prepared feedstock contained 15% w/w glucose, 15% w/w fructose.

Twelve runs were carried out using inverted molasses. It was of interest to compare these runs with those from section (5.2.3) where a synthetic feed mixture of glucose and fructose was used with none of the interfering ions or coloured solutes etc. The run conditions are outlined in Appendix (A.4). All runs were with the 150μ mean size dowex cation exchange resin in the calcium form. The eluent rate was 150 $gmin^{-1}$ and the feed rate was $4gmin^{-1}$.

The following correlation equations were obtained. The abscissa, (X), was rotation rate ($°h^{-1}$) at 20°C.

Table 5.19
Correlation Equations Relating Resolutions and Exit Peak Concentrations of the Constituents of Inverted Molasses to Rotation Rate

Ordinate (Y)	Correlation Equation Y = f (X)	R_{EX}	R_{10}
Resolution Glucose - Fructose	$Y = .7153 - 3.262 \times 10^{-4}X$	.25	.729
Resolution Ionic - Fructose	$Y = .3206 + 0.0029X$	.83	.729
Resolution Colour - Fructose	$Y = 0.449 + 0.0073X$	.73	.729
Resolution Betaine-Fructose	$Y = 0.227 + 0.0028X$	.58	.729
Glucose Concentration (% w/w)	$Y = 3.7652 - 0.0085X$	.70	.729
Fructose Concentration (% w/w)	$Y = 3.2025 - 0.0069X$	.59	.729
Ionic Concentration (µs)	$Y = 5.4996 - 0.0064X$	.46	.729
Colour Concentration (A)	$Y = 1.2948 + 0.001X$	.18	.729
Betaine Concentration (% w/w)	$Y = .3149 - 8.732 \times 10^{-4} X$	.63	.729

Apart from the glucose-fructose resolution the resolution correlates reasonably with rotation such that as rotation rate increases the resolution increases slightly. With a synthetic feed the correlation equation for glucose - fructose resolution was: $Y = 0.844 + 7.13 \times 10^{-4} X$ and $R = 0.30$. There appears to be a reduction in resolution with the inverted molasses feed which is due to the interference from the remaining constituents. A comparison between exit concentrations also shows that with inverted molasses the concentrations are lower. Thus there is an overall deterioration in performance of the rotating chromatograph when separating the invert molasses feed. The effect of rotation rate however follows the trends outlined in section (5.2.3). The reduction in glucose-fructose resolution shown by the

correlation equation is within the bounds of the scatter of the date as shown by the low correlation co-efficient.

The operating temperature was increased to 50°C and changes in the rotation rate (X) gave the following equations:

Table 5.20
Correlation Equations Relating Resolutions and Exit Peak Concentrations of the Constiuents of Inverted Molasses to Rotation Rate at 50°C

Ordinate (Y)	Correlation Equation Y = f (X)	R_{EX}	R_{10}
Resolution Glucose - Fructose	Y = 0.0235 + 0.0022X	.67	.729
Resolution Ionic - Fructose	Y = 0.3409 + 0.003X	.88	.729
Resolution Colour - Fructose	Y = 0.7856 + 0.0032X	.76	.729
Resolution Betaine-Fructose	Y = 0.321 + 0.0026X	.68	.729
Glucose Concentration (% w/w)	Y = 4.8226 - 0.009X	.97	.729
Fructose Concentration (% w/w)	Y = 4.7106 - 0.0103	.88	.729
Ionic Concentration (µs)	Y = 6.0375 - 0.0077X	.98	.729
Colour Concentration (A)	Y = 3.2348 - 0.0072X	.75	.729
Betaine Concentration (% w/w)	y = .4363 - 0.0052X	.71	.729

In general the 50°C runs correlate well with less evidence of the scatter associated with some of the results at 20°C. The glucose-fructose resolution increases as rotation increases but within the range of rotation rate values used in the experiments the resolution was higher at 20°C. The three remaining resolutions show an improvement in separation at 50°C. Thus high temperature operation at rotation rates over 300° h^{-1} is favourable to running at 20°C. The exit concentrations also increase at the higher temperature

though as rotation increases the concentrations appear to decrease at a faster rate than at 20°C. High temperature operation does offer some advantages with possibly improved separation and more concentrated products. There are also practical advantages to be gained from pumping a less viscous feed.

CHAPTER SIX
LIQUID DISTRIBUTION AROUND THE ANNULUS

6. Liquid Distribution Around the Annulus

6.1 Introduction

When collecting samples for analysis from the 50 exit lines from the annulus the volume of liquid in each collection beaker provided an indication of the uniformity of flow around the annulus. Ideally, when collecting samples from all positions over a specified collection time the liquid volume in each beaker should be approximately equal to the mean liquid volume. Should the liquid volume rise or fall significantly about the mean there is evidence of liquid maldistribution around the annulus. During the course of experiments on the rotating chromatograph it was observed that liquid maldistribution was taking place. To investigate further the main experimental programme was suspended and attention was turned to solving the problem of liquid maldistribution.

Various other workers in the continuous annular chromatography field have experienced difficulties with liquid maldistribution around the annulus. Svensson *et al* (17) found it impossible to get uniform rates of flow through all exits and Moskvin (68) cited non-uniform packing of sorbent as the reason for adverse separation performance and went on to use fabricated blocks of sorbent. Certainly separation will suffer if the liquid is not flowing uniformly throughout the annulus. Each solute in a feed mixture has a specific rate of vertical migration which depends upon its strength of sorption and also upon the mobile phase velocity. If the mobile phase velocity is everywhere constant the solute will acquire its own flow spiral in the rotating column. However if the solute is within a region where the mobile phase velocity is for some reason below average then the migration of the solute will be retarded and separation is made less predictable. It is also essential that separated solutes should not remix at the annulus exit just before leaving the column. At the

base of the annulus there is a groove into which fits a circular ring of porous polyethylene material. The ring sits above 100 exit holes equally spaced around the annulus. Separation is taking place within the annulus up until the ring whereupon the liquid streams through the pores of the 3 mm thick ring and falls through a hole or else has to travel slightly sideways before reaching a hole. The amount of sideways travel has been minimized in the rotating chromatograph by having a flat-bottomed groove design which ensures that at the annulus exit, the exit holes occupy a large percentage of the total annulus area. If this was not the case the sideways travel of liquid streams at the exit could lead to separated solutes being remixed before being able to leave the annulus. A report by C B Euston *et al* (69) failed to find the cause of maldistribution in their annulus after repacking several times and also after attempting to force their annulus into a more perfect shape. In their case the problem of maldistribution was so severe that they abandoned the apparatus altogether.

6.2 Liquid Maldistribution in the Rotating Annular Chromatograph

The problem of liquid maldistribution was identified by having the annulus stationery and flowing eluent only through the system. Fifty 250 ml collection beakers were positioned to receive the eluent at the annulus exit. Collection of eluent took place over a specified time after which the fifty beakers were weighed. Figure (6.1) shows a typical liquid profile with mass of liquid collected being plotted against collection position where position one is directly below the feed pipe. As the figure shows there is considerable deviation in mass collected. Only 42% of the collected weights were within ± 20% of the mean 88 grams. Such a liquid distribution profile is unacceptable

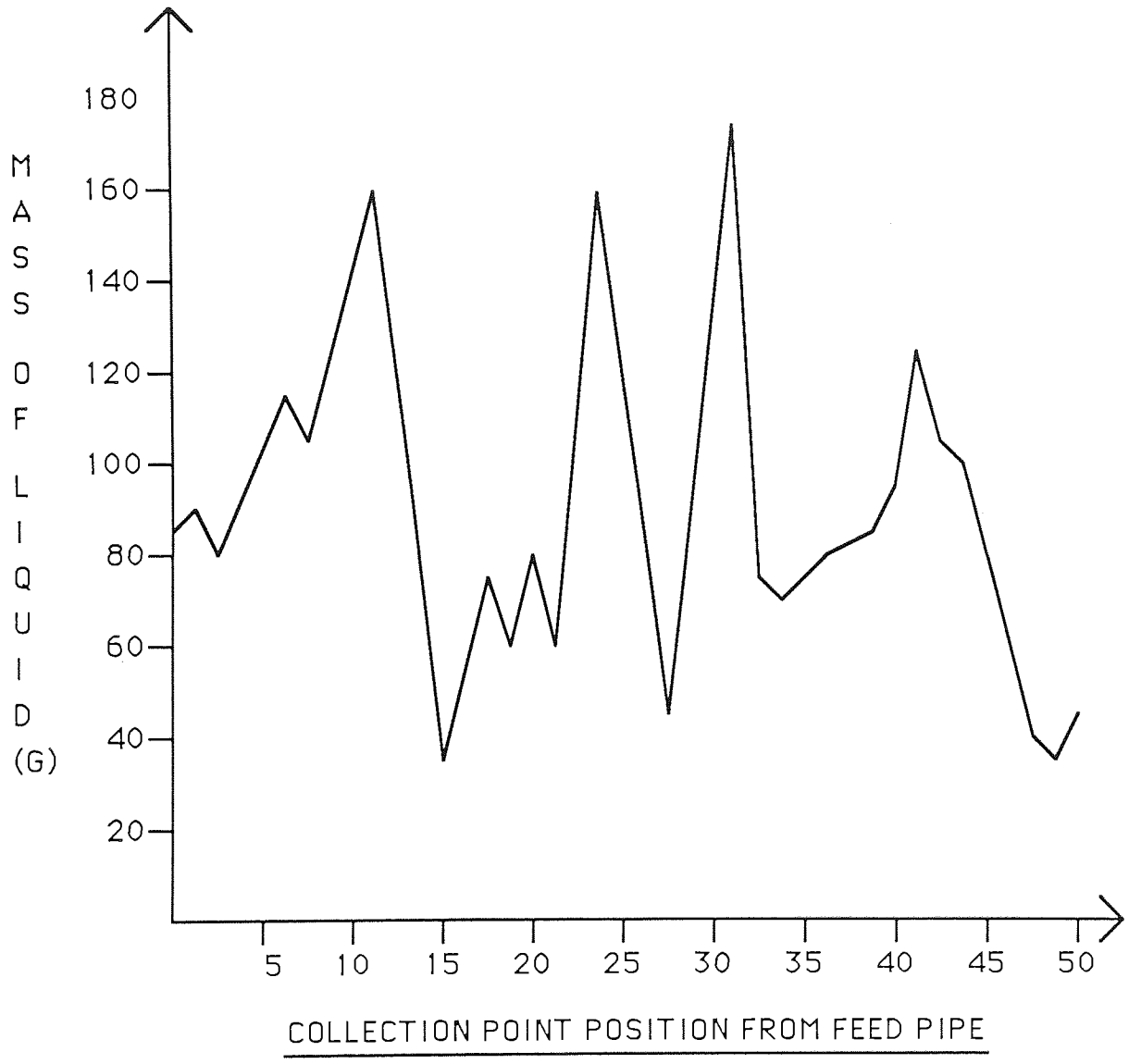

FIGURE 6.1 LIQUID DISTRIBUTION AROUND STATIONARY ANNULUS

with regards to measuring the separation performance of the annular chromatograph. In addition the profile marks a deterioration in distribution from an initially relatively even distribution when experiments on the chromatograph commenced. Thus time becomes a variable in experiments unless a means can be found to maintain indefinitely an even liquid distribution.

To test whether the profile shown in Figure (6.1) was caused by non-uniformities in the packing a solution of blue dextran was prepared and temporarily introduced as eluent into the stationary annular chromatograph. After the blue dextran the normal de-ionised water eluent was re-introduced. The blue dextran appeared in the sorbent bed as a blue band the front of which could be followed as it progressed down the bed. This front remained as a uniform ring around the annulus throughout the length of the bed. If the packing had been non-uniform the flow in some sections of the bed would have been greater than in others and the blue dextran front would advance at a greater rate in areas of high flow. As a result the front would break up and be uneven around the annulus. The fact that the blue dextran front remained uniform was indicative of a uniformly packed bed. However, as a further test the annulus was repacked. Uniformity in packing only needs to be attained horizontally and this can be visualized in the annulus as a series of horizontal rings which segment the bed vertically. Such a uniformity is achieved by slurry packing the annulus whilst rotating the annulus at a high rate. After repacking, the liquid distribution was found to be not significantly different from that shown in Figure (6.1). Subsequent repackings produced no improvement. Thus it was concluded that the liquid maldistribution evident in Figure (6.1) was not being caused by packing non-uniformities. The problem it was thought must lie with the porous polyethylene ring. Blockages in the ring would cause uneven liquid flow through it. It was not possible to examine

the porous ring without undertaking a major overhaul of the chromatograph. If the porous ring was blocked it might be possible to unblock it by using the backflush ring. The backflush ring fits underneath the annulus and was normally used to backflush the resin bed in order to remove fines and to re-stratify the bed. The porous ring was backflushed in-situ and the annulus was again re-packed. Subsequent liquid distribution analysis again showed no effective improvement over the distribution showed in Figure (6.1).

It was decided to overhaul the column to gain access to the porous polyethylene ring so that it could be examined under a scanning electron microscope (S.E.M.). S.E.M. analysis showed that the pores in the polyethylene ring were smaller by comparison with an unused sample of material. The pores had possibly been closed up by the effects of compression caused by the weight of the packed bed. However no evidence of blockages by extraneous matter could be seen although observation was hindered by the somewhat murky picture produced by the S.E.M. The pore size of an unused sample of porous polyethylene was difficult to define though an average of 70 microns was assigned. It was not possible to see directly through the 3 mm thick sample for the pores were interlinked in various directions so that liquid flowing through would have to follow a tortuous path. By comparison a 100 micron nylon mesh had a uniform and clearly definable pores size through which light readily passed. It was thought that this mesh was less prone to plugging by fines and would be a suitable alternative packing support medium. A mesh ring was cut and fitted into the annulus covering the exit holes and the entire chromatograph was re-assembled. Eluent was pumped through the system and the liquid distribution was found to be significantly worse than shown in Figure 6.1. Approximately 60% of the 100 exit holes had no liquid flowing through them and the bulk of the eluent flowed through only about 10 holes.

The problem of liquid maldistribution required further analysis but the somewhat unwieldy nature of the rotating annular chromatograph made analysis difficult. To investigate further a smaller test rig was designed and built which modelled the requisite features of the larger annular chromatograph.

6.3 A Test Rig to Study Liquid Distribution

The test rig was designed to be a scaled down model of the rotating annular chromatograph. The ratio of annulus area to bed length was the same for both units. The test rig annulus area was approximately 42 cm^2 and its bed length was 45 cm. The test rig annulus accommodated 36 exit holes. 6 cm diameter equi-spaced on a 14.4 cm pitch circle diameter. Although designed to be a model of the larger unit the test rig did incorporate some modifications to enhance portability and experimentation. One feature was that the packing support medium could be in the form of a ring or as discs. Two distributors, one for rings and one for discs were designed to fit into the base of the annulus and to provide a suitable seal between the inner and outer annulus walls. A pressure gauge was fitted to measure the pressure drop across these distributors. The pressure drop over the whole unit was measured by a gauge fitted into a top cover. The top cover screwed into the inner pipe and was sealed by a neoprene gasket against the outer pipe. Apart from the outer pipe which was constructed from PVC the remaining parts were of galvanised carbon steel. The test rig was designed to an operating pressure of 3 bar.

From observations made with the rotating annular chromatograph it was not considered necessary that the test rig should be able to rotate. Thus a means to rotate the test rig was not incorporated into the design. In effect the test rig

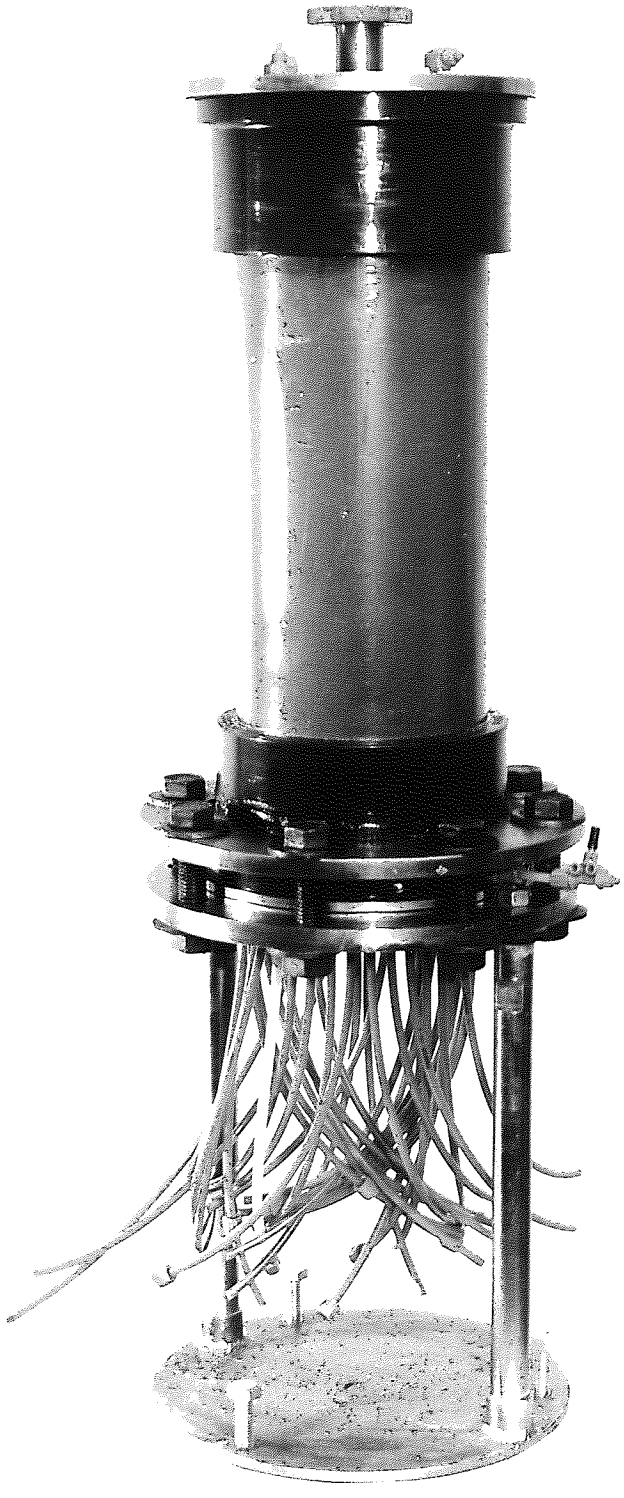

PLATE B TEST RIG

was not a chromatograph for it had no feed pipe either and the only fluid to be introduced into the rig was the eluent. Plastic pipes fitted into the holes underneath the annulus and the eluent ran through these into 36, 250 ml collection beakers. The liquid distribution profile was obtained by weighing the quantity of eluent collected in each of the 36 beakers over a specified time.

6.4 Experiments on the Test Rig

A ring of porous polyethylene of pitch circle diameter 14.4 cm was cut and fitted into the "ring" distributor. The test rig annulus was assembled with the "ring" distributor in place and the annulus was packed with Dowex Cation exchange resin. This resin had a mean particle size of 150 micron and had been used in experiments to separate carbohydrate feedstocks on the rotating annular chromatograph.

Liquid distribution was measured by pumping de-ionised water eluent through the test rig and collecting the eluent in 36 collection beakers located beneath the exit holes. Collection took place over a specified time after which the beakers were weighed. The liquid distribution was measured as a percentage of the collection beakers whose collected weights were within $\pm$ 20% of the mean.

The first experiment was designed to study liquid distribution with time. The liquid distribution was periodically measured over a succession of days and the pressure drops over the distributor and over the column were also recorded. Table (6.1) shows the results for this experiment. On day one for example 70% of the beakers had collected weights to within $\pm$ 20% of the mean. The remaining 30% of beakers and hence 30% of the annulus were

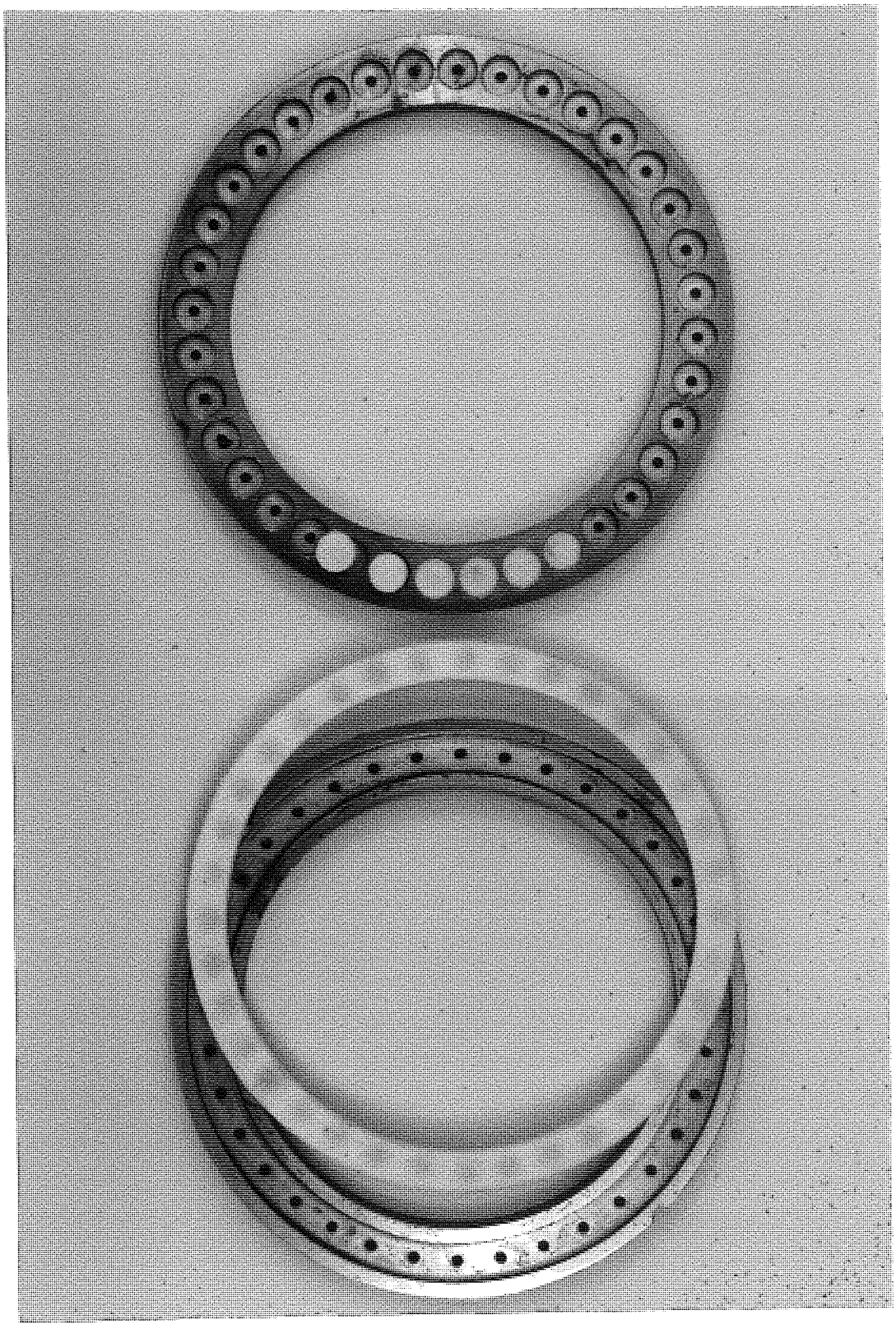

PLATE C RING AND DISC DISTRIBUTORS

suffering from liquid maldistribution. The eluent flowrate was constant throughout. From Table (6.1) the liquid distribution deteriorated with running time. After ten days of continuous running only 8% of the liquid was evenly distributed which represents severe maldistribution. The pressure drop over the column was entirely due to the pressure drop over the porous distributor. The test rig modelled the rotating annular chromatograph in that liquid distribution tended to deteriorate over time. Although liquid maldistribution occurred after only several days compared to months of operation with the larger unit, it was after continuous eluent flow rather than the intermittent operation of separation experiments. The increase in distributor pressure drop at constant eluent flow suggests that the distributor was becoming blocked. Examination of the porous ring showed it to be a dirty grey colour. The discolouration and blockages were believed to be caused by the de-ionised water eluent. Two 6 mm diameter porous polyethylene discs were punched out and fitted into the eluent pump delivery line and then the above experiment was repeated. The two discs were to act as in-line filters. Table (6.2) shows that the liquid distribution was invariant with time and that the distributor pressure drop was negligible. The in-line filter discs had to be regularly changed because they blocked quite rapidly creating very high pressure drops over the discs.

Table 6.1
Liquid Distribution Measured with Time
(No In-Line Filters)

Day Number	% Beakers with ± 20% of Mean	Pressure Drop Across Distributor Pdist (psi)	Pressure Drop Across Column Pcol (psi)
1	70	0	0
2	63	1	1
3	60	1	1
4	60	1	1
5	52	3	3
6	47	5	5
7	36	8	8
8	19	13	13
9	8	21	21
10	8	21	21

Table 6.2
Liquid Distribution Measured with Time
(With In-Line Filters)

Day Number	% Beakers with ± 20% of Mean	Pressure Drop Pdist (psi)	Pressure Drop Pcol (psi)
1	68	0	0
2	65	0	0
3	66	0	0
4	71	1	1
5	64	1	1
6	65	1	1
7	70	1	1

The problem of liquid maldistribution was being caused by fines introduced with the eluent clogging up the porous distributor. Although the eluent was de-ionised water, further filtration to remove fines was required. The porous polyethylene was thought to be a suitable filter for this purpose.

The results in Table 6.2 indicate that the liquid distribution was not uniform around the entire annulus of the test rig. Ideally the percentage of the collected weights in the beakers within $\pm$20% of the mean needed to be nearer 100%.

The results in Table (6.1) and (6.2) were for when a ringed liquid distributor was in place. The test rig had the facility to test porous discs as an alternative distributor configuration. Thirty-six 6mm diameter discs were punched out of the porous polyethylene material and inserted into the disc distributor which was then fitted into the base of the test rig annulus in place of the ring distributor. As before, eluent was passed through the system and the liquid distribution was measured periodically. The results for discs were comparable to those for the ring configuration and there appeared to be no advantage with regard to liquid distribution in using discs or a ring.

A porous teflon material was also tested as a possible alternative distributor to the porous polyethylene. The porous teflon had a similar pore size to the polyethylene, approximately 70 micron, and was a similar thickness, approximately 3 mm. In experiments on the test rig the teflon gave comparable results to the polyethylene so that no advantage was gained from using it as a replacement distributor material.

In the experiments outlined above the eluent flowrate was constant. In Table (6.1) the distributor pressure drop increased with time but the increase was caused by the blocking of the distributor pores by fines. Such blockages are

by nature randomly distributed so that the distributor effectively loses it uniform porous structure. By increasing the eluent flowrate the pressure drop over the distributor is increased while the distributor's uniform porous structure is maintained. Table (6.3) shows the results from experiments on the test rig studying the effect of eluent rate on liquid distribution.

Table 6.3
The Effect of Eluent Flowrate on Liquid Distribution

Eluent Flow ($Gmin^{-1}$)	Pdist (psi)	% Beakers within ± 20% of Mean
50	0	62
75	1	68
100	2	67
150	4	69
200	5	72
250	7	74
300	8	77
350	9	78

In this particular experiment porous polyethylene discs were used as distributor material.

As the eluent flowrate increased the distributor pressure drop increased and the liquid distribution improved.

6.5 Discussion of Results from Test Rig Experiments

In a packed bed, the flowpath is made up of many parallel and interconnecting channels. The channels are not fixed in diameter or direction. In flowing through these passages the fluid phase is repeatedly accelerated and experiences repeated kinetic energy losses. In addition the rough surfaces of the bed particles produce form drag and skin friction losses. Thus it is apparent that the bed develops a variety of pressure patterns which induce varying flows through different parts of a packed bed. If the bed is poorly packed these flow fluctuations lead to serious liquid flow maldistribution. However, even a well packed bed inevitably induces flow variations but these variations are normally insignificant and are corrected by increasing the pressure drop over the packing support (or distributor). As the distributor pressure drop increases the oncoming fluid is forced to re-arrange itself so that an equal amount is approaching each opening. Therefore, if the flow resistance across the distributor is greater than the resistance of the fluid to re-arrange itself, the re-arrangement takes place and an even liquid distribution through the distributor results. This is so because under these conditions, the path of least resistance to the total flow crossing the distributor is an equal flow through each opening. If the resistance through the distributor is negligible - such as was the case with the nylon mesh which was tested in the rotating annular chromatograph - the fluid is not forced to re-arrange itself and the flow through the distributor becomes unpredictable.

Apart from preventing leakage of solids from the annular bed it is apparent that the bed support must also act as a liquid distributor at the annulus exit. To function effectively the distributor pressure drop must be high enough so that the flow variations induced in even the most well packed beds are insignificant. The porous polyethylene material offers a greater resistance to

flow than the nylon mesh and is therefore a better distributor. Provided the porous polyethylene remains unblocked and maintains a uniform porous structure it gives acceptable liquid distributions at the annulus exit. The liquid distribution is improved when the distributor pressure drop is increased by increasing the eluent flowrate.

6.6 Implementation of Test Reg Findings

Two 20 mm diameter porous polyethylene discs were fitted into the feed and eluent pump delivery lines to serve as in-line filters. The pressure drop over these filters was measured and indicated when a particular disc was so blocked it needed replacing.

Despite taking the precaution of in-line filtering it was thought that some fines would still find a way into the annular chromatograph eventually blocking the porous packing support. Consequently the porous support would need replacing if it could not be unblocked in-situ. The unwieldy nature of the rotating annular chromatograph had previously made gaining access to the porous support a time consuming operation. A stainless steel ring was designed to fit externally underneath the lower stainless steel flange. The ring was 6 mm thick and on a circle of pitch diameter were drilled into the ring one hundred diameter holes to a depth 3 mm. The remaining 3 mm depth of the ring was drilled with holes 3 mm diameter thereby creating a recess into which fitted one hundred 6 mm diameter porous polyethylene discs. The holes in the stainless steel ring aligned with the exit holes in the lower flange. The ring was attached to the flange using allen screws with a neoprene rubber gasket sealed between the two metal surfaces.

Now that the porous polyethlene was housed in this stainless steel ring access to the polyethylene was more readily gained. By fitting a ring of nylon mesh to act as a packing support inside the annulus the discs fitted externally functioned as a liquid distributor at the chromatograph's exit.

After re-assembly the liquid distribution around the annulus was tested periodically over several days. The liquid distribution was found to be uniform and this uniformity was maintained throughout the experiments to be described in Chapter 7.

CHAPTER SEVEN

7 The Separation of Sucrose from Beet Molasses (2)

7.1 Introduction

Following the equipment modifications discussed in Chapter (6) the rotating annular chromatograph was used again to separate sucrose from beet molasses. All the runs in this section were carried out at 20° C and the results are in Appendix (A.5).

7.2 The Effect of Rotation Rate

From Table (7.1) the three resolution correlation equations support previous findings that as the rotation rate of the annular chromatograph increases the resolution between solutes increases. As with previous experimental findings the solute peak exit concentrations decrease as rotation increases . The correlation co-efficients for the various concentration equations show a considerable improvement compared to those for the inverted molasses runs discussed in section (5.2.4). This improved correlation is possibly a result of the improved liquid distribution. When liquid maldistribution was being experienced the operation of the rotating chromatograph was time dependent. Once maldistribution started to occur it generally worsened with increase use of the column so that repeatability of results was not satisfactory. The introduction of time as a variable leads to considerable scatter in experimental data and to the low correlation co-efficients previously experienced.

7.3 The Effect of Feed Rate

From Table (7.1) the resolution between sucrose and non-sugars in beet molasses constituents decreases as feed rate increases.

The correlation equations for the peak concentrations also indicate that the concentration increases as feed rate increases. However, Figure (7.1) shows that although there is a reasonable straight line correlation between sucrose concentration and feed rate a better correlation is given by the polynomial:

$$\text{Sucrose Conc.} = -0.6048 + 2.2988\,(\text{Feed Rate}) - 0.1751\,(\text{Feed Rate})^2 \qquad (R = 0.91)$$

The expression suggests that an optimum feed rate exists after which the sucrose exit concentration tends to decrease with increasing feed rate.

The maximum points for the sucrose polynomial is 6.56 which indicates that the optimum feed rate lies somewhere near this value. As the feed rate is increased above the optimum the deterioration in separation performance offsets the increase in exit concentration caused by higher feed rates.

7.4 The Effect of Feed Concentration

From Table (7.1) the effects of feed concentration and feed rate are found to be similar. The various resolutions between sucrose and the remaining solutes decrease as the concentration increases. However, the exit concentrations for sucrose and betaine have maximum values at feed concentrations 33% and 34% w/w sucrose respectively. At concentrations above these values the exit concentrations tend to decrease. Thus the feed concentration and feed rate have similar effects upon resolution and exit concentration. In particular, there is a limit to the exit peak concentration of sucrose attainable. Once this limit is reached further increases in either feed rate or feed concentration has the effect of decreasing exit concentration.

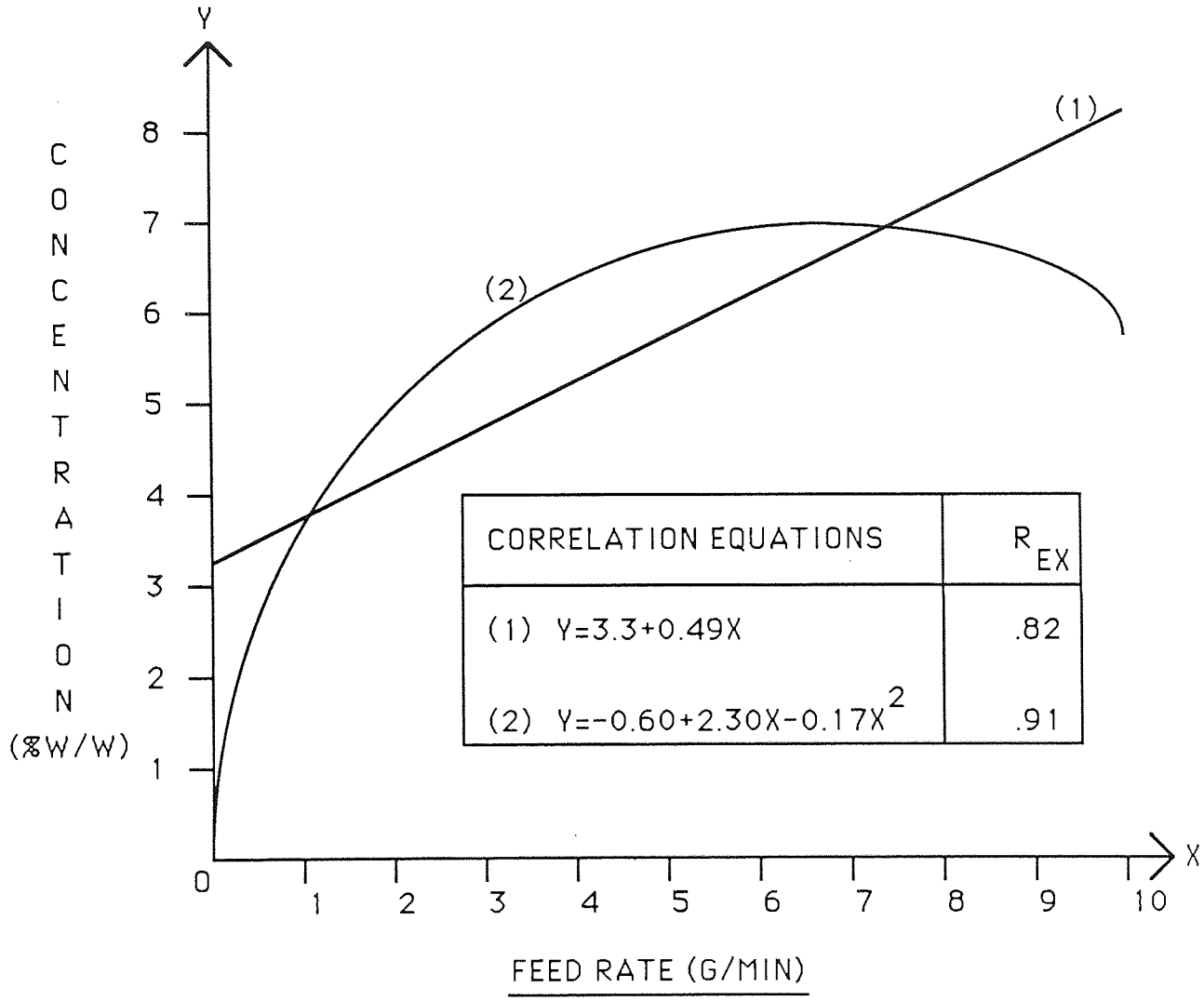

FIGURE 7.1 SUCROSE PEAK EXIT CONCENTRATION VERSUS FEED RATE OF BEET MOLASSES

Table 7.1
Correlation Equations for Beet Molasses Experiments

Ordinate (Y)	Abscissa (X)	Correlation Equation Y = f (X)	R_{EX}	R_{10}
Resolution Sucrose/Ionic	Rotation ($°h^{-1}$)	Y = 0.2785 + 0.0014X	.76	.55
Resolution Sucrose/Colour	Rotation ($°h^{-1}$)	Y = 0.5807 - 0.0021X	.60	.55
Resolution Sucrose/Betaine	Rotation ($°h^{-1}$)	Y = 0.2762 + 0.0082X	.74	.55
Sucrose Concentration (% w/w)	Rotation ($°h^{-1}$)	Y = 7.2273 - 0.0131X	.75	.55
Betaine Concentration (% w/w)	Rotation ($°h^{-1}$)	Y = 0.5763 - 9.824 X 10^{-4}X	.59	.55
Ionic Concentration (% w/w)	Rotation ($°h^{-1}$)	Y = 8.5673 - 0.0153X	.93	.55
Colour Concentration (% w/w)	Rotation ($°h^{-1}$)	Y = 0.8824 - 0.0016X	.83	.55
Resolution Sucrose/Ionic	Feed Rate ($gmin^{-1}$)	Y = 0.7128 - 0.058X	.90	.52
Resolution Sucrose/Colour	Feed Rate ($gmin^{-1}$)	Y = 1.6338 - 0.1408X	.77	.52
Resolution Sucrose/Betaine	Feed Rate ($gmin^{-1}$)	Y = 2.7936 - 0.3294X	.78	.52
Sucrose Concentration (% w/w)	Feed Rate ($gmin^{-1}$)	Y = 3.3007 + 4899X	.82	.52
Betaine Concentration (% w/w)	Feed Rate ($gmin^{-1}$)	Y =.1729 + 0.0608	.89	.52
Ionic Concentration (% w/w)	Feed Rate ($gmin^{-1}$)	Y = 4.0372 + .7762X	.9	.52
Colour Concentration(% w/w)	Feed Rate ($gmin^{-1}$)	Y = 0.3029 + 0.086	.73	.52
Resolution Sucrose/Ionic	Feed Concentration.(% w/w)	Y = 0.9015 - 0.0134X	.83	.52
Resolution Sucrose/Colour	Feed Concentration.(% w/w)	Y = 1.7709 - 0.0255X	.74	.52
Resolution Sucrose/Betaine	Feed Concentration.(% w/w)	Y = 3.5564 - 0.0617X	.65	.52
Sucrose Concentration (% w/w)	Feed Concentration.(% w/w)	Y = 3.4427 + .45X - 0.0068X^2	.9	.52
Betaine Concentration (% w/w)	Feed Concentration.(% w/w)	Y = .0585 + .0017X - 2.48 x $10^{-4}X^2$	.94	.52
Ionic Concentration (% w/w)	Feed Concentration.(% w/w)	Y = 3.7438 + 0.0809X	.84	.52
Colour Concentration (% w/w)	Feed Concentration.(% w/w)	Y = -.34 + .061X - 0.0011X^2	.76	.52

7.5 The Effect of Improved Liquid Distribution

The experimental correlation co-efficients given in Table (7.1) are all relatively high indicating that a high degree of confidence can be placed in the correlation equations. In previous experimental work the correlation co-efficients were not always greater than the R_{10} value and in some cases the co-efficients were much lower and it was not possible to correlate the experimental data at all. With the modifications described in Chapter (6) the liquid distribution remained uniform throughout the duration of the experiments. In previous experiments the liquid distribution tended to deteriorate with time so that time became an experimental variable. Once this condition was reached a means had to be found to restore a uniform liquid distribution. This could mean re-packing the bed or replacing the porous polyethylene ring at the annulus exit. Whatever steps were taken the operation of the annular chromatograph was severely interrupted and repeatability of experimental results was difficult to achieve. The objective of the modifications described in Chapter (6) was to establish a uniform liquid distribution around the annulus which would then be maintained for a considerably longer time period than had previously been experienced. For the experiment discussed in this section this objective was attained.

CHAPTER EIGHT
COMPUTER SIMULATION

8.1 Introduction

The classical theories of chromatography, from the plate model of Martin and Synge (37) to Giddings' statistical treatment (70), operate with the basic premise that the various sorbable species in the column do not interact. This assumption conveniently permits each multicomponent case to be treated as a superposition of independent single-component cases, which can be calculated separately. This assumption is entirely adequate for conventional analytical chromatography at low concentrations but becomes untenable when high concentrations in the mobile or stationary phase lead to interference of the sorbable species with one another, for example through their competition for the limited number of available sorption sites. The species can then no longer be considered separately, and each multicomponent case must be treated as a whole. This seemingly minor complication has serious consequences for the theoretical treatment and may be said to add a new dimension to chromatographic behaviour.

8.2 Equilibrium Chromatography of Two Interacting Solutes

If it could ever be developed, a "complete" theory of chromatography accounting for all possible effects would be of unmanageable complexity. In the following theoretical analysis the equilibrium chromatography of two interacting species is first considered with later extensions of the treatment to account for various band broadening disturbances and for more than two solutes. The term, "Equilibrium", as used in this context connotes the following conditions:

1 Local equilibrium is established between phases.

2 The effects of diffusion are negligible compared with convective transport, and there is no channelling.

In addition the chromatographic column is assumed to be "ideal", which implies the following further assumptions:

3 The system is one-dimensional in the direction of flow with uniform cross-sectional area.

4 The volumetric flow rate and the void fraction of the bed are constant.

5 The process is isothermal and isochoric.

The theoretical development considers first the conventional batch chromatographic process. A simple dimensional translation from time to angular position then enables the treatment to be extended to the continuous annular chromatograph.

The degree of nonequilibrium will be slight if the rate of sorptive-desorptive exchange (or mass transfer) is large or if the moving concentration pulse migrates through the column slowly thus preventing rapid concentration changes. A chromatograph zone is widened by the velocity divergence found within its boundaries and the rate of widening increases with the degree of nonequilibrium. Given the highly refined nonequilibrium theories that already account for disturbances one might ask whether it would be better to incorporate corrections for solute interaction into these theories rather than pursuing a rather primitive equilibrium theory of interaction which requires later corrections for disturbances. Unfortunately, this is impossible in principle. Although chromatography is intrinsically a dynamic process, its essential features are controlled by the equilibrium distributions of the species

between the mobile and stationary phases. Equilibrium properties determine the sequence, types, approximate forms, and propagation velocities of the composition variations arising under any given operating conditions, while kinetic and dynamic effects merely render all these variations somewhat more diffuse. Therefore, an equilibrium theory can be refined by corrections for non-equilibrium effects, but a greater complexity of equilibrium properties produced basically new effects which cannot be accounted for by corrections or minor modifications.

From Figure (8.1) a simple shell balance for a single chemical species which is adsorbed from a dilute solution in an inert solvent moving through the interstices of a bed of particles gives:

$$(VceA)_{z,t} - (VceA)_{z+\Delta z,\, t} = \frac{\partial}{\partial t} [\Delta zce\, A + \Delta zn(1 - e)A]_{\bar{z};t} \qquad (8.1)$$

where

$$z < \bar{z} < z + \Delta z$$

and

c	=	Concentration of solute in the mobile phase
n	=	Concentration of solute in the stationary phase
e	=	Bed voidage
V	=	Interstitial velocity of fluid through the bed
z	=	Axial coordinate
t	=	Time
Co(t)	=	Influent concentration of solute
A	=	Cross-sectional area of the bed.

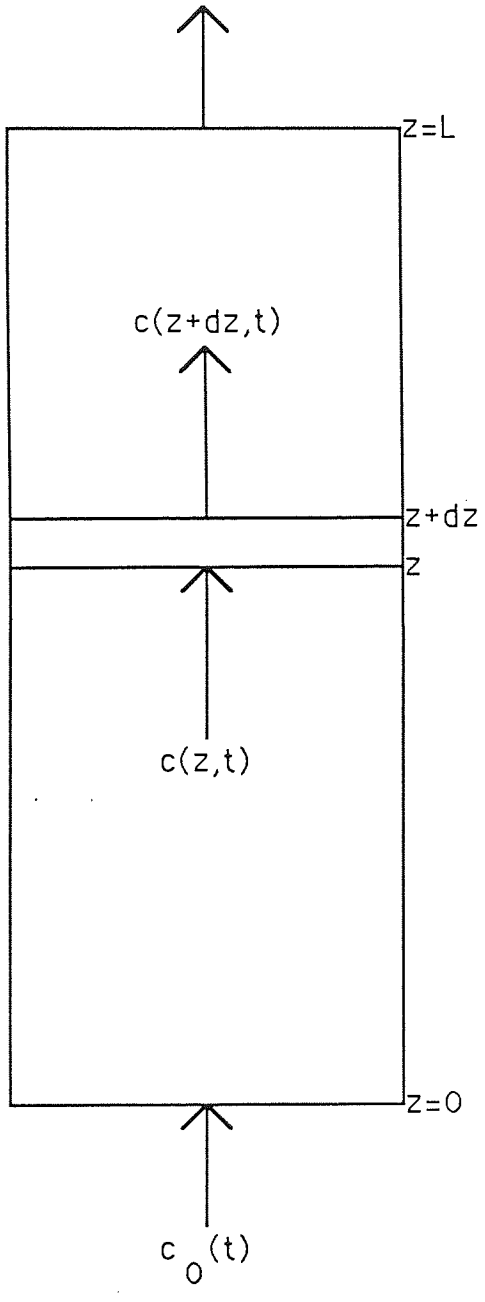

FIGURE 8.1 SIMPLE SHELL BALANCE

In equation (8.1) the left-hand side is the rate of flow of solute into the shell minus the rate of flow from the shell, and the right-hand side is the rate of accumulation of solute in the shell. With the assumptions of constant V, e and A, and taking the limit as t tends to zero we obtain for solute one:

$$V\frac{\partial c_1}{\partial z} + \frac{\partial c_1}{\partial t} + \frac{1 - e}{e}\frac{\partial n_1}{\partial t} = O \qquad 8.2\ (a)$$

and similarly for solute two:

$$V\frac{\partial c_2}{\partial z} + \frac{\partial c_2}{\partial t} + \frac{1 - e}{e}\frac{\partial n_2}{\partial t} = O \qquad 8.2\ (b)$$

When two solutes are present in concentrations c_1 and c_2 in the mobile phase, their equilibrium concentrations n_1 and n_2 in the stationary phase will be functions of both concentrations,,

$$n_1 = g_1\ (c_1, c_2)\ ,\quad n_2 = g_2\ (c_1, c_2) \qquad 8.3$$

The equilibrium relation which is usually called the adsorption isotherm is, in general, a complicated non-linear function of the mobile phase concentrations in which mutual influences among different solutes are taken into account. Since the ideal localized mono layer model was introduced by Langmuir (71), the Langmuir relation has been extensively employed not only for single solute systems but also for multiple solutes (72). A rigorous discussion was given by De Boer (73) and experimental evidence of its validity has been presented (74).

For each component, the Langmuir adsorption isotherm is:

$$n_i = \frac{n_o k_i c_i}{1 + \sum_{j=1}^{M} k_j c_j} \qquad (c = 1, 2, ..., M) \qquad 8.4$$

where

n_0 = limiting concentration of adsorbed solute

k_i = The reciprocal value of ci when half the sites are occupied by molecules of solute i and the other half are vacant.

With two solutes, if $k_2 > k_1$, solute two is more strongly adsorbed than solute one.

Equations (8.2a) and (8.2b) can be simplified by making the following transformation of the independent variables.

Let

$$x' = \frac{1 - e}{e} \frac{z}{V} \;, y' = t - \frac{z}{V} \qquad 8.5$$

Then equations (8.2a) and (8.2b) become:

$$\frac{\partial c_1}{\partial x'} + \frac{\partial n_1}{\partial y'} = O \qquad 8.6a$$

$$\frac{\partial c_2}{\partial x'} + \frac{\partial n_2}{\partial y'} = O \qquad 8.6b$$

From the Langmuir adsorption isotherm it is noticed that $k_1 c_1$ and $k_2 c_2$ generally keep together , so that, setting:

$$u = k_1 c_1 \ , \ v = k_2 c_2 \qquad 8.7$$

Equations (8.6a) and (8.6b) become:

$$\frac{1}{k_1} \frac{\partial u}{\partial x'} + n_O \frac{\partial}{\partial y'} \frac{u}{1 + u + v} = O$$

and

$$\frac{1}{k_2} \frac{\partial v}{\partial x'} + n_o \frac{\partial}{\partial y'} \frac{v}{1 + u + v} = O$$

This suggests that we put:

$$x = k_1 n_o x' \ , \ y = y' \ , \ k = \frac{k_1}{k_2} \qquad 8.8$$

and then:

$$\frac{\partial u}{\partial x} + \frac{1 + v}{\Delta^2} \frac{\partial u}{\partial y} - \frac{u}{\Delta^2} \frac{\partial v}{\partial y} = O \qquad 8.9$$

$$\frac{-v}{\Delta^2} \frac{\partial u}{\partial y} + k\frac{\partial v}{\partial x} + \frac{1 + u}{\Delta^2} \frac{\partial v}{\partial y} = O \qquad 8.10$$

where

$$\Delta = 1 + u + v$$

The dependent variables are dimensionless and the independent variables both have the dimensions of time. Nevertheless, because of their origin x can be thought of as space-like and y as time-like. Thus, for example, x = 0 gives the inlet or feed condition of the stream entering the column at z = 0. The case y = 0 gives the condition at z = Vt. Now z/V is the instant at which an element of the carrier fluid entering the column at t = 0 first reaches the point z. Hence the feed conditions cannot have any influence until y = 0. It is more convenient however to consider initial conditions specified on the line t = 0, i.e.,

$$y = \frac{-e}{1-e}\,\frac{x}{k_1 n_o} = -\lambda x \qquad 8.11$$

It is also observed that to recover the distribution of solutes in the column from the solutions u (x, y), v (x, y) at any instant t we must take sections by lines:

$$y = t - \lambda x, \quad \lambda = \frac{e}{(1-e)\,k_1 n_0} \qquad 8.12$$

The geometry of the variables is shown in Figure (8.2).

The simplification gained in the subsequent analysis of equations (8.9) and (8.10) justifies the reductions outlined above. These equations are an example of a "reducible" pair of first order partial differential equations. The reason for this is that their quasilinearity can be reduced to strict linearity by interchanging the roles of dependent and independent variables. This reduction which makes the equations much easier to handle is known as the hodograph transformation.

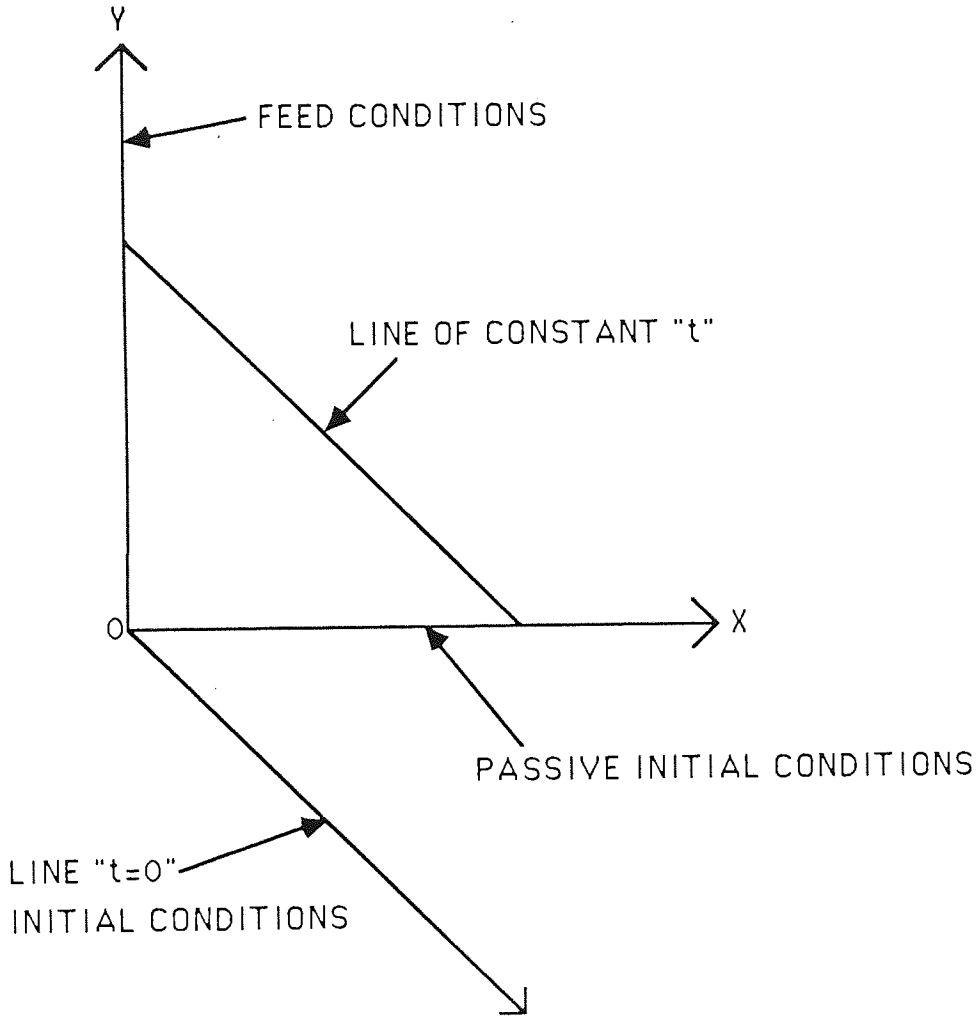

FIGURE 8.2 GEOMETRY OF VARIABLES

The general solution to the partial differential equations (8.9) and (8.10) is built up as the envelope of two one-parameter families of curves. These two families may be represented in the form β (x, y) = constant and α (x, y) = constant, and they form a curvilinear co-ordinate net of positive and negative curves. Thus β is constant along the positive curves C+ and α is constant along the negative curves C-. Accordingly at the point (x, y), two different directions which are given by dy/dx = σ+ on C+ and dy/dx = σ- on C- exist. Each direction represents a direction in which the derivatives of both u and v are taken in when equations (8.9) and (8.10) have been linearly combined. Once a fixed solution of equations (8.9) and (8.10) is inserted, the equations dy/dx = σ+ (x, y, u, v) and dy/dx = σ- (x, y, u, v) are two separate ordinary differential equations of the first order which define the two one-parametric families of characteristic curves or simply characteristics, C+ and C- in the (x, y) - plane, belonging to the solution u (x, y), v (x, y).

When the differential equations are reducible the characteristic curves Γ in the (u, v) plane, the images of the characteristics C in the (x, y) plane are independent of x and y. That is:

$$\text{For } \Gamma+, \frac{du}{dv} = \zeta+(u,v) \qquad \text{and for } \Gamma-, \frac{du}{dv} = \zeta-(u,v) \qquad 8.13$$

Equation (8.13) can be solved to give two families of characteristics Γ+ and Γ-. in the hodograph plane of u and v. The advantage of reducibility is that these characteristics can be laid down once and for all being independent of the particular solution u (x, y) v (x, y) considered.

Very often the following situation is encountered. In a region (I) of the (x, y) plane the solution (u,v) of the differential equations (8.9) and (8.10) or, as we shall simply say, the "flow" (u, v) is constant. This is the case for example in

the elution of a column initially saturated with constant concentrations of two solutes. The initial state and inlet conditions are both regions of constant state and are represented by single points in the (u, v) plane. Adjacent to these regions of constant state are other regions (II) in which u and v vary. When the differential equations are reducible the flow in such a region (II), adjacent to a region (I) of constant state, is of a particularly simple character for then u and v are functionally related. The region (II) of (x, y) plane in which u and v are functions of one another is represented by a characteristic curve Γ in the (u, v) plane and is called a simple wave region. Such a region in the (x, y) plane is covered by arcs of characteristics which carry constant values of u and v and hence are straight lines.

Thus, in the case of elution of a column initially saturated with two solutes, Figure (8.3) shows the (x, y) and the (u, v) planes. The initial state is represented by the point A (u_o,v_o), in the hodograph plane and the pure solvent feed is the origin O. These are marked on the axes of the (x, y) plane and we would like to fill this quadrant with straight-line characteristics so that it is a simple wave region. Now each of these characteristics will bear a pair of constant values u, v. The only place on the boundary where we can think of concentrations other than (0,0) and (u_o, v_o) being present is at the origin, where we can imagine that all concentrations between (0,0) and (u_o,v_o,) co-exist. The characteristics will all emanate from the origin of the (x, y) plane and we have what is known as a centered simple wave. It is also known from simple wave theory that the image of the simple wave region must consist of characteristics in the hodograph plane.

There are two ways of going from A to O: either along the Γ+ from A to D and then along the Γ- from D to O; or along the Γ- from A to B and down the Γ+

from B to O. With the second route there is overlapping of C- characteristics in the (x, y) plane but this does not occur with the path ADO.

Since the simple wave is centred, we can take any cross section by a line of constant time, $y = t - \lambda x$, and get the typical distribution of solute on the column. This is shown in Figure (8.3). The sector adjacent to the x-axis is a region of constant state A; a simple wave region D-A leads to another region of constant state D. Again a simple wave region O-D connects the plateau to the constant state O.

Considering instead the saturation of an initially empty bed with a mixture of concentrations u_o and v_o it is not possible to devise a simple wave solution. For, in this case, the state on the x-axis is O and on the y-axis A. But there is no way of going from O to A along Γ characteristics and preventing the C characteristics bearing constant values of u and v from overlapping.

Since it is impossible for more than one concentration to be present at any one point and instant such a solution is not physically acceptable and a line of discontinuity must be put in which allows the solution to be one valued. The trouble arises from the fact that the higher concentrations move faster than the lower. An advancing concentration wave with a sloping front gets progressively steeper as the higher concentrations overtake the lower. The only way to retain a physically meaningful solution is to introduce a discontinuity or shock. In the case of the saturation of an initially empty bed there is a shock from the very first, for the boundary conditions have a discontinuity at the origin.

Figure (8.4) shows the two shocks that are needed to join the state O on the x-axis to state A on the y-axis. The intermediate state has to be state B rather than D for with the latter the shock from O to D has a greater slope than the

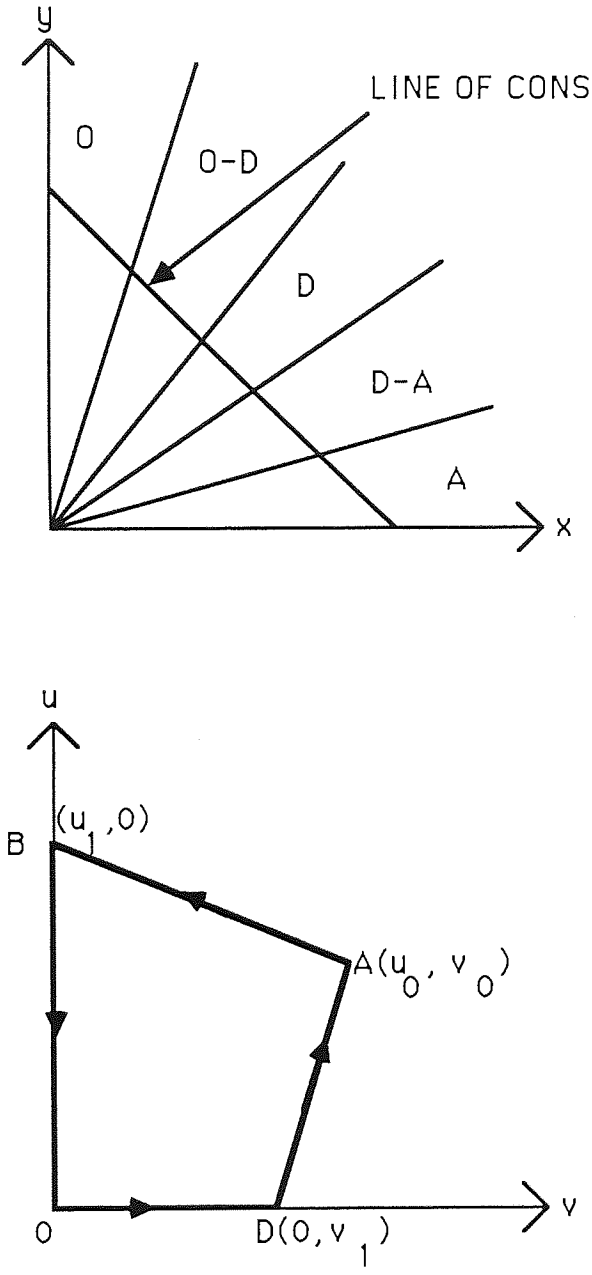

FIGURE 8.3 (x,y) AND (u,v) PLANES FOR THE ELUTION OF A COLUMN INITIALLY SATURATED WITH CONSTANT CONCENTRATIONS OF TWO SOLUTES

shock from D to A. It follows that the two shocks must be as in Figure (8.4) and a section by a line of constant time gives the distribution of the two solute concentrations shown in Figure (8.5).

In a chromatographic separation the two solutes to be separated are put onto the column as a mixture over a short period of time. This is akin to the saturation process described above so that initially two shocks are formed. Following the feed pulse injection however there is a period of elution which can be related to the simple wave solution previously discussed. In effect we have a combination of Figures (8.3) and (8.4) with interference of the two patterns eventually taking place. The simple wave solution overtakes first one shock then another and by reducing the strength of the shocks causes the shock paths to curve.

8.3 The Chromatographic Cycle

It has been observed that separation of different solutes may be accomplished by applying the saturation and elution processes successively. Suppose a clean bed of sorbent is first irrigated with a fluid mixture. After a finite period of time $t = y$, the inlet stream is changed from the mixture to pure solvent so that the chromatogram starts to be eluted.

Figure (8.6) shows the (x, y) plane which will be described by looking at the distribution of the two solutes at various typical instants. This will correspond to a section of the plane by lines $y = t - \lambda x$ for various values of t. Figure (8.7) shows the distribution of solutes along the column at the various times.

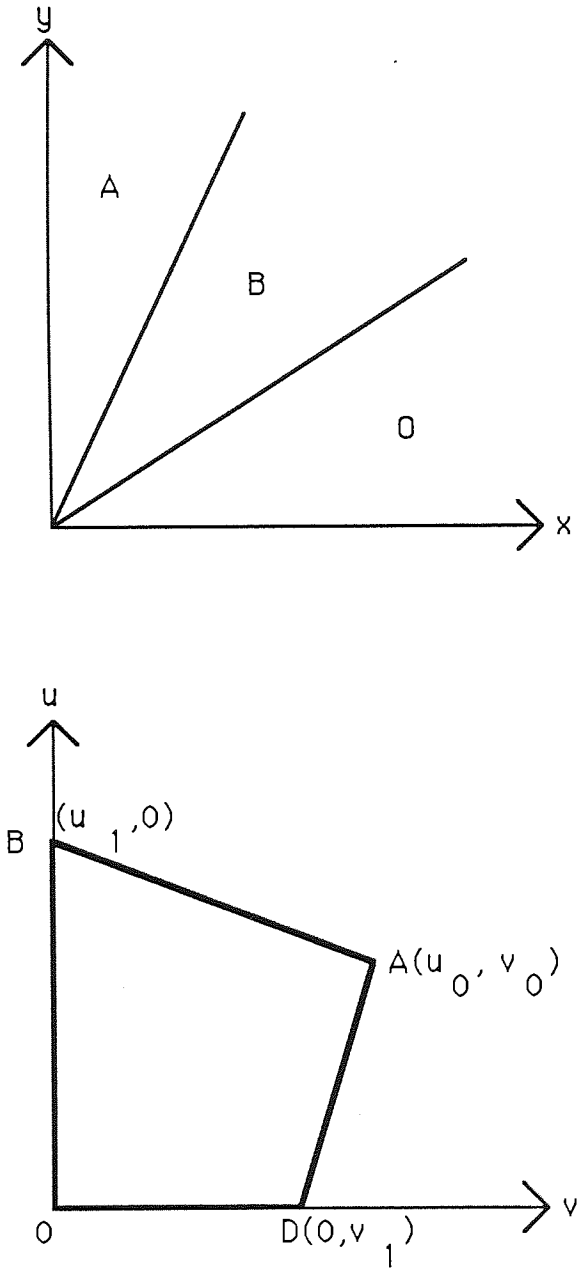

FIGURE 8.4 (x,y) AND (u,v) PLANES FOR THE SATURATION OF AN INITIALLY EMPTY COLUMN

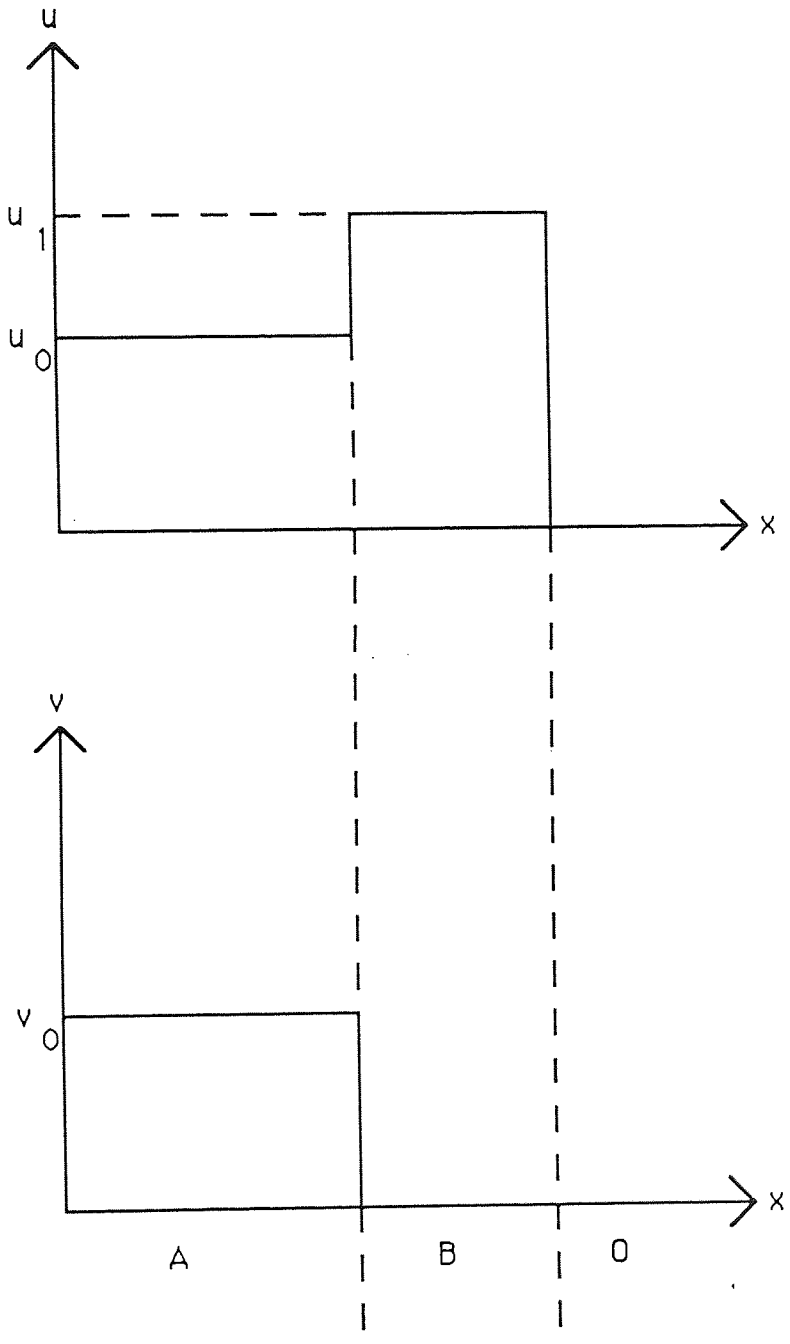

FIGURE 8.5 DISTRIBUTION OF TWO SOLUTE CONCENTRATIONS FOR THE SATURATION OF AN INITIALLY EMPTY BED

At $t=t_1$ the feed mixture has been completely put on the column. The flow of pure solvent starts to elute the saturated part of the bed and the distribution of solutes is represented by the cycle:

O—> D—> A—> B—> O

In moving from state O to D the concentration of solute two increases from 0 to v_1 while solute one has zero concentration. From D to A solute one increases from zero to the feed concentration u_o and solute two increases from v_1 to v_o. From A to B the second solute immediately falls to zero and the first solute increases further to u_1 before itself decreasing to zero from B to 0. The change in states from O to D is a gradual change because it takes place across the simple wave (AD) whereas the change from state A to B is a discontinuous increase or decrease because it takes place across the shock (AB).

At $t = t_2$ the (AD) simple wave starts to overtake the (AB) shock wave and constant state A disappears as the (AB) shock cannot maintain its full strength. When $t = t_3$ the interaction is over and the (DO) shock line separates solute two from solute one from left to right. Thus separation is complete at this instant. At $t = t_4$ (where t_4 could be greater or less than t_3) the (AD) simple wave which has been transmitted into a (BO) simple wave starts an interaction with the (BO) shock wave so that the shock at the head of the chromatogram begins to decay and constant state B disappears. At $t = t_5$ the (DO) shock wave decays for behind it is the simple wave (DO) bringing concentration pairs $u = 0$, $v < v_1$. The two solutes are separated by a region of constant state O which broadens as t increases.

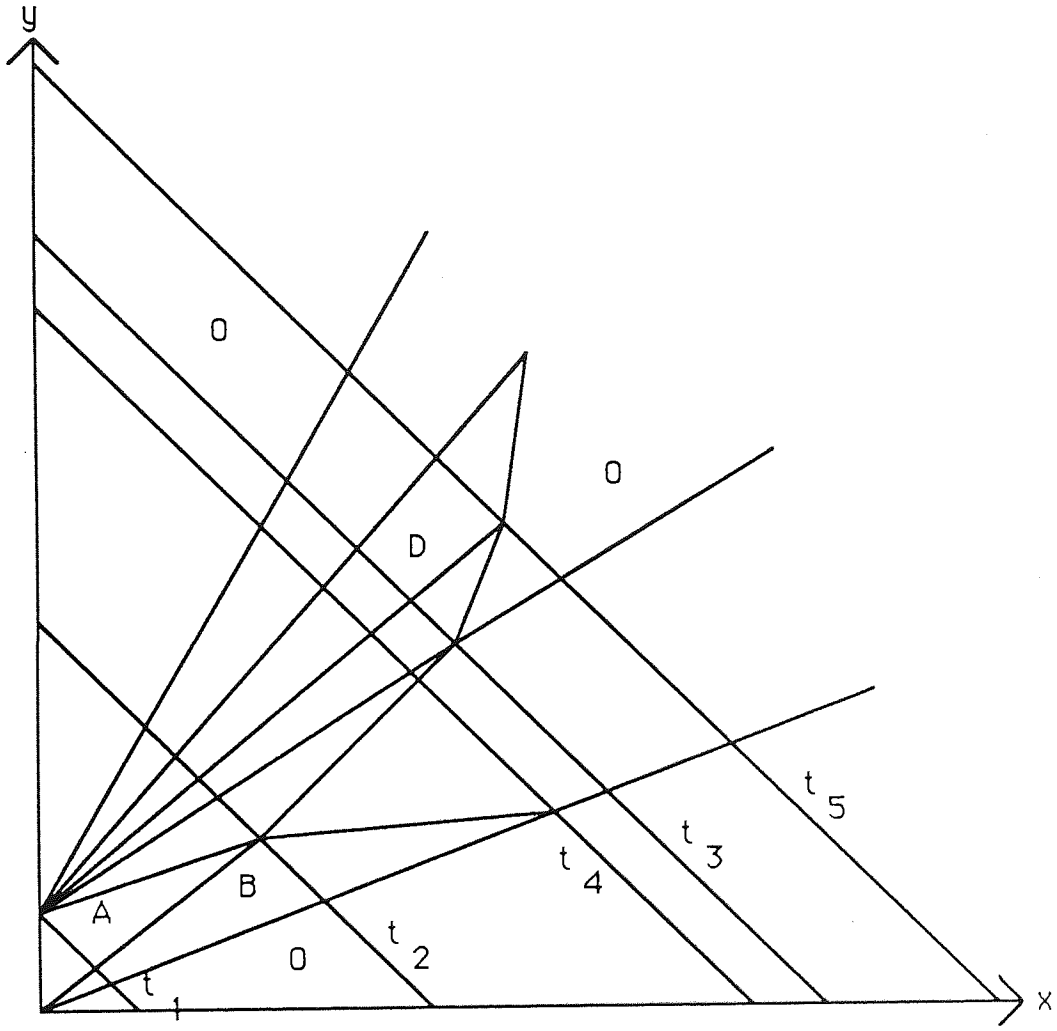

FIGURE 8.6 (x,y) PLANE FOR CHROMATOGRAPHIC SEPARATION

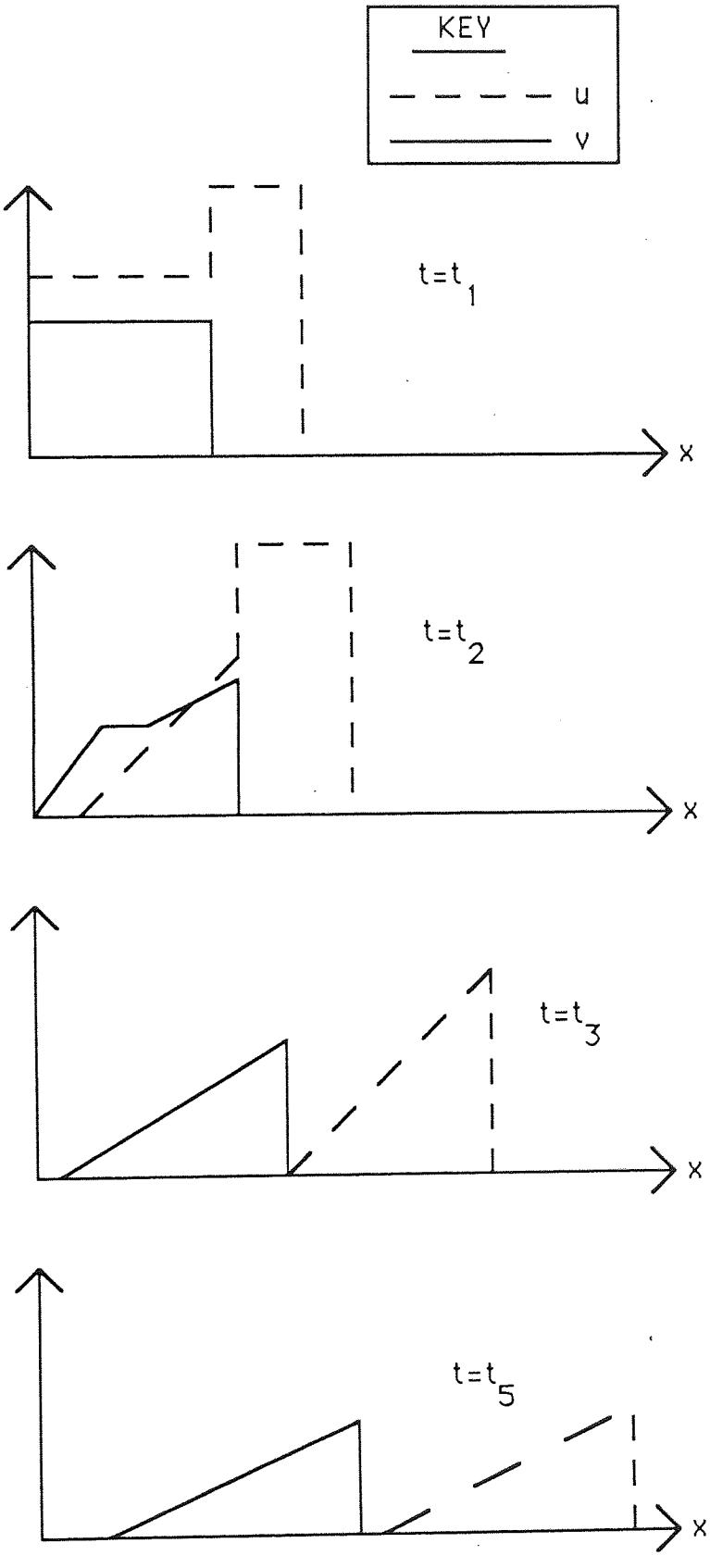

FIGURE 8.7 DISTRIBUTION OF SOLUTES AT DIFFERENT TIMES

8.4 Extensions of Theoretical Analysis

8.4.1 Disturbances

The various effects loosely referred to as disturbances are:

1 Deviations from local equilibrium because of finite mass-transfer resistance to sorption and desorption (non equilibrium).

2 Molecular diffusion in the axial direction (axial diffusion).

3 Back-mixing of volume elements of the mobile phase because of branching and rejoining of stream paths, flow velocity variations, etc. (eddy dispersion).

4 Distortions of the flow-velocity profile because of packing irregularities or wall effects (channeling) or hydrodynamic instability (fingering).

5 Volume changes of the sorbent particles constituting the bed.

The general effect of any disturbance is dispersive, i.e. makes all concentration variations more diffuse than they would be otherwise. The effect produced is in proportion to the sharpness of the composition variations. The H.E.T.P. concept models the combined effect of all disturbances as back-mixing on fictitious "plates", on which the mobile phase undergoes successive equilibrations. A similar approach is used here whereby the disturbances are all lumped together. Such an oversimplified approach is unable to discriminate fully between species with different equilibrium and kinetic properties but is convenient at this stage of the development of the model.

The validity of a diffusion equation is postulated to account for disturbances or band-broadening processes.

The differential equation of diffusion reduces to:

$$\frac{\partial c}{\partial t} = D_z \frac{\partial^2 c}{\partial z^2} \qquad 8.14$$

if diffusion is one-dimensional i.e., if there is a gradient of concentration only in the z-direction and the diffusion co-efficient D_z is constant.

c = Concentration of diffusing solute

t = time

D_z = Diffusion co-efficient

z = Axial co-ordinate

The solution:

$$c = \frac{M}{2(\pi D_z t)^{1/2}} \quad EXP(-z^2/4D_z t) \qquad 8.15$$

of equation (8.14) described the spreading by diffusion of an amount of substance M deposited at time t = 0 in the plane z = 0.

Equation (8.15) gives distributions at various times which may be superimposed on the chromatographic profiles given in Figure (8.7) to account for band broadening processes. Certain adjustments in the variables in Equation (8.15) have to be made to make the equation compatible with the equations which give rise to the profiles in Figure (8.7). The finished profile from Figure (8.7) is divided into strips such that each strip has a characteristic elution time. Then a strip represents the amount of substance M deposited at t = 0 in the plane z = L, where L = column length. Thus each strip gives a

profile according to equation (8.15) and the completed chromatogram is produced by superimposing all the profiles.

8.4.2 Transformation from Time Dependent Separations To Steady State Separations

The chromatographic process which takes place on the rotating annular chromatograph is a steady state separation occurring in the z and θ directions. This two dimensional flow path contrasts with the conventional batch system where separation occurs only in the z-direction and is time dependent. Wankat (44) compared the material and energy balances, equilibrium relations, and mass transfer expressions for the time dependent, one-dimensional and the steady state, two-dimensional separations. He found that the equations and appropriate boundary conditions for the one-dimensional system can be transformed into the equations and boundary conditions for the two-dimensional system if the transform $\theta = \omega t$ is made where t is time, θ is the angular co-ordinate, and ω is rotation rate.

8.4.3 Extension of model to the separation of more than two solutes.

Rhee *et al* (46) present a rigorous treatment of the theory of multicomponent chromatography for more than two components. The principles are the same though the calculations are necessarily more involved than when considering only a binary separation.

Having developed the binary model in this chapter this model was applied to multicomponent separations by selecting a key feed component and by

considering the binary separations of this component from all remaining components in succession.

8.5 Simulation of Glucose-Fructose Separation

8.5.1 Introduction

It was assumed that the adsorption isotherms were of the type proposed by Langmuir.

The model was used to simulate the separation of the isomers glucose and fructose on the rotating annular chromatograph. The relevant experimental results were discussed in Section (5.2) and further experimental details are in Appendix A.2.

To use the model the operating run conditions have to be supplied together with solute values for the Langmuir isotherm parameter, K_i, and diffusion co-efficient, D_i. K_i values for glucose and fructose were obtained by fitting the model to the first six glucose-fructose runs (GF1 to GF6). The best fit between the model and these six runs was obtained when the following K_i values were assigned; K (glucose) = 0.5, K (fructose) = 0.9. The diffusion co-efficient was similarly obtained by fitting the model to the same six runs and the best fit was obtained when the following diffusivities were assigned; D (glucose) = 2.3 $cm^2\ min^{-1}$, D (fructose) = 4.0 $cm^2\ min^{-1}$. Figure (8.8) shows a comparison between experimental and model profiles for the run GF1 with the various K_i and D_i values assigned as above.

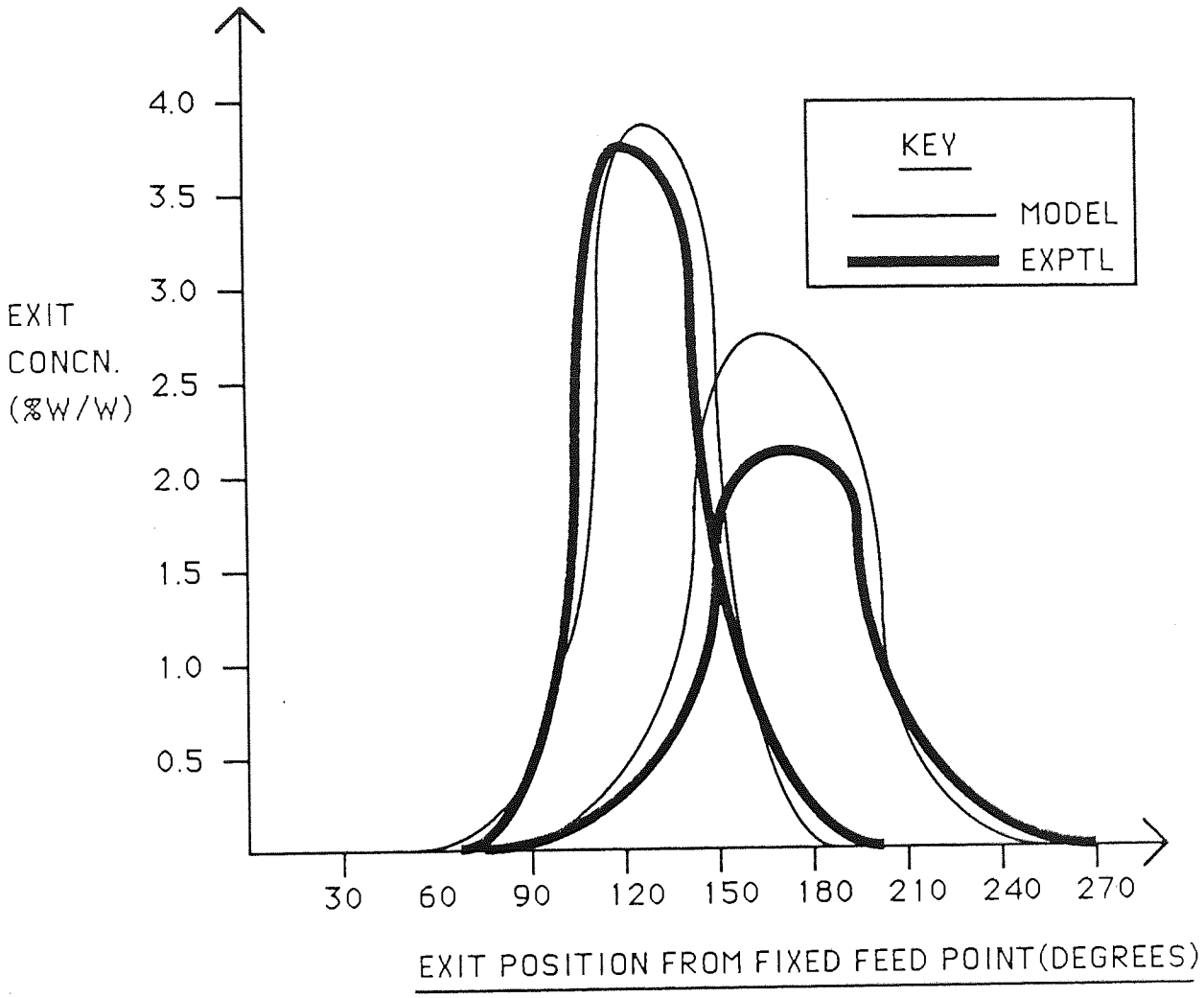

FIGURE 8.8 COMPARISON BETWEEN SIMULATED(MODEL) AND EXPERIMENTAL PROFILES FOR RUN GF1

8.5.2 Effect of Rotation Rate

Figures (8.9) and (8.10) show the variation of exit bandwidths with rotation rate as found experimentally and as predicted by the model.

From Figures (8.9) and (8.10) the model correctly predicts the trend of an increase in exit bandwidth as rotation rate increases. The increase predicted by the model is generally less than found by experiment. The model also predicts an increase in solute exit peak position with rotation rate as shown in Figures (8.11) and (8.12). Even though the model quite accurately predicts bandwidths and peak positions the comparison between model and experimental findings for resolution shows some discrepancy (Figure 8.14). According to experiments the resolution increases only slightly as rotation increases whereas the model predicts a more significant increase in resolution. In Figure (8.13) the exit peak concentration of glucose is plotted as a function of rotation rate. Again the model and experimental results have the same trend namely rotation rate increases the concentration decreases.

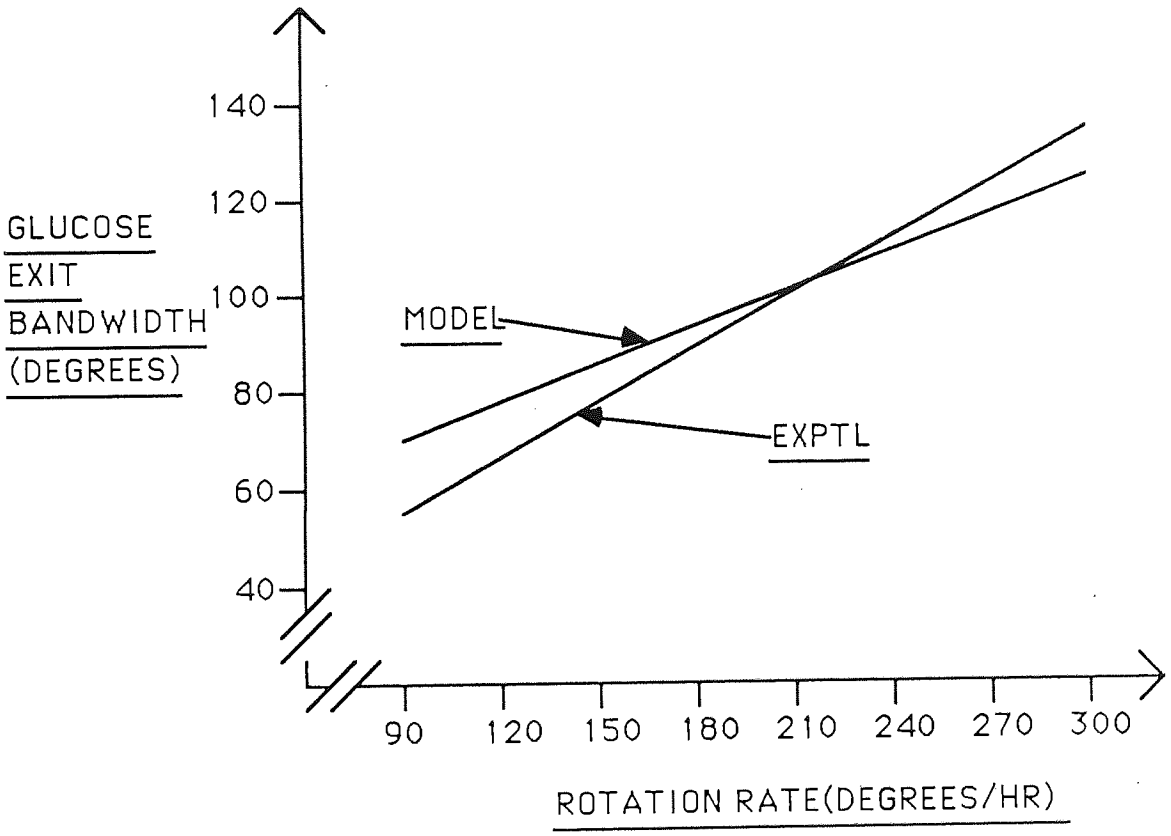

FIGURE 8.9 EXPERIMENTAL AND MODEL GLUCOSE EXIT BANDWIDTH VERSUS ROTATION RATE

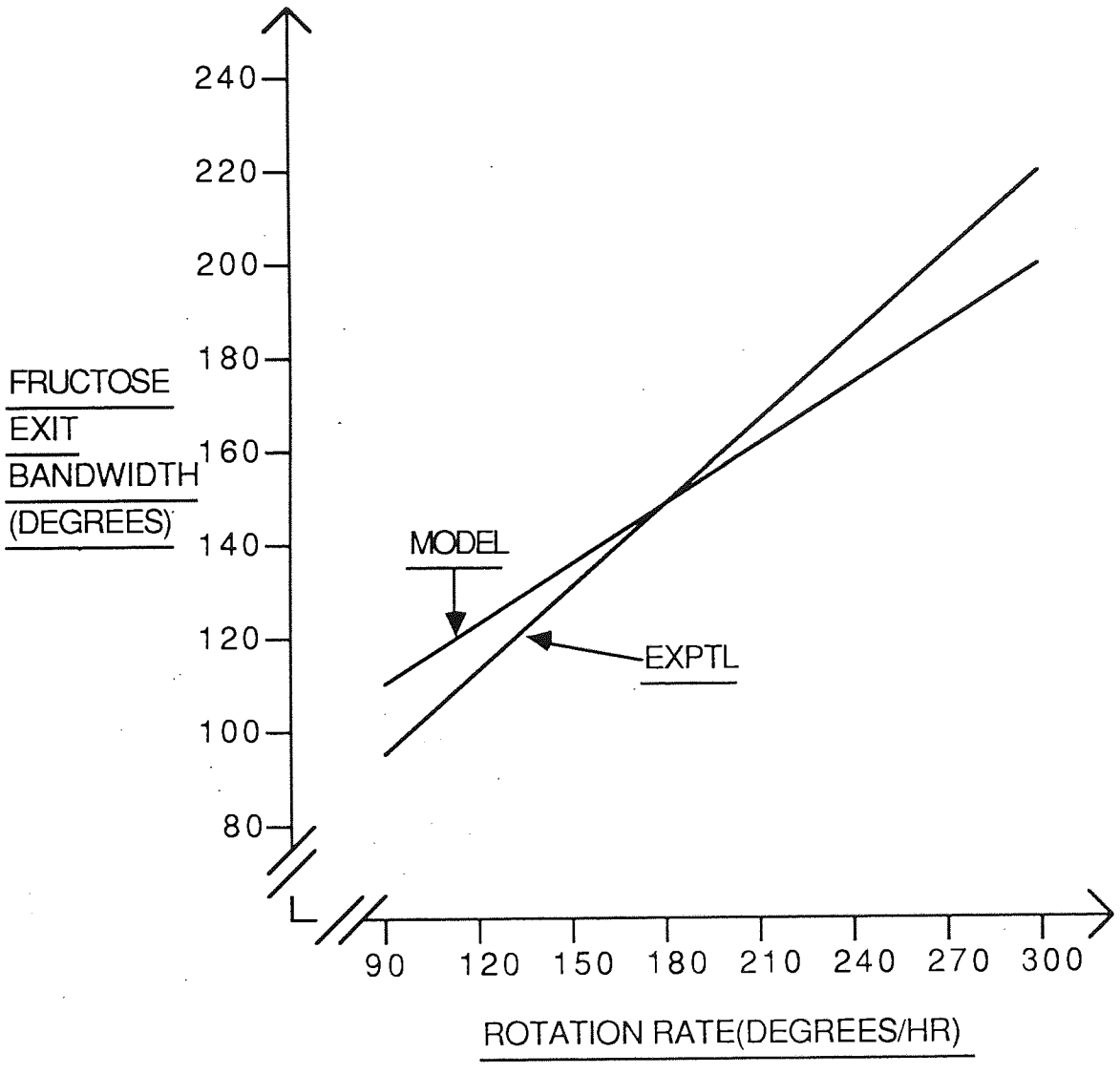

FIGURE 8.10 EXPERIMENTAL AND MODEL FRUCTOSE EXIT BANDWIDTH VERSUS ROTATION RATE

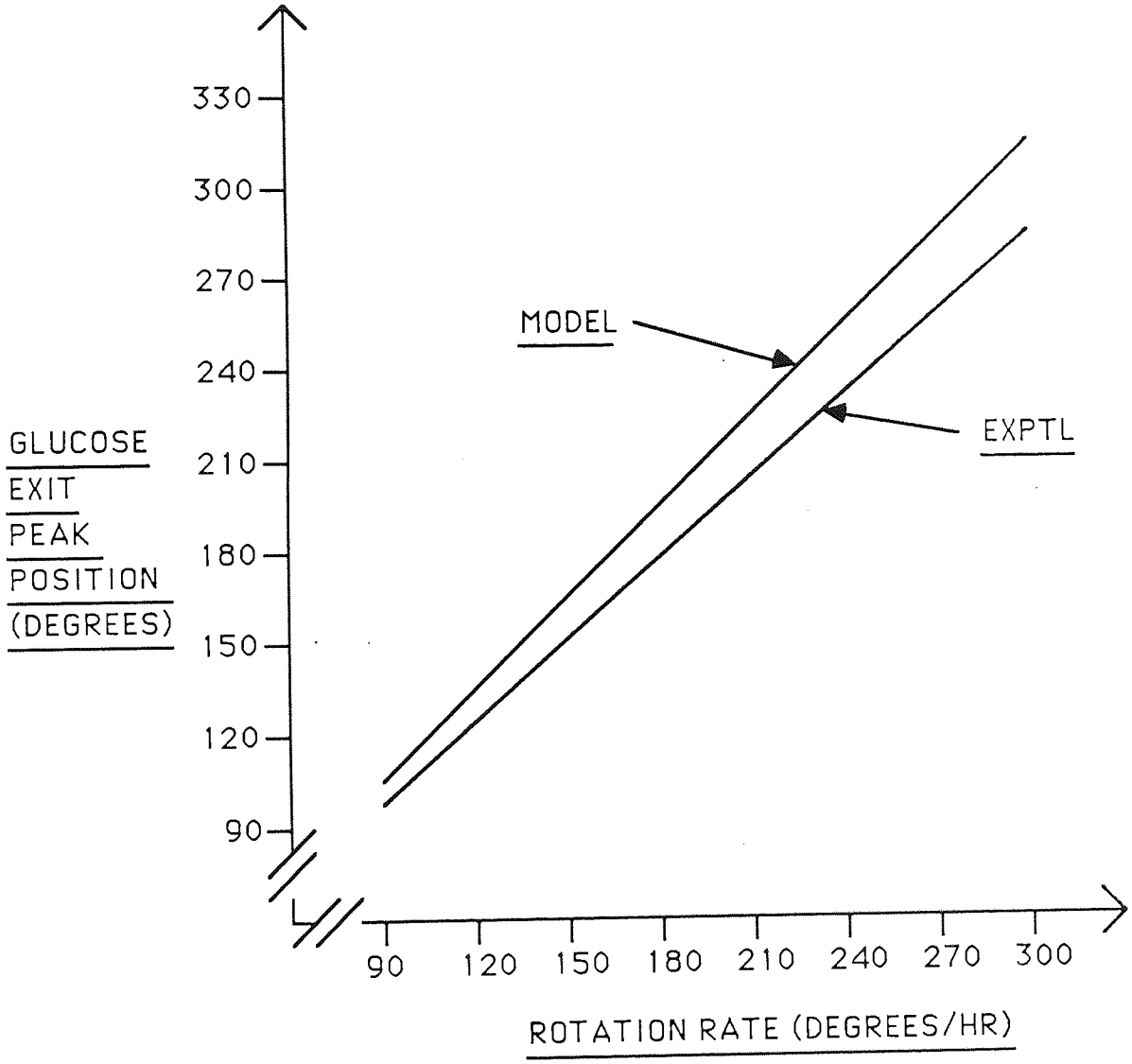

FIGURE 8.11 EXPERIMENTAL AND MODEL GLUCOSE EXIT PEAK POSITION VERSUS ROTATION RATE

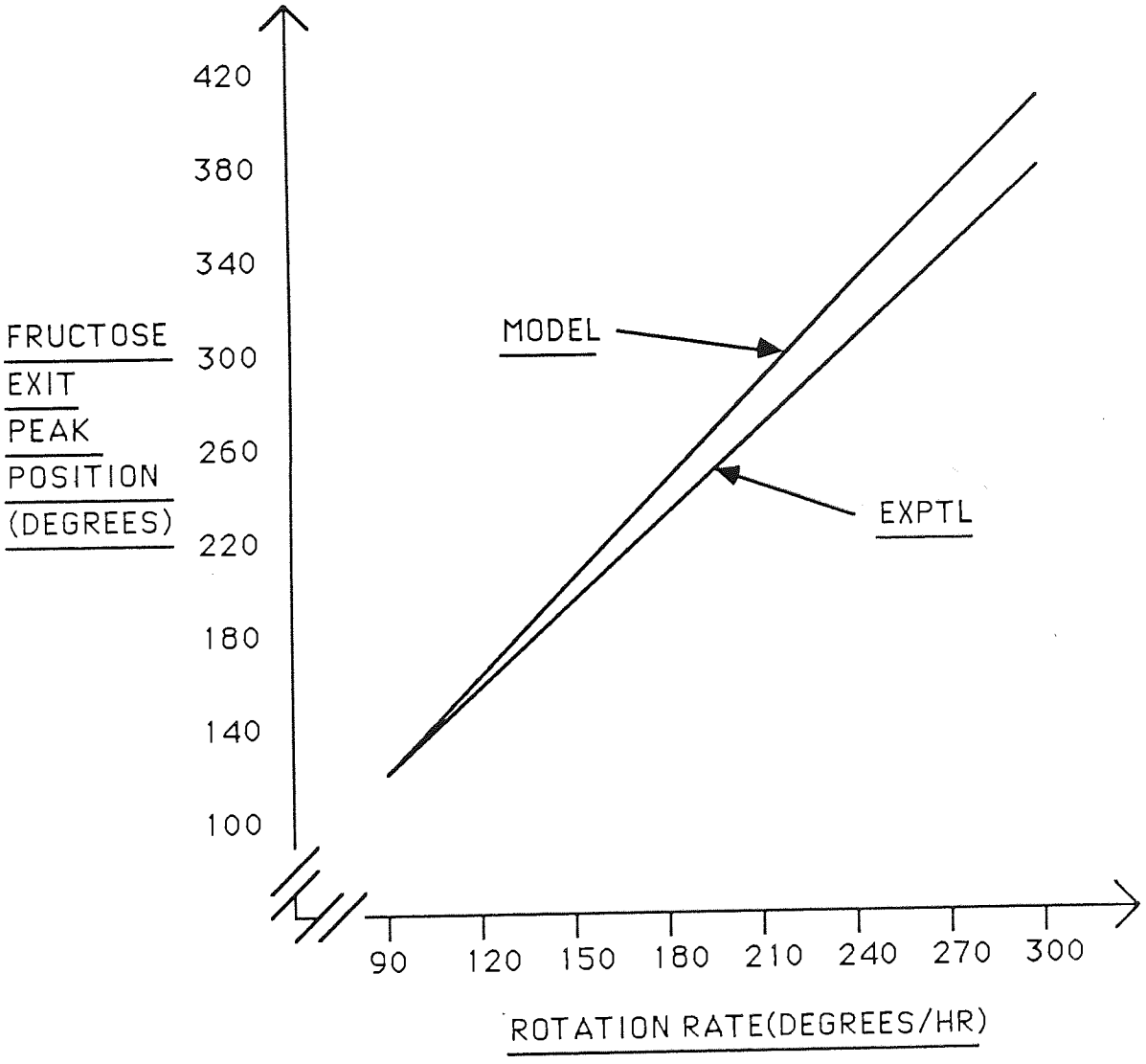

FIGURE 8.12 EXPERIMENTAL AND MODEL FRUCTOSE EXIT PEAK POSITION VERSUS ROTATION RATE

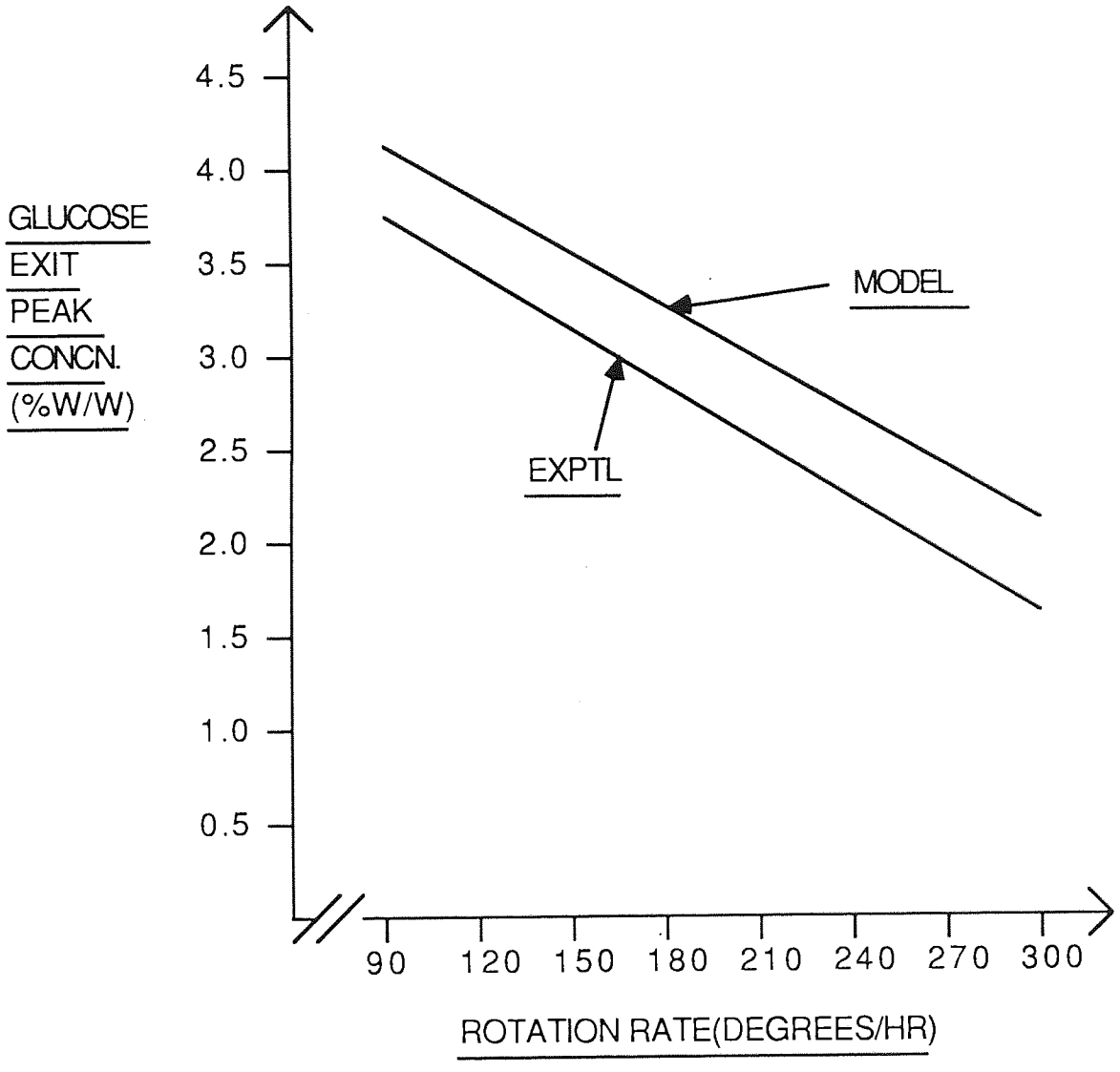

FIGURE 8.13 EXPERIMENTAL AND MODEL GLUCOSE EXIT PEAK CONCENTRATION VERSUS ROTATION RATE

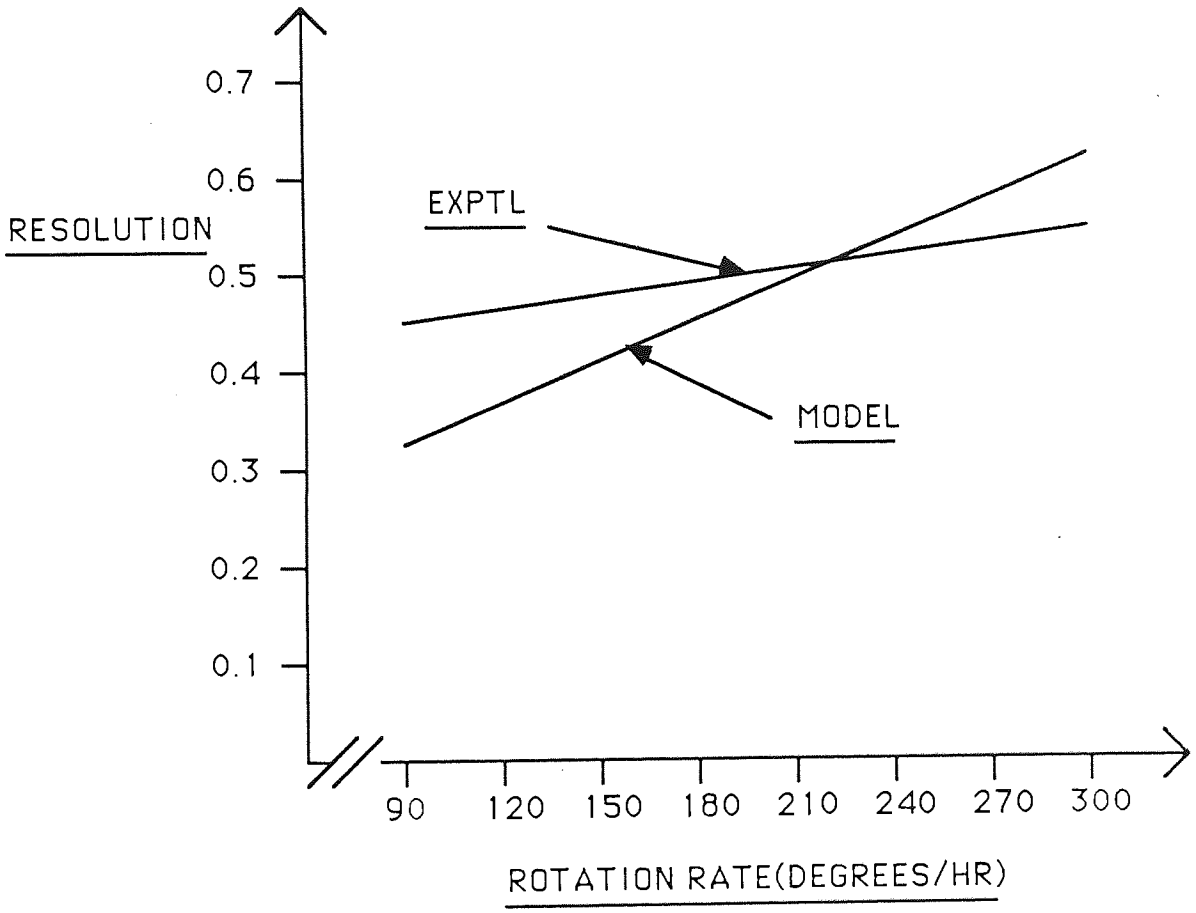

FIGURE 8.14 EXPERIMENTAL AND MODEL GLUCOSE-FRUCTOSE RESOLUTION VERSUS ROTATION RATE

8.5.3 Effect of Eluent Rate

The model prediction that exit bandwidth decreases as the eluent rate increases is consistent with experimental findings as Figures (8.15) and (8.16) show. One expects a decrease in band spreading as the eluent rate increases because of the reduction caused in the solute column residence time which means that the solute has less time to undergo band spreading processes. Figures (8.17) and (8.18) show an accurate prediction by the model of glucose and fructose exit peak positions as the eluent rate varies. This similarity between model and experimental data shows that the chosen values for the Langmuir isotherm parameters were consistent with experimental results. The model predicts that the glucose-fructose resolution is invariant with increase in eluent rate whereas the experimentally determined resolution decreased. The predicted decreases in bandwidths and peak positions are such that the resolution is unaffected as also is the exit glucose concentration. In the case of the exit concentration the dilution caused by higher eluent rates is predicted to be exactly offset by the concentrating effect of lower solute column residence times giving a constant concentration. The experimental evidence however suggested a decrease in concentration as the eluent rate increased.

8.5.4 Effect of Feed Rate

Figures (8.19) and (8.20) show that as the glucose-fructose feed rate increases the model gives a modest increase in exit bandwidths whereas the experimental results show a decrease. The experimental trend is surprising in view of the increase in initial bandwidths at higher feed rates but it could possibly be the effect of variations of the isotherm parameters and diffusion

co-efficients induced by high feed rates. The model assumes that these parameters are constant for all operating conditions whereas in practice they can vary.

The peak position was found experimentally to be constant as the feed rate was varied and this trend was predicted by the model also. Figures (8.21) and (8.22) show the effect of feed rate on the glucose exit peak concentration and resolution respectively. There are discrepancies between model and experimental data in these two figures but the overall trend is correctly predicted.

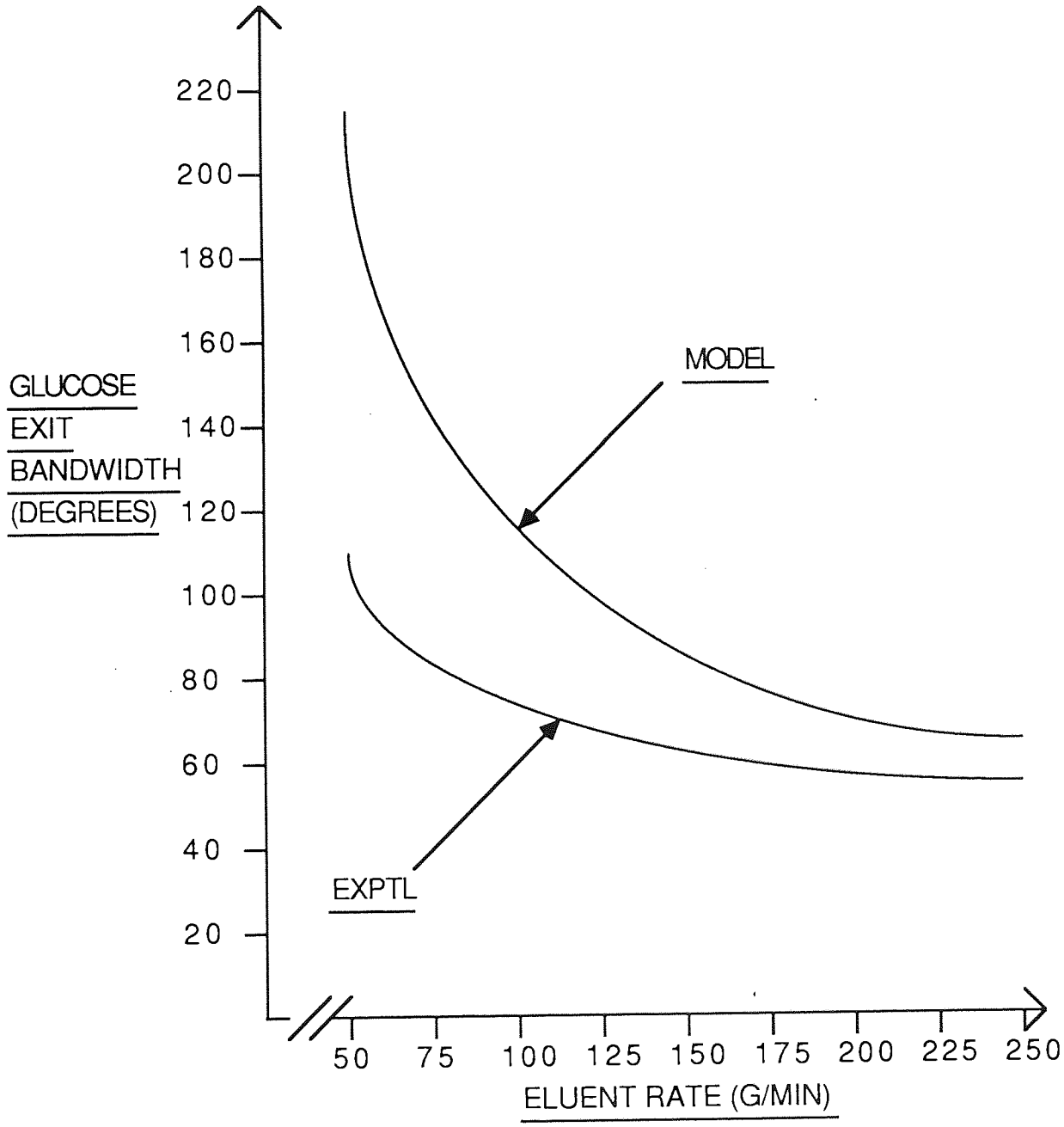

FIGURE 8.15 EXPERIMENTAL AND MODEL GLUCOSE EXIT BANDWIDTH VERSUS ELUENT RATE

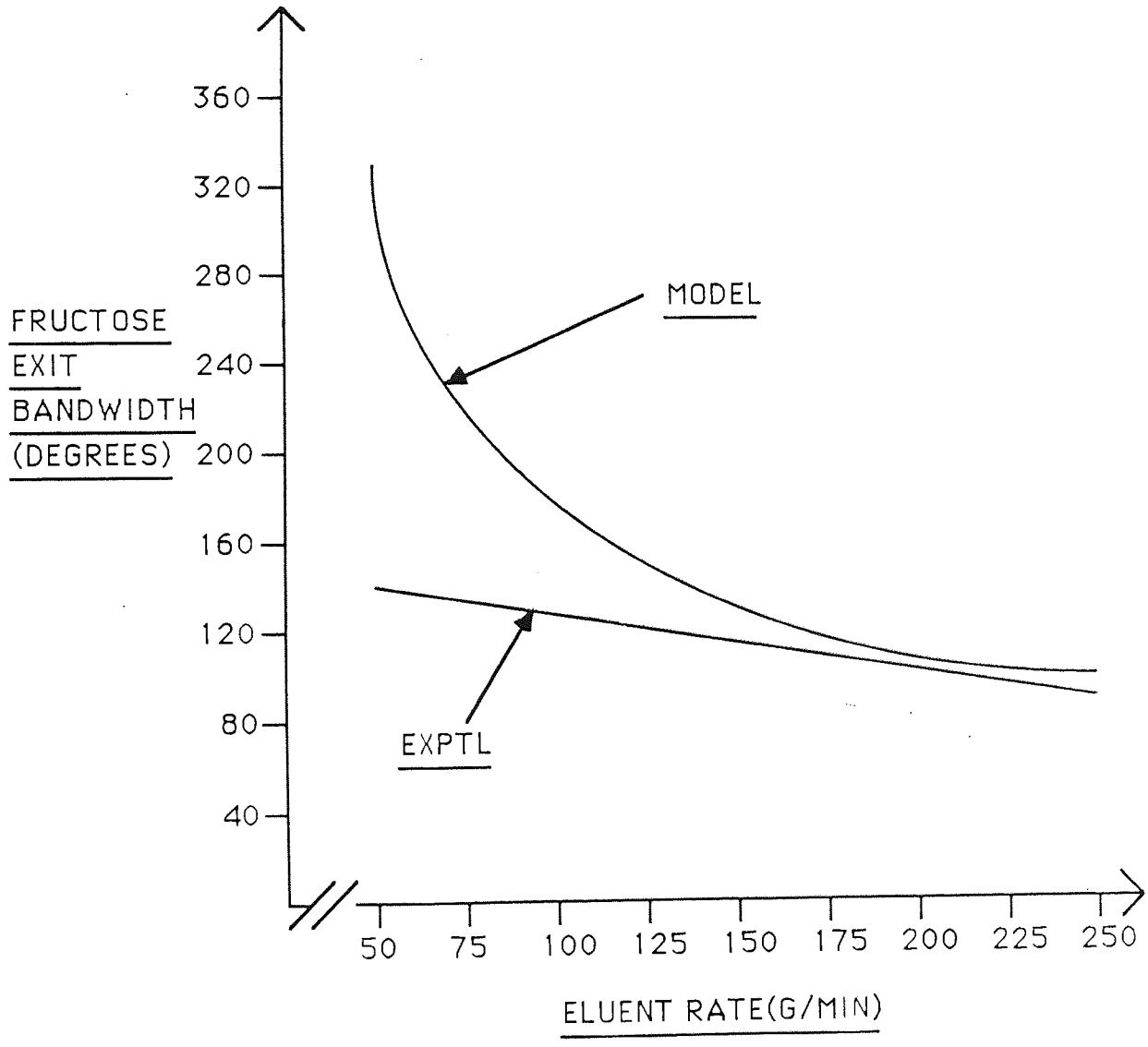

FIGURE 8.16 EXPERIMENTAL AND MODEL FRUCTOSE EXIT BANDWIDTH VERSUS ELUENT RATE(G/MIN)

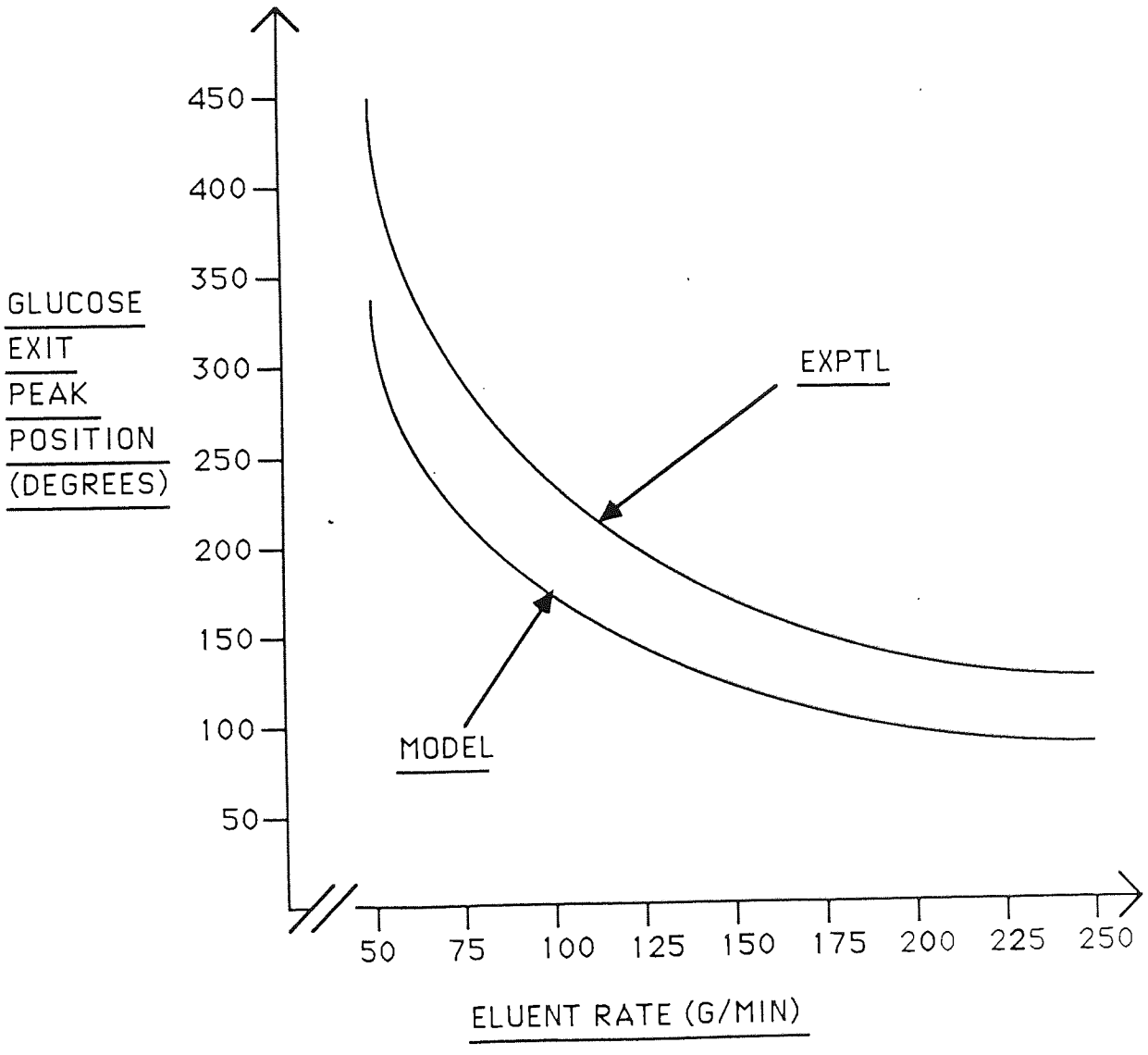

FIGURE 8.17 EXPERIMENTAL AND MODEL GLUCOSE EXIT PEAK POSITION VERSUS ELUENT RATE

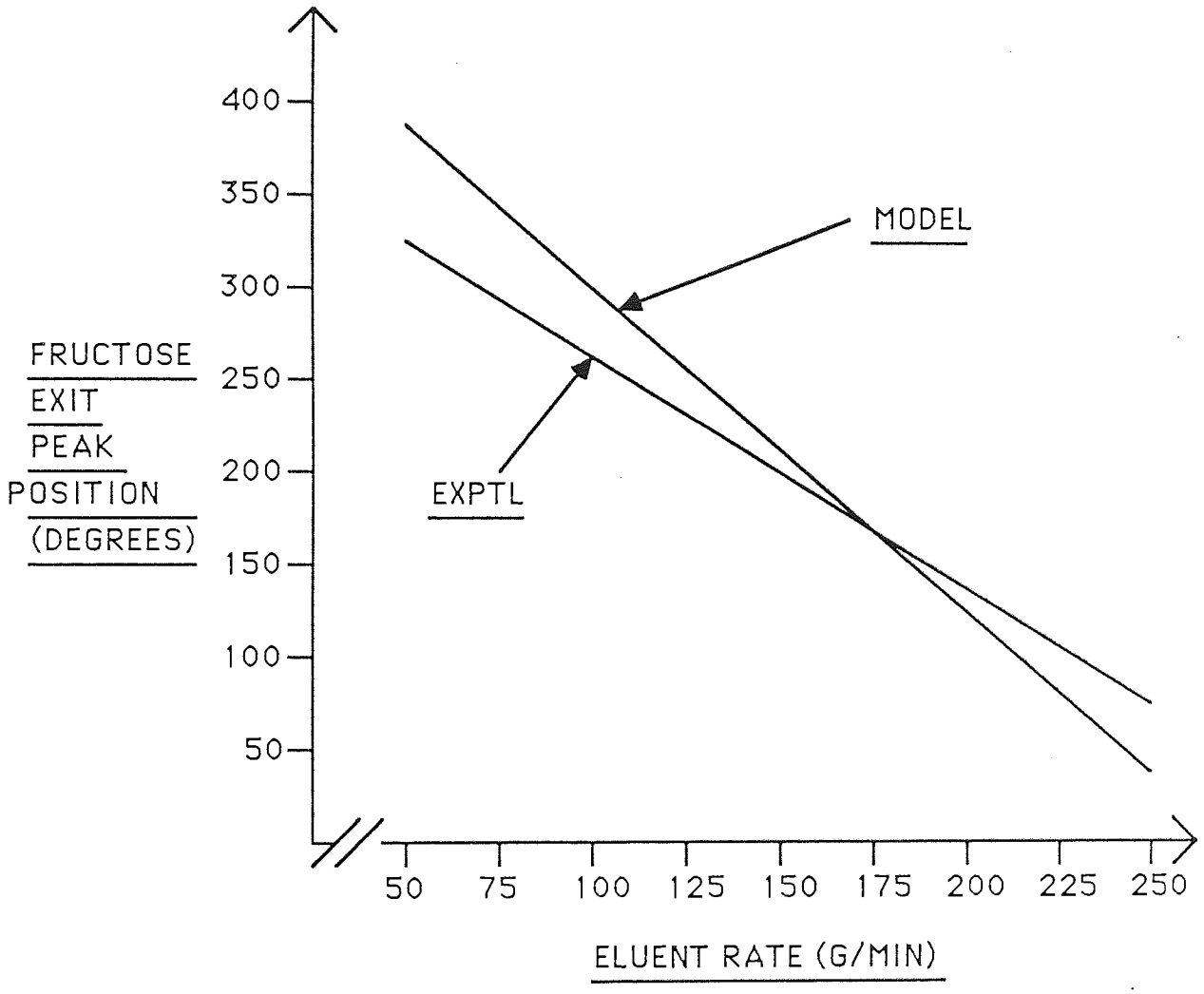

FIGURE 8.18 EXPERIMENTAL AND MODEL FRUCTOSE EXIT PEAK POSITION VERSUS ELUENT RATE

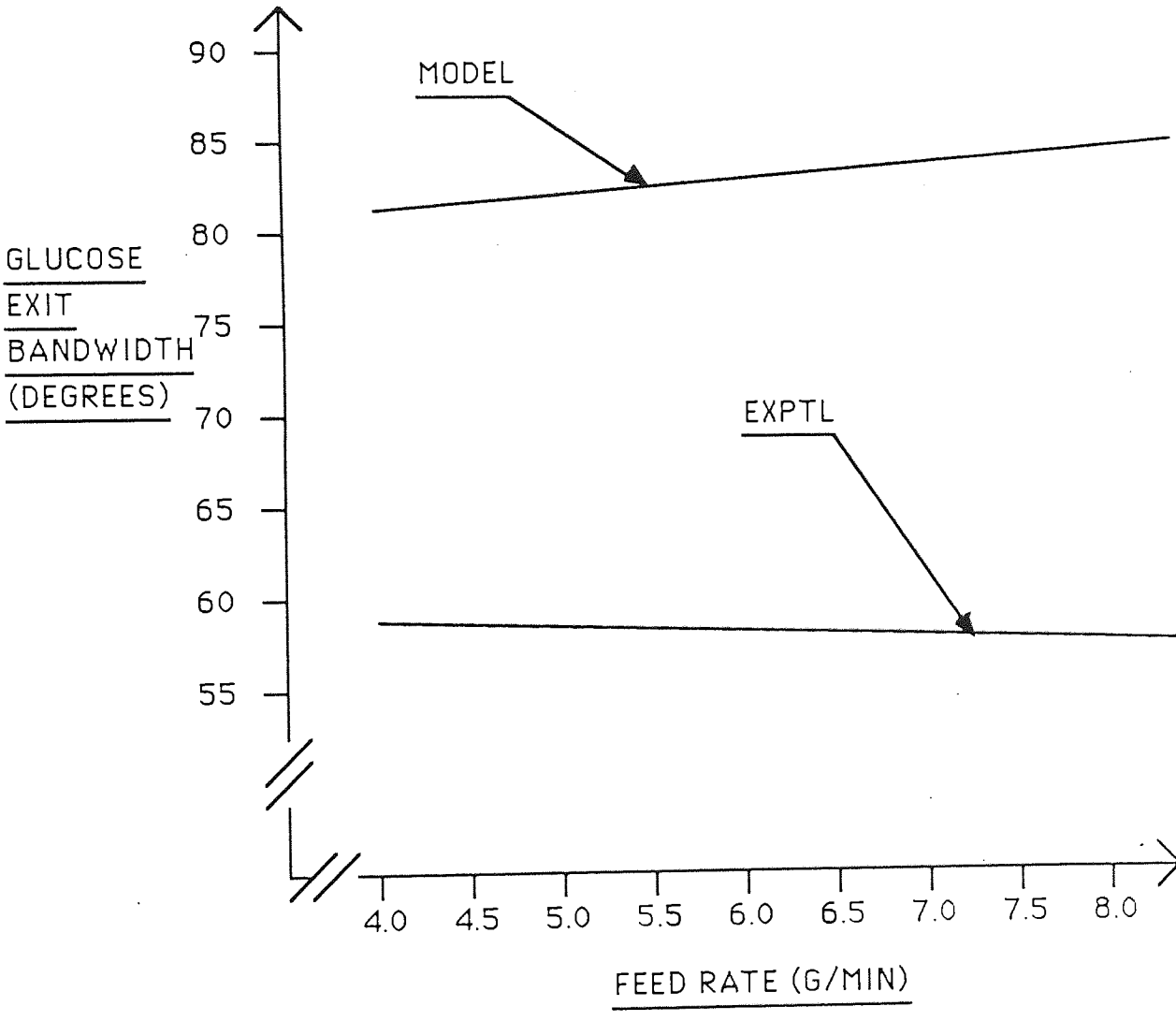

FIGURE 8.19 EXPERIMENTAL AND MODEL GLUCOSE EXIT BANDWIDTH VERSUS FEED RATE

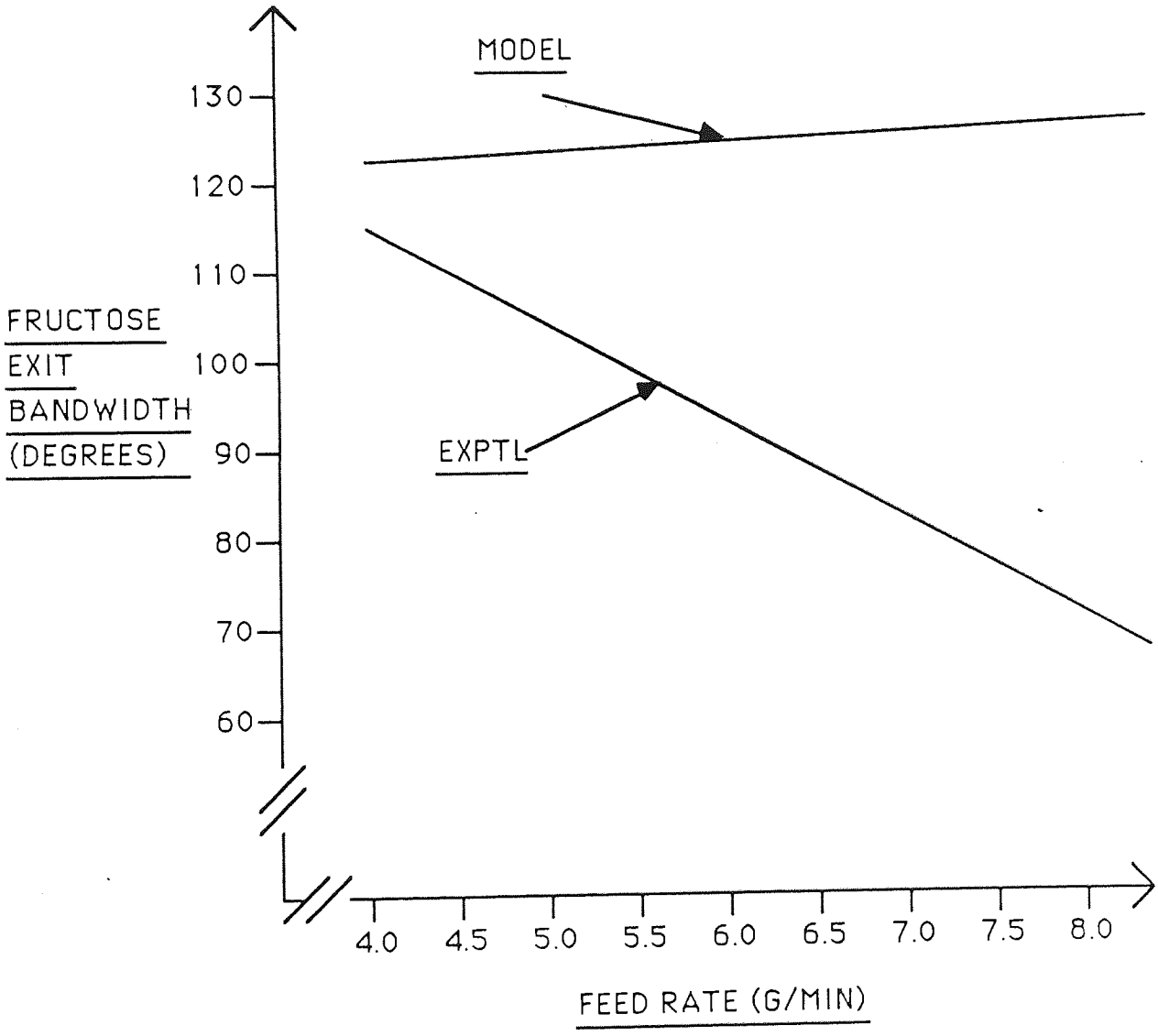

FIGURE 8.20 EXPERIMENTAL AND MODEL FRUCTOSE EXIT BANDWIDTH VERSUS FEED RATE

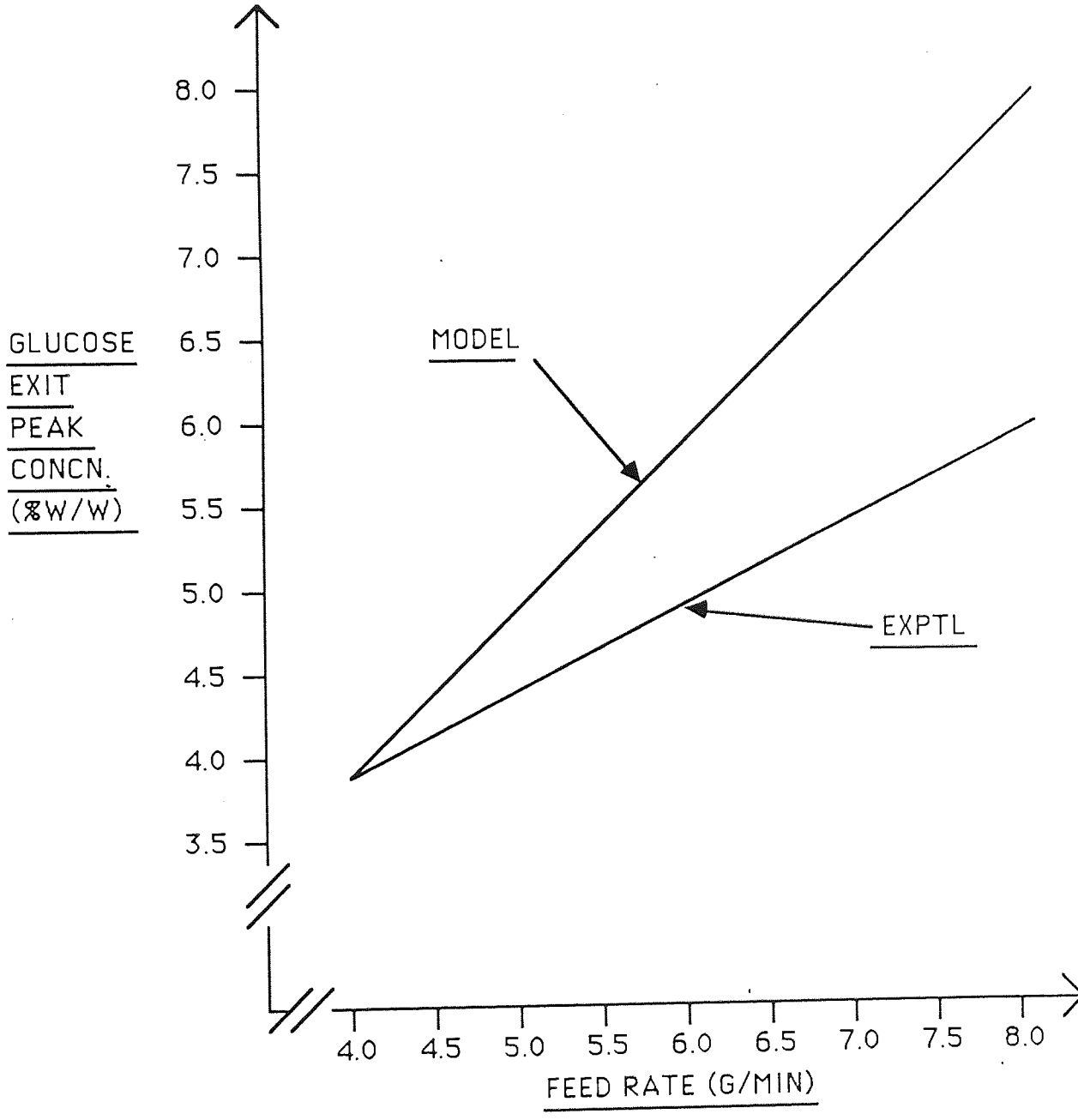

FIGURE 8.21 EXPERIMENTAL AND MODEL GLUCOSE PEAK EXIT CONCENTRATION VERSUS FEED RATE

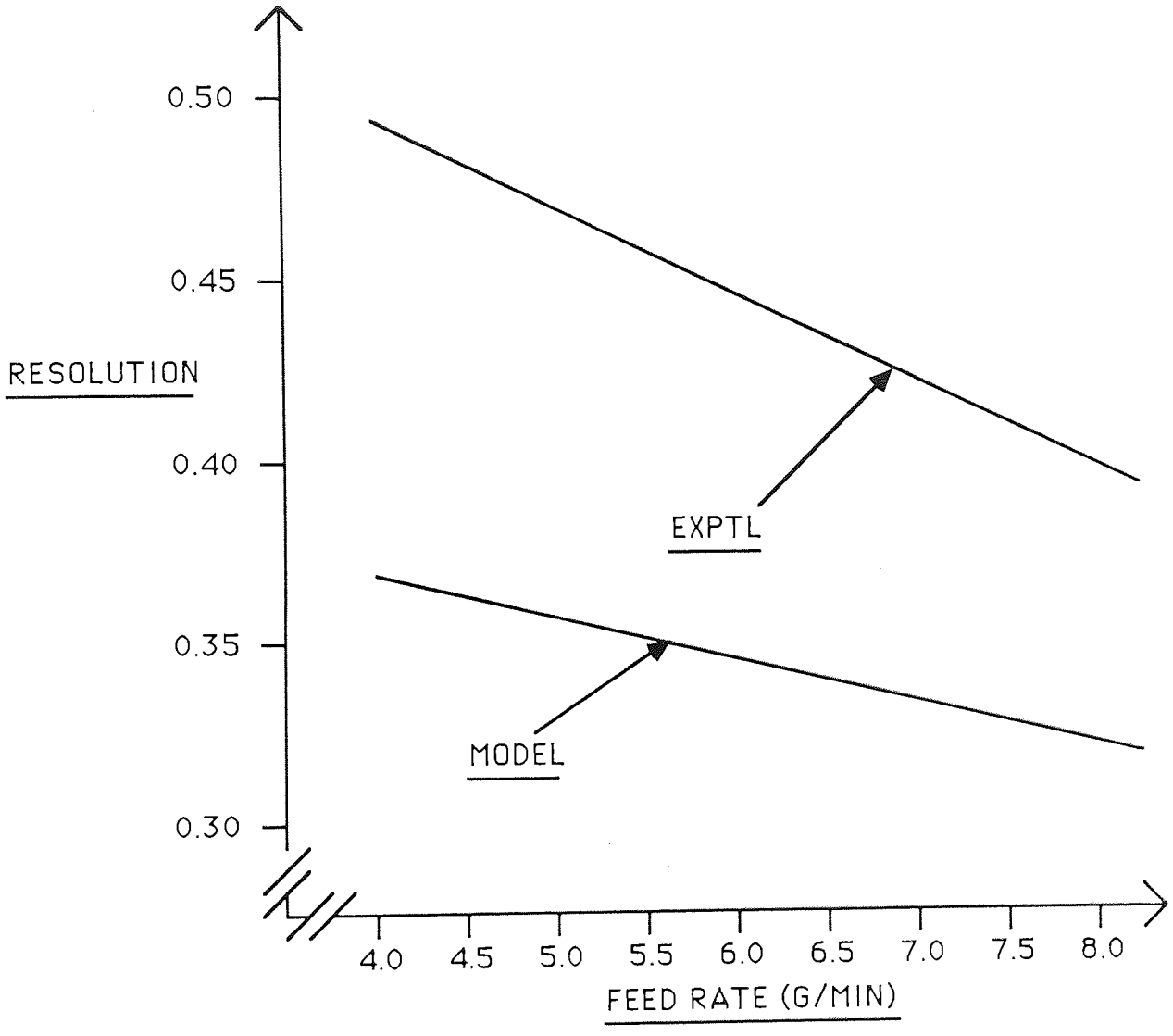

FIGURE 8.22 EXPERIMENTAL AND MODEL GLUCOSE-FRUCTOSE RESOLUTION VERSUS FEED RATE.

CHAPTER NINE

9 Conclusions

9.1 Introduction

Various experiments were conducted on the rotating annular chromatograph with beet molasses and other carbohydrate feedstocks where the underlying aim was to achieve a good separation of constituents while minimizing the dilution suffered by the constituents within the chromatograph. The somewhat narrow range of operating conditions employed in the beet molasses experiments were extended when investigating with glucose/fructose feeds. The separation performance of the chromatograph when separating glucose from fructose was found to deteriorate when using inverted molasses feed as opposed to synthetic glucose/fructose mixtures. Throughout the experimental work ways were constantly sought to improve the operation and ease of running of the equipment of which the main breakthrough was a means to ensure good liquid distribution around the annulus.

9.2 Beet Molasses Experiments

The rotating annular chromatograph was used to separate sucrose from the remaining constituents in the multicomponent feedstock beet molasses. High feed rates and concentrations achieve higher throughputs and product concentrations but reduce the separation between sucrose and the remaining solids. Low eluent rates were found to be preferable to separation while having little effect on the outlet concentration. The disadvantage of low eluent rates however are that a greater volume of bed is utilized to achieve separation and also that the feed at the feed nozzle has a greater tendency to diffuse sideways and upwards such that if not checked it can escape from the top of the bed. This tendency can be reduced by operating the column at

higher rotation rates so that the feed is more thinly spread. Rotating the annulus below $90°h^{-1}$ was found to reduce the separation performance markedly but once above this minimum value rotation rate had little effect. In view of the possibility of employing multiple feed points with the rotating chromatograph a low rotation rate is required.

9.3 Glucose-Fructose Experiments

Glucose/Fructose separation was carried out over a wide range of operating conditions and with synthetic and inverted molasses feeds. As rotation rate was increased there was a fall in exit peak concentration which was not observed in the beet molasses runs. The resolution between glucose and fructose also improved slightly at higher rotation rates. If the feed rate to rotation rate ratio was kept constant then as the rotation rate increased the exit concentrations increased though there was less of an improvement in resolution. The effect of feed rate on separation performance was similar to that with beet molasses but increases in eluent rate were found to reduce exit peak concentrations of both glucose and fructose.

Reducing the bed particle size from a mean of 420 micron to 150 micron produced a 100% increase in glucose/fructose resolution. The exit peak concentrations were approximately 25% higher also.

When separating glucose and fructose using inverted molasses the separation performance deteriorated compared to when using syntnetic feed.

The presence of the other constituents in the molasses were detrimental to performance. However, operating at higher temperature (50°C) was found to

be of some advantage with invert molasses although not with the synthetic feed.

9.4 Liquid Distribution Around The Annulus

Previous workers in the annular chromatography field have experienced liquid maldistribution around the annulus. In this research work a means was found to ensure that liquid distribution was uniform. A detachable ring located and sealed at the annulus base housed the polyethylene bed support material in the form of discs. This material is prone to clogging by fines and was the cause of liquid maldistribution in the annulus. Previously the bed support was housed internally which owing to the unweildy nature of the chromatograph meant that it was difficult to get at and replace once clogged.

9.5 Computer Simulation

A simulation model of the rotating annular chromatograph incorporating the effects of interference between solutes was developed. The model was capable of predicting the experimental trends of the chromatograph over a wide range of operating conditions.

9.6 Recommendations For Future Work

1 Carry out more separation experiments to improve the reliability of the relationships derived to predict the effect of various operating parameters.

2 High temperature operating particularly needs further investigation with possible improvements to be made to the heating system so that temperatures up to 80°C could be used.

3 Use the rotating annular chromatograph as a reactor-separator. Initial studies demonstrate its applicability for the inversion of sucrose by the enzyme invertase followed by the chromatographic separation of the glucose/fructose product.

4 To achieve higher throughput capacity the volume of the annular bed can be increased by increasing the outside diameter. The existing glass shell can be replaced by a wider diameter stainless steel shell enabling operating at high pressures.

5 A rigorous extension of the simulation model to multicomponent feedstocks. Experimentally derived distribution co-efficients and diffusion co-efficients will improve the accuracy of the model.

APPENDIX A.1

This Appendix includes the experimental results from 16 runs which were performed on the rotating annular chromatograph to separate the constituents of beet molasses. For each run, the peak position (θ) relative to the stationary feed point at which a solute's exit concentration was a maximum was recorded. The peak concentration was measured in micro-siemens (μs) for the ionic component, in an absorbance unit (A) for the colour and in %w/w for sucrose and betaine. The solute exit bandwidth (W) was measured in degrees. The resolution of each solute from sucrose was calculated using Equation (6). The concentration ratio, C_3, was calculated by dividing the sucrose peak concentration by the sucrose feed concentration.

In addition to the 16 runs which formed a factorial experiment a further 3 runs were carried out which were replications of run 2 and another 3 runs which studied the effect of feed rate in more detail.

Table A.1 (1) Results of Factorial Experiment

Run 1: $\omega = 180°h^{-1}$, V = 12lh, $F = 120cm^3h^{-1}$ (35% w/w sucrose)

Component	θ	W	Peak Concentration	Resolution
Colour	86.4	52.5	2.59	0.20
Ionic	100.8	62.3	5.95	0.00
Sucrose	100.8	80.7	2.27	/
Betaine	189.2	100.8	0.20	0.95

Concentration Ratio, $C_3 = 0.065$

Run 2: $\omega = 120°h^{-1}$, $V = 9lh^{-1}$, $F = 120cm^3h^{-1}$ (24% w/w sucrose)

Component	θ	W	Peak Concentration	Resolution
Colour	72.0	67.4	3.03	0.46
Ionic	72.0	55.4	4.70	0.51
Sucrose	100.8	57.9	1.64	/
Betaine	144.0	75.3	0.16	0.65

Concentration Ratio, $C_3 = 0.068$

Table A.1 (1) continued

Run 3: $\omega = 120°h^{-1}$, $V = 9\ lh^{-1}$, $F = 120cm^3h^{-1}$ (35% w/w sucrose)

Component	θ	W	Peak Concentration	Resolution
Colour	86.4	89.4	3.66	0.40
Ionic	86.4	49.9	7.42	0.56
Sucrose	115.2	53.1	3.62	/
Betaine	172.8	68.3	0.26	0.56

Concentration Ratio, $C_3 = 0.103$

Run 4: $\omega = 120°h^{-1}$, $V = 12lh^{-1}$, $F = 180\ cm^3h^{-1}$ (24%w/w sucrose)

Component	θ	W	Peak Concentration	Resolution
Colour	57.6	55.8	1.30	0.25
Ionic	57.6	36.7	7.41	0.30
Sucrose	72.0	57.5	3.63	/
Betaine	129.6	72.0	0.29	0.89

Concentration Ratio, $C_3 = 0.151$

Table A.1 (1) continued

Run 5: $\omega = 180°h^{-1}$, $V = 9lh^{-1}$, $F = 180cm^3h^{-1}$ (24% w/w sucrose)

Component	θ	W	Peak Concentration	Resolution
Colour	100.8	84.6	1.97	0.39
Ionic	115.2	91.6	5.44	0.25
Sucrose	144.0	138.8	2.68	/
Betaine	230.4	86.4	0.10	0.77

Concentration Ratio, $C_3 = 0.117$

Run 6: $\omega = 120°h^{-1}$, $V = 9lh^{-1}$, $F = 180cm^3h^{-1}$ (35% w/w sucrose)

Component	θ	W	Peak Concentration	Resolution
Colour	86.4	44.7	6.34	0.26
Ionic	86.4	65.8	9.25	0.22
Sucrose	100.8	64.5	4.55	/
Betaine	172.8	98.6	0.42	0.88

Concentration Ratio, $C_3 = 0.13$

Table A.1 (1) continued

Run 7: $\omega = 180°h^{-1}$, $V = 9lh^{-1}$, $F = 180cm^3h^{-1}$ (35% w/w sucrose)

Component	θ	W	Peak Concentration	Resolution
Colour	144.0	94.4	6.25	0.26
Ionic	158.4	74.3	8.25	0.14
Sucrose	172.8	129.9	4.21	/
Betaine	273.6	100.8	0.12	0.87

Concentration Ratio, $C_3 = 0.12$

Run 8: $\omega = 180°h^{-1}$, $V = 12lh^{-1}$, $F = 120cm^3h^{-1}$ (24% w/w sucrose)

Component	θ	W	Peak Concentration	Resolution
Colour	100.8	34.4	3.06	0.46
Ionic	100.8	43.0	4.80	0.43
Sucrose	129.6	89.7	1.88	/
Betaine	201.6	100.8	0.16	0.76

Concentration Ratio, $C_3 = 0.078$

Table A.1 (1) continued

Run 9: $\omega = 180°h^{-1}$, $V = 12lh^{-1}$, $F = 180cm^3h^{-1}$ (35% w/w sucrose)

Component	θ	W	Peak Concentration	Resolution
Colour	100.8	59.6	6.18	0.18
Ionic	100.8	91.9	6.42	0.15
Sucrose	115.2	101.3	3.39	/
Betaine	172.8	92.0	0.25	0.60

Concentration Ratio, $C_3 = 0.097$

Run 10: $\omega = 180°h^{-1}$, $V = 9lh^{-1}$, $F = 120cm^3h^{-1}$ (24% w/w sucrose)

Component	θ	W	Peak Concentration	Resolution
Colour	115.2	40.0	2.35	0.45
Ionic	115.2	67.2	4.35	0.37
Sucrose	144.0	89.4	1.61	/
Betaine	259.2	81.6	0.14	1.35

Concentration Ratio, $C_3 = 0.067$

Table A.1 (1) continued

Run 11: $\omega = 120°h^{-1}$, $V = 12lh^{-1}$, $F = 180cm^3h^{-1}$ (35% w/w sucrose)

Component	θ	W	Peak Concentration	Resolution
Colour	72.0	42.6	3.86	0.27
Ionic	72.0	38.1	8.95	0.30
Sucrose	86.4	59.0	5.41	/
Betaine	129.6	85.6	0.38	0.59

Concentration Ratio, $C_3 = 0.154$

Run 12: $\omega = 180°h^{-1}$, $V = 9lh^{-1}$, $F = 120cm^3h^{-1}$ (35% w/w sucrose)

Component	θ	W	Peak Concentration	Resolution
Colour	115.2	62.3	4.85	0.49
Ionic	129.6	59.2	7.37	0.33
Sucrose	158.4	114.4	2.98	/
Betaine	273.6	120.8	0.26	0.98

Concentration Ratio, $C_3 = 0.085$

Table A.1 (1) continued

Run 13: $\omega = 120°h^{-1}$, $V = 12lh^{-1}$, $F = 120cm^3h^{-1}$ (24% w/w sucrose)

Component	θ	W	Peak Concentration	Resolution
Colour	72.0	32.6	3.28	0.35
Ionic	72.0	33.9	4.71	0.35
Sucrose	86.4	48.9	1.93	/
Betaine	129.6	72.0	0.18	0.72

Concentration Ratio, $C_3 = 0.08$

Run 14: $\omega = 180°h^{-1}$, $V = 12lh^{-1}$, $F = 180cm^3h^{-1}$ (24% w/w sucrose)

Component	θ	W	Peak Concentration	Resolution
Colour	86.4	44.3	5.17	0.39
Ionic	100.8	65.5	6.00	0.17
Sucrose	115.2	103.6	2.62	/
Betaine	201.6	109.4	0.18	0.81

Concentration Ratio, $C_3 = .109$

Table A.1 (1) continued

Run 15: $\omega = 120°h^{-1}$, $V = 12lh^{-1}$, $F = 120cm^3h^{-1}$ (35% w/w sucrose)

Component	θ	W	Peak Concentration	Resolution
Colour	57.6	43.0	7.32	0.49
Ionic	72.0	53.6	6.70	0.22
Sucrose	86.4	74.9	3.78	/
Betaine	144.0	101.7	0.28	0.65

Concentration Ratio, $C_3 = .108$

Run 16: $\omega = 120°h-1$, $v = 9lh-1$, $F = 180\ cm^3h-1$ (24% w/w sucrose)

Component	θ	W	Peak Concentration	Resolution
Colour	72.0	52.0	6.84	0.42
Ionic	72.0	56.8	7.37	0.41
Sucrose	100.0	85.4	4.05	/
Betaine	158.4	114.0	0.33	0.58

Concentration Ratio, $C_3 = 0.169$

Table A.1 (1) continued

Run 17: $\omega = 120°h^{-1}$, $V = 12lh^{-1}$, $F = 260cm^3h^{-1}$ (35% w/w sucrose)

Component	θ	W	Peak Concentration	Resolution
Colour	72.0	81.8	5.63	0.4
Ionic	86.4	61.4	11.45	0.23
Sucrose	100.8	63.4	7.72	
Betaine	144.0	81.8	0.57	0.60

Concentration Ratio, $C_3 = .22$

Run 18: $\omega = 120°h^{-1}$, $V = 12lh^{-1}$, $F - 340\ cm^3h^{-1}$ (35% w/w sucrose)

Component	θ	W	Peak Concentration	Resolution
Colour	72	41.1	6.90	0.46
Ionic	79.2	39.1	11.65	0.31
Sucrose	93.6	53.5	9.74	
Betaine	122.4	69.9	0.73	0.47

Concentration Ratio, $C_3 = 0.28$

Table A.1 (1) continued

Run 19: $\omega = 120°h^{-1}$, $V = 12lh^{-1}$, $F = 160cm^3h^{-1}$ (35% w/w sucrose)

Component	θ	W	Peak Concentration	Resolution
Colour	64.8	39.1	3.98	.53
Ionic	79.2	41.2	8.10	.17
Sucrose	86.6	42.2	4.73	/
Betaine	115.2	47.4	0.36	.64

Concentration Ratio, $C_3 = 0.13$

Table A.1 (2) Results of Replicated Run 2

Run 2b: $\omega = 120°h^{-1}$, $V = 9lh^{-1}$, $F = 120cm^3h^{-1}$ (24% w/w sucrose)

Component	θ	W	Peak Concentration	Resolution
Colour	72.0	60.2	2.94	.48
Ionic	72.0	51.0	4.13	.52
Sucrose	100.8	59.8	0.96	
Betaine	144.0	63.6	0.09	.70

Concentration Ratio, $C_3 = 0.04$

Run 2c: $\omega = 120°h^{-1}$, V - $9lh^{-1}$, F =- $120cm^3h^{-1}$ (24% w/w sucrose)

Component	θ	W	Peak Concentration	Resolution
Colour	72	80.0	2.52	.51
Ionic	72	85.7	4.17	.49
Sucrose	108	61.2	2.02	/
Betaine	144	47.9	.19	.66

Concentration Ratio, $C_3 = 0.084$

Run 2d: $\omega = 120°h^{-1}$, $V = 9lh^{-1}$, $F = 120cm^3h^{-1}$ (24% w/w sucrose)

Component	θ	W	Peak Concentration	Resolution
Colour	79.2	41.7	2.74	.45
Ionic	72.0	58.6	4.29	.51
Sucrose	100.8	54.3	2.64	
Betaine	136.8	61.8	0.16	.62

Concentration Ratio, $C_3 = 0.110$

APPENDIX A.2

Contains details of 28 runs separating a synthetic glucose-fructose feedstock. For each run the feed concentration was 15% w/w glucose, 15% w/w fructose and all runs were carried out using duolite cation exchange resin, mean particle size 420 micron.

Table A.2

Experimental Results for Glucose-Fructose runs using Duolite Cation Exchange Resin

Run No	Eluent Velocity ($gmin^{-1}$)	Feed Rate ($gmin^{-1}$)	Rotation Rate ($^{\circ} h^{-1}$)	Resolution Glucose/ Fructose	Peak Concentrations Glucose (% w/w)	Fructose (% w/w)
GF1	150	4.0	129	9.59	3.7	2.2
GF2	150	4.0	180	0.52	2.7	1.7
GF3	150	4.0	240	0.50	2.0	1.3
GF4	150	4.0	300	0.55	1.5	1.0
GF5	200	4.0	120	0.38	2.9	2.2
GF6	250	4.0	120	0.34	3.0	2.0
GF7	100	4.0	120	0.58	4.0	3.1
GF8	150	4.7	120	0.54	4.7	3.1
GF9	150	5.9	120	0.44	4.8	3.6
GF10	150	7.1	120	0.40	5.8	4.5
GF11	150	4.7	140	0.51	3.1	2.1
GF12	150	5.9	177	0.43	3.4	2.4
GF13	150	7.1	210	0.56	3.3	2.2
GF14	150	8.3	248	0.45	3.3	2.7
GF15	176	4.7	120	0.49	4.1	2.3
GF16	100	2.6	120	0.58	3.0	2.0
GF17	263	7.1	120	0.36	4.4	3.2
GF18	150	3.0	90	0.36	2.0	2.2
GF19	150	4.0	90	0.40	3.7	2.5
GF20	150	10.0	300	0.48	3.3	2.4
GF21	150	4.0	120	0.46	3.5	2.9
GF22	55	4.0	120	0.54	4.8	3.5
GF23	150	8.3	120	0.41	5.6	4.1
GF24	75	4.0	120	0.55	3.5	3.3
GF25	150	4.0	143	0.49	2.4	1.6
GF26	150	6.8	204	0.41	3.6	2.0
GF27	150	4.0	240	0.46	2.0	1.3
GF28	221	5.9	120	0.42	3.9	2.9

APPENDIX A.3

This contains details of 26 runs separating a synthetic glucose-fructose feedstock. For each run the feed concentration was 15% w/w glucose, 15% w/w fructose and all runs were carried out using the Dowex cation exchange resin, mean particle size 150 micron.

Table A.3

Experimental Results for Glucose-Fructose runs using Duolite Cation Exchange Resin

Run No	Eluent Velocity ($gmin^{-1}$)	Feed Rate ($gmin^{-1}$)	Rotation Rate ($° h^{-1}$)	Temp. (°C)	Resolution Glucose/ Fructose	Peak Concentrations Glucose (% w/w)	Fructose (% w/w)
GF29	150	4.0	130	20	1.11	4.8	3.1
GF30	150	4.0	208	20	1.22	2.6	2.4
GF31	150	4.0	300	20	0.96	2.1	2.0
GF32	150	4.0	180	20	1.00	3.6	2.5
GF33	150	4.0	120	20	0.79	4.6	3.0
GF34	100	4.0	120	20	0.80	4.6	3.6
GF35	100	4.0	240	20	1.74	2.6	3.1
GF36	100	4.0	120	20	1.38	4.7	4.1
GF37	150	5.9	120	20	0.83	5.2	5.1
GF38	150	2.7	120	20	0.86	2.9	2.6
GF39	100	4.0	240	20	1.12	3.3	2.3
GF40	150	4.0	240	20	0.99	2.7	2.1
GF41	100	4.0	288	20	1.42	2.5	2.1
GF42	150	4.0	190	50	1.18	4.0	5.2
GF43	150	4.0	280	50	0.42	1.6	1.8
GF44	150	4.0	375	50	0.78	1.8	1.4
GF45	150	4.0	140	50	0.79	3.7	2.7
GF46	150	7.1	120	20	0.60	6.9	5.0
GF47	150	4.0	260	50	0.87	3.2	2.4
GF48	150	4.0	120	50	0.54	4.4	3.2
GF49	150	4.0	210	50	0.90	3.2	2.8
GF50	150	4.0	170	50	0.56	2.7	2.5
GF51	150	4.0	240	50	0.77	3.2	2.4
GF52	150	4.0	144	20	0.77	2.9	2.9
GF53	150	4.0	240	20	1.03	2.4	2.1
GF54	150	4.0	205	20	0.99	2.6	2.8
GF55	100	4.0	180	20	1.24	3.7	2.7
GF56	100	4.0	205	20	1.38	2.9	2.3
GF57	150	4.8	120	20	0.94	4.8	3.9

APPENDIX A.4

This contains the experimental results for runs using inverted molasses feedstock. The separations were carried out using Dowex Cation Exchange Resin (mean size 150 micron) in the calcium form. The feed concentration was 15% w/w glucose, 15% w/w fructose.

The peak concentrations at the exit were measured in % w/w for glucose, fructose and betaine, micro-siemens for the ionic fraction and absorbance units (A) for the colour.

Table A4

Experimental Results for runs using Invert Molasses Feedstocks

Run IM1: $\omega = 160°h^{-1}$, $V = 150gmin^{-1}$, $F = 4gmin^{-1}$ $T = 20°C$

Solute	Peak Position (θ) (Degrees)	Bandwidth (W) (Degrees)	Peak Concentration (% w/w)	Resolution
Glucose	194.4	50.4	2.87	0.61
Fructose	244.8	115.2	1.12	
Ionic	172.8	122.4	3.45	0.61
Colour	144.0	115.2	1.15	0.88

Run IM2: $\omega = 230°h^{-1}$, $V = 150gmin^{-1}$, $F = 4gmin^{-1}$ $T = 20°C$

Solute	Peak Position (θ) (Degrees)	Bandwidth (W) (Degrees)	Peak Concentration (% w/w)	Resolution
Glucose	259.2	64.8	1.65	0.76
Fructose	352.8	180.0	1.73	
Ionic	194.4	108.6	4.05	1.10
Colour	165.6	115.2	1.20	1.27

Run IM3: $\omega = 230°h^{-1}$, $V = 150gmin^{-1}$, $F = 4gmin^{-1}$ $T = 50°C$

Solute	Peak Position (θ) (Degrees)	Bandwidth (W) (Degrees)	Peak Concentration (% w/w)	Resolution
Glucose	331.2	136.8	2.96	0.36
Fructose	388.8	180.0	2.60	
Ionic	223.2	129.6	4.20	1.07
Colour	172.8	100.8	1.30	1.54

Run IM4: $\omega = 150°h^{-1}$, $V = 150gmin^{-1}$, $F = 4gmin^{-1}$ $T = 50°C$

Solute	Peak Position (θ) (Degrees)	Bandwidth (W) (Degrees)	Peak Concentration (% w/w)	Resolution
Glucose	223.2	82.8	3.64	0.34
Fructose	252.0	86.4	3.78	
Ionic	151.2	122.4	4.91	0.97
Colour	136.8	86.4	1.65	1.33

Run IM5: $\omega = 200°h^{-1}$, $V = 150gmin^{-1}$, $F = 4gmin^{-1}$ $T = 20°C$

Solute	Peak Position (θ) (Degrees)	Bandwidth (W) (Degrees)	Peak Concentration (% w/w)	Resolution
Glucose	259.2	100.8	1.49	0.60
Fructose	324.0	115.2	2.13	
Ionic	208.8	129.6	4.22	0.94
Colour	151.2	57.6	1.82	2.00

Run IM6: $\omega = 275°h^{-1}$, $V = 150gmin^{-1}$, $F = 4gmin^{-1}$ $T = 20°C$

Solute	Peak Position (θ) (Degrees)	Bandwidth (W) (Degrees)	Peak Concentration (% w/w)	Resolution
Glucose	345.6	151.2	1.90	0.57
Fructose	432.0	151.2	1.20	
Ionic	266.4	158.4	3.38	1.07
Colour	208.8	64.8	1.88	2.07

Run IM7: $\omega = 183°h^{-1}$, $V = 150gmin^{-1}$, $F = 4gmin^{-1}$ $T = 20°C$

Solute	Peak Position (θ) (Degrees)	Bandwidth (W) (Degrees)	Peak Concentration (% w/w)	Resolution
Glucose	288	115.2	1.76	0.68
Fructose	316.8	93.6	2.20	
Ionic	216.0	144.0	5.38	0.85
Colour	151.2	100.8	1.50	1.70

Run IM8: $\omega = 122°h^{-1}$, $V = 150gmin^{-1}$, $F = 4gmin^{-1}$ $T = 20°C$

Solute	Peak Position (θ) (Degrees)	Bandwidth (W) (Degrees)	Peak Concentration (% w/w)	Resolution
Glucose	165.5	115.2	2.98	0.69
Fructose	237.6	93.6	2.75	
Ionic	122.4	208.8	4.78	0.76
Colour	115.2	187.2	1.65	0.88

Run IM9: $\omega = 300°h^{-1}$, $V = 150gmin^{-1}$, $F = 4gmin^{-1}$ $T = 50°C$

Solute	Peak Position (θ) (Degrees)	Bandwidth (W) (Degrees)	Peak Concentration (% w/w)	Resolution
Glucose	374.4	158.4	2.05	0.48
Fructose	460.8	208.8	1.65	
Ionic	259.2	136.8	3.68	1.17
Colour	194.4	108.0	1.21	1.70

Run IM10: $\omega = 180°h^{-1}$, V = 150gmin^{-1}, F = 4gmin^{-1} T = 50°C

Solute	Peak Position (θ) (Degrees)	Bandwidth (W) (Degrees)	Peak Concentration (% w/w)	Resolution
Glucose	273.6	93.6	2.95	0.30
Fructose	309.6	144	2.70	
Ionic	194.4	151.2	4.44	0.79
Colour	172.8	129.6	1.63	1.00

Run IM11: $\omega = 270°h^{-1}$, V = 150gmin^{-1}, F = 4gmin^{-1} T = 50°C

Solute	Peak Position (θ) (Degrees)	Bandwidth (W) (Degrees)	Peak Concentration (% w/w)	Resolution
Glucose	338.4	151.2	2.42	0.90
Fructose	482.4	165.6	1.66	
Ionic	295.2	136.8	4.07	1.24
Colour	237.6	100.8	1.58	1.82

Run IM12: $\omega = 120°h^{-1}$, V = 150gmin^{-1}, F = 4gmin^{-1} T = 50°C

Solute	Peak Position (θ) (Degrees)	Bandwidth (W) (Degrees)	Peak Concentration (% w/w)	Resolution
Glucose	158.4	93.6	3.70	0.27
Fructose	187.2	136.8	3.02	
Ionic	122.4	79.2	5.20	0.60
Colour	86.4	72.0	3.07	1.32

APPENDIX A.5

This contains the experimental results for runs using beet molasses feedsotck. The runs were carried out at 20°C using Dowex Cation Exchange Resin (mean particle size 150 micron) in the sodium form. These runs also followed the equipment modifications outlined in Chapter 6 which were designed to improve liquid distribution around the annulus such that the distribution would not alter with time.

Table A.5

Experimental Results for Beet Molasses

Runs Following Design Changes to Improve Liquid Distribution

Run No	Eluent Rate ($gmin^{-1}$)	Feed Rate ($gmin^{-1}$)	Feed Conc. (% sucrose)	Rotation Rate ($°h^{-1}$)	Peak concentration				Resolution Between Sucrose and:		
					Sucrose (%w/w)	Betaine (%w/w)	Ionic (µs)	Colour (A)	Ionic	Colour	Betaine
1	150	2.59	30.0	200	5.29	0.31	5.57	0.73	0.73	1.08	1.62
2	150	2.59	30.0	130	5.17	0.40	7.00	0.70	0.50	0.74	1.39
3	150	2.59	30.0	90	6.37	0.61	6.55	0.78	0.34	0.77	1.02
4	150	2.59	30.0	280	3.38	0.30	4.50	0.55	0.69	1.31	1.90
5	150	2.59	30.0	165	4.24	0.40	5.72	0.63	0.49	0.86	1.29
6	150	2.59	30.0	50	8.10	0.67	7.72	0.72	0.22	0.40	0.58
7	150	2.59	30.0	340	4.03	0.42	2.89	0.23	0.60	0.93	3.43
8	150	2.59	30.0	180	4.39	0.31	5.45	0.58	0.66	1.23	3.33
9	150	7.40	30.0	180	6.92	0.59	10.10	1.07	0.28	0.54	0.43
10	150	7.40	30.0	180	6.46	0.57	9.78	0.85	0.31	0.52	0.39
11	150	6.83	30.0	180	7.20	0.66	8.13	0.64	0.34	0.84	0.59
12	150	2.59	33.0	180	4.10	0.42	5.93	0.46	0.52	1.03	1.66
13	150	2.59	37.5	180	3.60	0.46	6.90	0.32	0.40	0.82	1.03
14	150	2.59	30.0	180	4.52	0.22	5.78	0.52	0.58	0.92	1.80
15	150	3.67	30.0	180	5.95	0.32	7.00	0.63	0.38	1.65	0.80
16	150	4.52	30.0	180	6.30	0.52	8.50	0.52	0.40	0.63	0.77
17	150	6.83	30.0	180	5.91	0.32	9.62	1.30	0.31	0.83	0.64

Table A5 Continued

Run No	Eluent Rate ($gmin^{-1}$)	Feed Rate ($gmin^{-1}$)	Feed Conc (% sucrose)	Rotation Rate ($°h^{-1}$)	Peak concentration				Resolution between sucrose and:		
					Sucrose (%w/w)	Betaine (% w/w)	Ionic (µs)	Colour (A)	Ionic	Colour	Betaine
18	150	8.28	30.0	180	6.89	0.61	11.32	1.00	0.19	0.31	0.26
19	150	5.75	30.0	180	7.15	0.63	7.10	0.65	0.47	0.90	0.52
20	150	2.59	40.0	180	3.75	0.60	7.20	0.13	0.29	0.66	1.13
21	150	2.59	20.0	180	2.77	0.22	5.88	0.35	0.55	0.97	1.88
22	150	2.59	30.0	180	3.25	0.36	7.00	0.60	0.53	1.37	1.16
23	150	2.59	35.0	180	3.94	0.46	6.40	0.40	0.43	1.02	1.43
24	150	2.59	25.0	180	3.40	0.25	5.70	0.43	0.56	1.15	1.26
25	150	2.59	15.0	180	1.83	0.14	4.90	0.35	0.63	1.30	2.89
26	150	2.59	45.0	180	3.10	0.59	7.60	0.25	0.21	0.34	0.53

COMPUTER PROGRAM

TY STEVE.FOR

```
      PROGRAM CHROMA
      IMPLICIT REAL(A-Z)
      INTEGER COUNT
      COMMON D(10),C(2,10),N(2,10),THI(2,10),A(2,10),W(2,10)
      COMMON K1,K2,J10,J14,J15,J16,P1,P2,P3,EV,DM
      COMMON XOA,TOA,XOB,TOB,XOC,TOC,XOD,TOD
      DIMENSION CANG(2000,2),DZ(2),PEAK(2)
      DIMENSION BANDW(2),HOP(2),FRED(2),RED(2)
      DIMENSION LEK(2),PEK(2),MEK(2),DEC(2000,2),FEC(2000,2)
      PRINT*,'READ IN ROT(DEG/MIN),SUPVEL(CM/MIN),FEED RATE(G/MIN)'
      READ*,WR,VEL,QF
      DELTA=3.6*QF/WR
      PRINT*,'READ IN NO. OF COMPONENTS,NCOMP'
      READ*,NCOMP
      PRINT*,'IDENTIFY A KEY COMPONENT.THE PROGRAM HANDLES BINARY
     CMIXTURES SO THAT THE SEPARATION OF MORE THAN TWO SOLUTES IS
     CCALCULATED BY CONSIDERING SUCCESSIVE SEPARATIONS BETWEEN A
     CKEY COMPONENT AND EACH OF THE REMAINING COMPONENTS IN TURN.
     CCOMPONENT ONE IN EACH CASE MUST BE THE COMPONENT WITH THE
     CLOWEST K-VALUE.'
   45 PRINT*,'READ IN FEED CONCS,CF1,CF2'
      READ*,CF1,CF2
      PRINT*,'READ IN K1,K2'
      READ*,K1,K2
      IF(K1.EQ.0) K1=0.001
      EV=.4
      L=140
   47 PRINT*,'TIME FOR CALC'
      READ*,TIME
      PRINT*,'READ IN DZ(1) AND DZ(2)'
      READ*,DZ(1),DZ(2)
      IPO=100
      C(1,1)=0
      C(2,1)=0
      D(1)=1
      N(1,1)=0
      N(2,1)=0
      A(1,1)=K1
      A(2,1)=K2
      W(1,1)=K1
      W(2,1)=K2
      THI(1,1)=0
      THI(2,1)=0
      C(1,7)=0
      C(2,7)=0
      D(7)=1
      N(1,7)=0
      N(2,7)=0
      A(1,7)=K1
      A(2,7)=K2
      W(1,7)=K1
      W(2,7)=K2
      THI(1,7)=0
      THI(2,7)=0
      C(1,9)=0
      C(2,9)=0
      D(9)=1
      N(1,9)=0
      N(2,9)=0
      A(1,9)=K1
```

```
A(2,9)=K2
W(1,9)=K1
W(2,9)=K2
THI(1,9)=0
THI(2,9)=0

C STATE THREE

C(1,3)=CF1
C(2,3)=CF2
THI(1,3)=K1*C(1,3)
THI(2,3)=K2*C(2,3)
D(3)=1+THI(1,3)+THI(2,3)
N(1,3)=THI(1,3)/D(3)

N(2,3)=THI(2,3)/D(3)

BB=K1*(1-N(1,3))+K2*(1-N(2,3))
CC=K1*K2*(1-N(1,3)-N(2,3))

W(1,3)=(BB-SQRT((BB*BB)-(4*CC)))/2
W(2,3)=(BB+SQRT((BB*BB)-(4*CC)))/2
A(1,3)=W(1,3)*D(3)
A(2,3)=W(2,3)*D(3)

C STATE TWO

IN=2
W(1,2)=W(1,3)
W(2,2)=W(2,1)

CALL HDE(IN,T,DELTA,L)
C STATE SIX

IN=6
W(1,6)=W(1,9)
W(2,6)=W(2,3)
CALL HDE(IN,T,DELTA,L)

SIGZ=EV+(1-EV)*W(1,1)/D(2)
SIGY=EV+(1-EV)*W(2,2)/D(3)
SIGX=EV+(1-EV)*(A(1,3)/(D(3)*D(3)))
SIGW=EV+(1-EV)*(A(1,3)/(D(6)*D(6)))
SIGV=EV+(1-EV)*(A(2,6)/(D(6)*D(6)))
SIGU=EV+(1-EV)*W(2,9)/D(9)
SIGT=EV+(1-EV)*W(2,7)/D(6)
SIGS=EV+(1-EV)*(A(1,7)/(D(7)*D(7)))
SIGR=EV+(1-EV)*(A(1,2)/(D(2)*D(2)))
XOA=DELTA/(SIGY-SIGX)
TOA=SIGY*XOA
C PRINT*,'SIGZ,SGY,SIGX,SIGW,SIGV',SIGZ,SIGY,SIGX,SIGW,SIGV
C PRINT*,'SIGU,SIGT,SIGS,SIGR',SIGU,SIGT,SIGS,SIGR

AER=D(2)/D(3)
BER=D(3)-A(1,3)/W(2,2)
CER=D(2)-A(1,3)/W(2,2)
XOB=XOA*(AER*BER/CER)**2
TOB=SIGW*XOB+DELTA

XOC=(TOA-(SIGR*XOA))/(SIGZ-SIGR)
TOC=SIGZ*XOC

XOD=((SIGT*XOB)+DELTA-TOB)/(SIGT-SIGV)
TOD=SIGV*XOD+DELTA
J1=SIGX*XOA
J2=A(1,3)/W(2,2)
```

```
J3=D(3)
J4=XOA
J5=A(1,3)*(1-EV)*W(2,2)/W(2,3)
J6=EV
J7=(1-EV)*A(1,3)
J8=D(3)/D(2)
J9=J4*((J3-J2)/J3)**2
J10=J4*J6-J1
J11=J4*J5
J12=J7-J5
J13=J9*J12
J14=J13/(J8*J8)
J15=J2/J8
J16=J11/(J8*J8)
P1=(XOC-XOA)*((1-(D(1)/D(2)))**2)
P2=D(1)/((1-EV)*A(1,2))
P3=J10*D(2)-(J14/(D(2)-J15))-(J16/D(2))
C PRINT*,'XOA,XOB,XOC,XOD',XOA,XOB,XOC,XOD
C PRINT*,'TOA,TOB,TOC,TOD',TOA,TOB,TOC,TOD
C PRINT*,'DTOT=',D
C START THE CLOCK

 DO 11 T=1,TIME

 IF(T.LT.DELTA) THEN
 IN=1
 IF(L.GT.0.AND.L.LE.T/SIGY) IN=3
 IF(L.GT.T/SIGY.AND.L.LE.T/SIGZ) IN=2

 ELSE IF(L.GT.0.AND.L.LE.(T-DELTA)/SIGU) THEN
 IN=9

 ELSE IF(T.GT.TOD) THEN
 AL=(T-DELTA)-((EV*XOD)*((1-(D(7)/D(6)))**2))
 BL=2*(D(7)*(T-DELTA))
 CL1=(T-DELTA)*(D(7)**2)
 CL2=(1-EV)*A(2,6)*XOD*((1-(D(7)/D(6)))**2)
 CL=CL1-CL2
 QL=(BL*BL)-(4*AL*CL)
 DL=BL+SQRT(QL)
 EL=2*AL
 FL=DL/EL
 D(8)=FL
 X30=XOD*((1-D(7)/D(6))/(1-D(7)/D(8)))**2
C PRINT*,'X30=',X30
 IF(L.GT.(T-DELTA)/SIGU.AND.L.LE.X30) THEN
 IN=8
 CALL HDE(IN,T,DELTA,L)
 ELSE IF(L.GT.X30.AND.L.LE.((T-TOB)/SIGS+XOB)) THEN
 IN=7
 ELSE
 CALL RT(T,IN,SIGS,SIGR,SIGZ,L)
 ENDIF

 ELSE IF(L.GT.(T-DELTA)/SIGU.AND.L.LE.(T-DELTA)/SIGV) THEN
 IN=8
 CALL HDE(IN,T,DELTA,L)

 ELSE IF(T.GT.TOB.AND.T.LE.TOD) THEN
 IF(L.GT.(T-DELTA)/SIGV.AND.L.LE.(T-TOB)/SIGT+XOB) IN=6
 IF(L.GT.(T-TOB)/SIGT+XOB.AND.L.LE.(T-TOB)/SIGS+XOB) IN=7
 IF(IN.NE.6.AND.IN.NE.7) THEN
 CALL RT(T,IN,SIGS,SIGR,SIGZ,L)
 ENDIF

 ELSE IF(L.GT.(T-DELTA)/SIGV.AND.L.LE.(T-DELTA)/SIGW) THEN
```

```
      IN=6
      ELSE IF(T.GT.TOA.AND.T.LE.TOB) THEN
      SS=(T-DELTA)/XOA
      SI=(D(3)/(D(3)-(A(1,3)/W(2,2))))**2
      SK=SS*SI
      VS=A(1,3)/W(2,2)
      VV=(1-EV)*A(1,3)
      AF=1-EV/SK
      BF=2*VS
      CF=(VS**2)-(VV/SK)
      DK=(BF+SQRT((BF*BF)-(4*AF*CF)))/(2*AF)
      X0=XOA*((DK*(D(3)-VS))/(D(3)*(DK-VS)))**2
      IF(L.GT.(T-DELTA)/SIGW.AND.L.LE.X0) THEN
      IN=4
      CALL HDE(IN,T,DELTA,L)

      ELSE IF(T.LT.TOC) THEN
      IF(L.GT.X0.AND.L.LE.(T-TOA)/SIGR+XOA) THEN
      IN=5
      EP=0
      FP=1
      CALL HDE(IN,T,DELTA,L)

      ELSE IF(L.GT.(T-TOA)/SIGR+XOA.AND.L.LE.T/SIGZ) THEN
      IN=2

      ELSE
      IN=1

      ENDIF

      ELSE
      FP=0
      EP=1
      IN=5
      CALL FALSI(IN,T,EP,FP,X00,L)
     C PRINT*,'X00=',X00
      IF(L.GT.X0.AND.L.LE.X00) THEN
      IN=5
      FP=1
      EP=0
      CALL HDE(IN,T,DELTA,L)
      ELSE
      IN=1
      ENDIF
      ENDIF
      ELSE IF(L.GT.(T-DELTA)/SIGW.AND.L.LE.(T-DELTA)/SIGX) THEN
      IN=4
      CALL HDE(IN,T,DELTA,L)
      ELSE IF(L.GT.(T-DELTA)/SIGX.AND.L.LE.T/SIGY) THEN
      IN=3
      ELSE IF(L.GT.T/SIGY.AND.L.LE.T/SIGZ) THEN
      IN=2
      ELSE
      IN=1
      ENDIF
      IF(D(IN).GT.1) THEN
      CANG(T,1)=C(1,IN)
      CANG(T,2)=C(2,IN)
      ENDIF

   11 CONTINUE
      IG=0
      IH=0
      DO 36 T=1,TIME
      THETA=(WR/VEL)*T
```

```
      IF(CANG(T,1).GT.0.AND.IG.EQ.0) THEN
      LEK(1)=T
      KLIP=LEK(1)*WR/VEL
      IG=1
      ENDIF
      IF(CANG(T,1).EQ.0.AND.IG.EQ.1) THEN
      MEK(1)=T
      IG=2
      ENDIF
      IF(CANG(T,2).GT.0.AND.IH.EQ.0) THEN
      LEK(2)=T
      KLOP=LEK(2)*WR/VEL
      IH=1
      ENDIF
      IF(CANG(T,2).EQ.0.AND.IH.EQ.1) THEN
      MEK(2)=T
      IH=2
      ENDIF
   36 CONTINUE
      DO 102 ICP=1,2
      POL=LEK(ICP)
      IF(POL.EQ.0) GO TO 47
      DOL=MEK(ICP)
      DO 103 ZX=POL,DOL
      DO 104 PHI=0,IPO
      FC1=CANG(ZX,ICP)/(2*SQRT(3.14*DZ(ICP)*ZX/WR))
      FC2=EXP(-((PHI*PHI)/(4*DZ(ICP)*ZX/WR)))
      FEC(ZX+PHI,ICP)=FC1*FC2
      DCP=DEC(ZX+PHI,ICP)
      DCQ=DEC(ZX-PHI,ICP)
      DEC(ZX+PHI,ICP)=FEC(ZX+PHI,ICP)+DCP
      DEC(ZX-PHI,ICP)=FEC(ZX+PHI,ICP)+DCQ
  104 CONTINUE
  103 CONTINUE
  102 CONTINUE
      HOP(1)=0
      HOP(2)=0
      DO 222 SID=1,2
      DO 223 T=1,TIME
      IF(DEC(T,SID).GT.DEC(T-1,SID)) THEN
      RED(SID)=DEC(T,SID)
      PEAK(SID)=T*WR/VEL
      ENDIF
  223 CONTINUE
  222 CONTINUE
      PRINT*,'CONCS',RED(1),RED(2)
      FRED(1)=0.6*RED(1)
      FRED(2)=0.6*RED(2)
      PRINT*,'PEAKS=',PEAK(1),PEAK(2)
      PRINT*,'FREDS',FRED(1),FRED(2)
      DO 322 MIK=1,2
      DO 323 T=1,TIME
      IF(DEC(T,MIK).GT.FRED(MIK)) THEN
      HOP(MIK)=HOP(MIK)+1
      ENDIF
  323 CONTINUE
  322 CONTINUE
      PRINT*,'HOPS',HOP(1),HOP(2)
      BANDW(1)=2*HOP(1)*WR/VEL
      BANDW(2)=2*HOP(2)*WR/VEL
      PRINT*,'W1,W2=',BANDW(1),BANDW(2)
      RESOL=2*(PEAK(2)-PEAK(1))/(BANDW(1)+BANDW(2))
      PRINT*,'RESOLUTION=',RESOL
      DO 123 T=1,TIME
      THETA=(WR/VEL)*T
      PRINT*,THETA,DEC(T,1),DEC(T,2)
```

```
123 CONTINUE
    NCOMP=NCOMP-1
    IF(NCOMP.GT.1) GO TO 45
    END
    SUBROUTINE HDE(IN,T,DELTA,L)
    IMPLICIT REAL(A-Z)
    COMMON D(10),C(2,10),N(2,10),THI(2,10),A(2,10),W(2,10)
    COMMON K1,K2,J10,J14,J15,J16,P1,P2,P3,EV,DM
    COMMON XOA,TOA,XOB,TOB,XOC,TOC,XOD,TOD
    DIMENSION AN(10),BN(10),CN(10),DN(10)
    IF(IN.EQ.2.OR.IN.EQ.6) GO TO 61
    IF(IN.EQ.8) THEN
    D(8)=SQRT(((1-EV)*A(2,6))/(((T-DELTA)/L)-EV))
    W(2,8)=A(2,6)/D(8)
    W(1,8)=W(1,6)

    ELSE IF(IN.EQ.4) THEN
    D(4)=SQRT(((1-EV)*A(1,3))/(((T-DELTA)/L)-EV))
    W(1,4)=A(1,3)/D(4)
    W(2,4)=W(2,3)

    ELSE
    IN=5
  C STATE 5 NEEDS ITERATION TO SOLVE D.
    EP=0
    FP=1
    X00=0
    CALL FALSI(IN,T,EP,FP,X00,L)
  C PRINT*,'X00=',X00
    W(1,5)=A(1,2)/D(5)
    W(2,5)=W(2,2)
    ENDIF
 61 CONTINUE
 62 IF(W(1,IN).EQ.K1) THEN
    N(2,IN)=(K2-W(2,IN))/K2
    N(1,IN)=0
    ELSE IF(W(2,IN).EQ.K2) THEN
    N(1,IN)=(K1-W(1,IN))/K1
    N(2,IN)=0
    ELSE
    AN(IN)=K2/(K2-W(2,IN))
    BN(IN)=K2/(K2-W(1,IN))
    CN(IN)=K1/(K1-W(1,IN))
    DN(IN)=K1/(K1-W(2,IN))
    N(1,IN)=(AN(IN)-BN(IN))/((AN(IN)*CN(IN))-(BN(IN)*DN(IN)))
    N(2,IN)=(DN(IN)-CN(IN))/((DN(IN)*BN(IN))-(CN(IN)*AN(IN)))
    ENDIF
    THI(1,IN)=N(1,IN)/(1-N(1,IN)-N(2,IN))
    THI(2,IN)=N(2,IN)/(1-N(1,IN)-N(2,IN))
    C(1,IN)=THI(1,IN)/K1
    C(2,IN)=THI(2,IN)/K2
    D(IN)=1+THI(1,IN)+THI(2,IN)
    A(1,IN)=W(1,IN)*D(IN)
    A(2,IN)=W(2,IN)*D(IN)
    END
    SUBROUTINE FALSI(IN,T,EP,FP,X00,L)
    IMPLICIT REAL(A-Z)
    COMMON D(10),C(2,10),N(2,10),THI(2,10),A(2,10),W(2,10)
    COMMON K1,K2,J10,J14,J15,J16,P1,P2,P3,EV,DM
    COMMON XOA,TOA,XOB,TOB,XOC,TOC,XOD,TOD
    TDSH(DD)=(J14/(DD-J15)**2)+J16/(DD*DD)+J10
    THIE(DD)=EV+(((1-EV)*A(1,2))/(DD*DD))
    AQ(DD)=P1/((1-(D(1)/DD))**2)
    BQ(DD)=P2*(DD/(DD-D(1)))**2
    CQ(DD)=(DD-D(1))*TDSH(DD)-(J10*DD)+(J14/(DD-J15))+J16/DD+P3
    XDSH(DD)=((L-XOA)*FP)+(EP*(AQ(DD)+(BQ(DD)*CQ(DD))))
```

```
      FN(DD)=T-TOA-(THIE(DD)*XDSH(DD))-TDSH(DD)
      IF(IN.EQ.4) THEN
      D1=D(3)-0.1
      D2=D(6)+0.1
      ELSE IF(IN.EQ.8) THEN
      D1=D(6)+0.1
      D2=D(9)-0.1
      ELSE
      D1=D(2)+0.031
      D2=D(7)-0.031
      ENDIF
   20 D3=D1-((FN(D1)*(D1-D2))/(FN(D1)-FN(D2)))
      IF(FN(D1).EQ.SIGN(FN(D1),FN(D2))) THEN
      D1=D1+0.1
      D2=D2-0.1
      GO TO 20
      ENDIF
      IF(FN(D3).EQ.SIGN(FN(D3),FN(D1))) THEN
      QQ=ABS(D3-D1)
      D1=D3
      ELSE
      QQ=ABS(D3-D2)
      D2=D3
      ENDIF
      IF(ABS(D3).GT.1.0) QQ=QQ/ABS(D3)
      IF(QQ.GT.1.0E-5) GO TO 20
      IF(FP.EQ.0) THEN
     C PRINT*,'D3=',D3
      X00D=XDSH(D3)
      X00=X00D+XOA
     C PRINT*,'X00=',X00
      ENDIF
      IF(IN.EQ.4.OR.IN.EQ.5.OR.IN.EQ.8) THEN
      D(IN)=D3
     C IF(IN.EQ.4) THEN
     C W(1,4)=A(1,3)/D(IN)
     C W(2,4)=W(2,3)
     C ELSE IF(IN.EQ.5) THEN
     C W(1,5)=A(1,2)/D(IN)
     C W(2,5)=W(2,2)
     C ELSE
     C W(1,8)=W(1,6)
     C W(2,8)=A(2,6)/D(IN)
     C ENDIF
      ENDIF
      END
      SUBROUTINE RT(T,IN,SIGS,SIGR,SIGZ,L)
      IMPLICIT REAL(A-Z)
      COMMON D(10),C(2,10),N(2,10),THI(2,10),A(2,10),W(2,10)
      COMMON K1,K2,J10,J14,J15,J16,P1,P2,P3,EV,DM
      COMMON XOA,TOA,XOB,TOB,XOC,TOC,XOD,TOD
      IF(T.GT.TOC) THEN
      EP=1
      FP=0
      CALL FALSI(IN,T,EP,FP,X00,L)
      IF(L.GT.((T-TOB)/SIGS)+XOB.AND.L.LE.X00) THEN
      IN=5
      CALL HDE(IN,T,DELTA,L)
      ELSE
      IN=1
      ENDIF
      ELSEIF(L.GT.((T-TOB)/SIGS)+XOB.AND.L.LE.((T-TOA)/SIGR)+XOA)THEN
      IN=5
      CALL HDE(IN,T,DELTA,L)
      ELSE IF(L.GT.((T-TOA)/SIGR)+XOA.AND.L.LE.T/SIGZ) THEN
      IN=2
```

```
ELSE
IN=1
ENDIF
END
```

NOMENCLATURE

A	=	Column area; Eddy diffusion constant
B	=	Longitudinal diffusion constant
C	=	Mass transfer constant; concentration
c	=	Concentration in mobile phase
dp	=	Particle size
D	=	Dispersion co-efficient
e	=	Voidage
F	=	Feed flowrate
H	=	HETP
K_D	=	Distribution co-efficient
k	=	Reciprocal value of c when half of the sites are occupied by molecules of solute i and the other half are vacant.
L	=	Column length
M	=	Mass; Concentration of solute in mobile phase
N	=	Number of theoretical plates
n	=	Concentration of solute in stationary phase
n_o	=	Limiting concentration of adsorbed solute
n^*	=	Equilibrium value of n
R	=	Resolution; Correlation co-efficient
t	=	Time
U	=	Mobile phase flowrate
u	=	Mobile phase velocity
V	=	Interstitial velocity
W	=	Bandwidth
x	=	Dependant (space-like) variable in Equation 8.8
y	=	Dependant (time-like) variable in Equation 8.8
z	=	Axial co-ordinate

Greek Letters

ω	=	Rotation rate
θ	=	Angular co-ordinate
$\overline{\theta}$	=	Peak position
Δ	=	Defined by Equations 8.9 and 8.10
λ	=	Defined by Equation 8.12
Γ	=	Characteristic curve
ζ	=	Slope of characteristic curve in (u,v) plane
σ	=	Slope of characteristic curve in (x,y) plane

Subscripts

i, j	=	Identify different solutes
1,2	=	Identify different solutes
0	=	Initial state
θ, z	=	Referring to co-ordinate system
I	=	Component I
Ex	=	Experimental value
+, -	=	Positive or negative characteristic curves

REFERENCES

1 Thawait S, PhD Thesis, University of Aston, Birmingham (1983).

2 Hongisto HJ, Int Sug J, 79, 100, (1977).

3 Heikkila H, Chem Eng, Jan 24, 50 (1983).

4 Schneider HG, Mikule J, Int Sug. J. 77, 259-264, 294-298, (1975).

5 Munir M, Int Sug. J, 78, 100 (1976).

6 Boehringer CF, Haftung SGMB, of Maunheim-Waldhof, British Patent 10855696 (1967).

7 Sayama K, Senba Y, Kawamoto T, Proc. Res. Soc. Japan Sugar Refineries Technol. 29, (1980).

8 Fornalek W, Szulc T, Jarosz A, Ligowska M, Gaz. Cukrow, 89, 131, (1981).

9 Barker, P.E., ("Developments in Continuous Chromatographic Refining"), Dev. Chromatogr. 1, 41-86, (1978).

10 Barker, P.E., Deeble, R.E., British Patent 1418503.

11 Barker, P.E., Deeble, R.E.,Anal. Chem. 45, (1973).

12 Barker, P.E., Ganetsos, G, J Chem Tech. Biotechnol 35B, 217, (1985).

13 Barker, P.E., Thawait, S, Chem Eng. Res. Des., 64, 302, (1986).

14 Barker, P.E., Chuah, C.H, The Chemical Engineer, 389, Aug/Sept., (1981).

15 Martin, A.V.P., Disc. Faraday Soc. 7, 332, (1949).

16 Giddings, J.C., Anal. Chem. 34, 37, (1962).

17 Svensson H, Agrell CE, Dehlen SO, Hagdahl L, Science Tools, 2 (2), 17, (1955).

18 Dinelli D, Polezzo S, Taramasso M, J. Chromatogr., 7, 477, (1962).

19 Fox J.B., J. Chromatogr., 43, 55, (1969).

20 Fox J.B., Calhoun R.C., Eglinton W.J., J. Chromatogr., 43, 48, (1969).

21 Nicholas R.A., Fox J.B., J. Chromatogr, 43, 61, (1969).

22 Solms J.J., British Patent, 786896, (1957).

23 Strain H.H., Sullivan J.C., Anal. Chem. 189, 100, (1962).

24 Durrum E.L., J.Am.Chem.Soc. 73, 4875, (1951).

25 Sussman M.V., Huang C.C., Science, 156, 974, (1976).

26 Sussman M.V., U.S. Patent, 3503712.

27 Sussman M.V., Astill K.N., Rombach R, Cerullo A, Chen SS, IEC Fundamentals II, 181, (1972a).

28 Moskvin LN, Mozzhukin AV, Tsaritsyna LG, J. Anal. Chem. USSR, 30 (1), 29, (1975).

29 Moskvin LN, Mel'nikov VA, J.Anal. Chem.USSR., 33 (1), 28, (1978).

30 Pronin AY, Goryaeva NA, Chmutov KV, J Appl Chem of the USSR. 53 (7), 1127, (1980).

31 Scott CD, Spence RD, Sisson WG, J Chromatogr., 126, 381, (1976).

32 Begovich JM, PhD Dissertation, The University of Tennessee, Knoxville, USA, (1982).

33 Begovich JM, Sisson WG, Resources and Conservation, 9, 219, (1982).

34 Howard AJ, M.S. Thesis, The University of Virginia, Charlottesville, USA (1987).

35 Byers CH, Holmes JM, Oak Ridge Nat. Lab. Report, ORNL 6783, (1988).

36 Van Deemter JJ, Zuiderweg FJ, Klinkenberg A, Chem. Eng. Sci, 5, 271, (1956).

37 Martin MJP, Synge RLM, Biochem J, 35, 1959 (1941).

38 Aris R, Amundson NR, Mathematical Methods in Chemical Engineering, Vol 2, 1973, Prentice Hall.

39 Rhee HK, Bodin BF, Amundson NR, Chem Eng Sci, 26, 1571, (1971).

40 Rhee HK, Amundson NR, Chem Eng Sci, 27, 199, (1972).

41 DeVault D, J.Am. Chem Soc. 65, 532, (1943).

42 Lapidus L, Amundson NR, J Phys. Chem., 56, 984, (1952).

43 Houghton G, J. Phys. Chem., 67, 84, (1963).

44 Wankat PC, AICheJ., 23 (6), 859, (1977).

45 Gluekauf E, Disc. Faraday Soc. 7, 12, (1949).

46 Rhee HK, Aris R, Amundson NR, Phil Trans. Roy. Soc. London, 267A, 419, (1970).

47 Helfferich F, Klein G, Multicomponent Chromatography, 1970, Marcel Dekker, N.Y.

48 McGinnis (Ed), Beet Sugar Technology, 2nd Ed., Beet Sugar Development Foundation.

49 Lofton LH, Hartmann EM, Sugar J., 36 (1), 26, (1973).

50 German Patent Q391, IVA/89H, 22nd April 1955.

51 German Patent Application, P2362, 211.9-41, of 14th December 1973. DT-A5 23, 62, 211.

52 Gross D, Int. Sug. Jou. 73, 298-301, 330-334, (1971).

53 Schneider HG, Mikule J, Int. Sugar J, 77, 259-264, 294-298, (1975).

54 Kunin R, Applications of Ion-Exchange, XVIII. Industrial Application Sugar Processing and Inversion, Rohm and Haas Research Labs (1969).

55 Ferrier RJ, Collins PM, Monosaccharides Chemistry, Penguin Library London, (1972).

56 Hyvonen L, Pertti V, Kovistoinen P, J of Food Science, 42 (3), 652, (1977).

57 Asher DR, Ind Eng Chem, 48, 1465 (1956).

58 Norman L, Rorabaugh G, Keller H, Journal of the A.S.S.B.T. Vol. 12, No. 5, April (1963).

59 Charley PJ, Abstract from Rendleman JA, Adv. in Carbohydrate Chemistry, 8, 233, (1980).

60 Angyal SJ, J. Chem. 25, 1957, (1972).

61 Angyal SJ, J. Chem. 27, 1447, (1974).

62 Angyal SJ, J. Chem, 28, 1279, (1975).

63 Angyal SJ, J. Chem, 28, 1541, (1975).

64 Davies OL, Design and Analysis of Industrial Experiments, 2ed, Oliver and Boyd, (1971).

66 Joshi K, PhD Thesis, University of Aston, Birmingham, (1988).

67 Davies OL, Goldsmith PL, Eds), Statistical Methods in Research and Production, 4th ed, Oliver and Boyd, (1972).

68 Moskvin LN, J. Anal. Chem. USSR. 33 (1), 38, (1978).

69 Euston CH, Peters J, Debbrecht FJ, Kauss JM, A Complete Continuous Chromatograph for Purification of Boron Compounds, Prepeared for Office or Aerospace Research, U.S.A.F., AFCRL-62-731.

70 Giddings JC, Dynamics of Chromatography, Part 1, Marcel Dekker, N.Y. 1965.

71 Langmuir I, J.Am. Chem Soc., 38, 2221, (1916).

72 Gluekauf E, Proc. Roy. Soc. Lond., A186, 35, (1946).

73 DeBoer JH, The Dynamical Character of Adsorption, Oxford Clarendon Press, (1953).

74 Shen J, Smith J.M, Ind Eng Chem Fund, 7, 106 (1968).

75 Thirkill C, PhD Thesis, University of Aston, Birmingham (1988)